### Title
3D Visualizations and Non-Destructive Spectroscopic Analysis of a Pre-Hispanic Chilean Child Mummy Bundle



**Author**
Burton, Marci Jefcoat

**Publication Date**
2018

Peer reviewed|Thesis/dissertation

UNIVERSITY OF CALIFORNIA

Los Angeles

# 3D Visualizations and Non-Destructive Spectroscopic Analysis of a Pre-Hispanic Chilean Child Mummy Bundle

A thesis submitted in partial satisfaction

of the requirements for the degree Master of Arts

in Conservation of Archaeological and Ethnographic Materials

by

Marci Jefcoat Burton

2018

ABSTRACT OF THE THESIS

3D Visualizations and Non-Destructive Spectroscopic Analysis

of a Pre-Hispanic Chilean Child Mummy Bundle

by

Marci Jefcoat Burton

Master of Arts in Conservation of Archaeological and Ethnographic Materials

University of California, Los Angeles, 2018

Professor Ioanna Kakoulli, Co-Chair

Professor Christian Jean Mar Fischer, Co-Chair

This thesis is a technical investigation of a pre-Hispanic child mummy bundle from the San Miguel de Azapa region in the Arica Valley of northern Chile. The mummy bundle was accessioned into the collections of the Fowler Museum at the University of California, Los Angeles (UCLA) in 1966, along with an assortment of separate human bones assumed to originate from the assemblage. No form of technical study has been conducted on the mummy bundle, and its contents and provenance are unconfirmed. With non and minimally invasive scientific analysis techniques, this study investigates the construction and dye composition of the exterior textiles, as well as an optical biopsy of the interior contents. The results confirm the mummy bundle contents, which include the remains of a young child and funerary artifacts characteristic of the Late Intermediate Period (900 – 1450 CE) in Arica, Chile. Additionally, the

origin of the separate human bones accessioned with the mummy bundle is established.

The thesis of Marci Jefcoat Burton is approved.

Daniel B. Ennis

Wendy Giddens Teeter

Samantha L. Cox

Ioanna Kakoulli, Committee Co-Chair

Christian Jean Mar Fischer, Committee Co-Chair

University of California, Los Angeles

2018

## Table of Contents

## List of Figures

## List of Tables

# Acknowledgements

The author would like to thank the following people for their generous help with this study: Xuanyi Wu (Graduate Student Researcher, Department of Materials Science and Engineering, UCLA), Christian de Brer (Conservator, Fowler Museum at UCLA), Elena Phipps (Conservator, Metropolitan Museum of Art, New York), Janet Monge (Department of Anthropology, University of Pennsylvania), Maria Ines Boechat (Radiology and Pediatrics, UCLA) and Kambiz Motamedi (Diagnostic Radiology, Department of Radiological Sciences, UCLA). A special thank you to Jessica Martinez (Magnetic Resonance Research Labs, UCLA), who without her 3D renders of the CT analysis, this thesis could not be possible. The author is most grateful to her thesis committee members: Wendy Giddens Teeter (Fowler Museum at UCLA), Daniel B. Ennis (Professor of Radiological Sciences, Bioengineering and Biomedical Physics, Department of Radiological Sciences, David Geffen School of Medicine, UCLA) and Samantha L. Cox (Department of Anthropology, University of Pennsylvania) for their encouragement, guidance and assistance in this technical study.

The author is especially thankful to Committee Co-Chairs, Prof. Ioanna Kakoulli (Department of Materials Science and Engineering/UCLA/Getty Conservation IDP) and Prof. Christian Fischer (UCLA/Getty Conservation IDP) for finding this meaningful thesis project and offering their patience and continuous help with all aspects of the study. Thank you to the UCLA/Getty Conservation Program: Prof. Ellen Pearlstein, Prof. David Scott and Vanessa Muros for all your instruction and mentorship. Finally, the author would like to acknowledge the moral support of her parents Mark Jefcoat and Debra Jefcoat, as well as her husband, Andrew Burton. Thank you for all your love, support and keeping me motivated throughout this process.

# 1 Introduction

Mummification is a transformative process in which a once-living body or tissue, is preserved in a state of arrested decay (Aufderheide, 2003: 41). Mummies are a form of preserved human remains, and the ones that survive today are usually found in desiccated and even extremely wet environments, such as the deserts of South America (Atacama) and Egypt (Sahara), or the bogs of northern Europe. The oldest known mummies originate from the Chinchorro culture (7500 – 1500 BCE), of present-day Arica located on the Pacific coast in the Atacama Desert near the modern-day Peruvian-Chilean boarder (Arriaza, 1998). The Chinchorro practiced anthropomorphic, or artificial mummification, where soft tissues were removed and replaced with mud and vegetal material, or hide was stitched over the bones (Aufderheide, 2003: 143). After the Chinchorro, subsequent pre-Hispanic cultures from the Andean Mountain range continued the practice of mummification. They wrapped the dead and associated funerary objects together in woven textiles bundles, and buried them in the dry, desiccating soils in the region, which would mummify the remains. Known as mummy bundles, these assemblages of wrapped and preserved human remains are frequently discovered at archaeological excavations in the coastal and inland areas in the western coastline of South America (see map, Figure 1-1).


Figure 1-1: Map of the Andean region in South America. Arica is marked with a yellow star. Maps courtesy of (left): University of Minnesota, http://open.lib.umn.edu/worldgeography/chapter/6-2-urban-north-and-andean-west/ and (right); the International Research Institute for Climate and Society, Earth Institute and Columbia University, http://iridl.ldeo.columbia.edu/maproom/.Regional/.S_America/.

Coastal Arica and the Azapa Valley of northern Chile hold a long tradition of pre-Hispanic funerary practices in South America. Influence from Southern Peruvian and Northern Chilean groups intermixed and shared cultural traits and resources, leading to shared technology and aesthetics that are reflected in the objects and textiles incorporated into mummy bundles from the region. Preparation of the bundle and the objects interred with the human remains offer clues to the technology and customs of their life, values in death, and can assist with attribution of a provenance and cultural association. While their study can offer tremendous knowledge into the life and death of pre-Hispanic civilizations, research of mummy bundles requires a delicate and thoughtful approach. Previous intrusive methods of study included removal of all textile wrappings, performing autopsies and even separation of human remain components and removal of associated burial objects. These former approaches are now deemed too invasive and discourteous towards the integrity of the mummified individual, and are no longer approved in practice. Similar to artifact looting, where people disturb burials to collect valuable artifacts for profit, the early days of archaeology often involved disruption of the mummy bundle integrity. Often times, mummies were unwrapped, and the objects considered valuable such as ceramics and metal, were removed. The human remains were left scattered and exposed to the desert environment, and their textiles discarded from the body and left crumpled in the sand. Cassman (2000) notes this treatment for burial textiles in early to mid-twentieth century excavations.

The modern treatment and analysis of human remains, including mummy bundles, are carried out with handling, examination and analytical techniques that are preferably non to minimally invasive. It is no longer acceptable to unwrap mummy bundles to view their contents, and instead, X-radiographic procedures are employed. Computed Tomography (CT) is a popular radiography technique developed as a diagnostic tool in the medical field, but has tremendous potential with the analysis of mummies (Brown and Martin, 2014; Davey, Stewart and Drummer, 2013; Applbaum and Applbaum, 2005; Aufderheide, 2003). A major advantage CT has over standard X-radiographs is the collection of continuous measurements, or, "slices" of digital images that provide a full image of the object in cross-sections (Niemeyer et al., 2013; Applbaum and Applbaum, 2005). Standard two-dimensional X-radiography can be difficult to interpret superimposed and overlapping objects, which can obscure and at times, completely inhibit the observation of objects in layered assemblages. Even the weave of the textiles can be superimposed and hinder observation. The three-dimensionality of the mummy bundle would also be lost with traditional X-rays.

CT slices offer a convenient and non-invasive approach to an assessment of the objects' interiors in a mummy bundle. The slice distance, however, can pose a limitation on certain details. Surface features (i.e., painted decoration, color, surface sheen, etc.), textures (wood grain, follicle patterns on hide, distinction between materials of similar radiopacities, etc.) and condition issues (i.e., salt efflorescence, discoloration and staining, soiling, accretions, etc.) are difficult to distinguish with CT (Conlogue, 2015). Additionally, soft tissues, such as skin, are difficult to observe with CT due to its lack of hydration, and therefore, heightened radiopacity (Conlogue, 2015). The incorporation of a small camera, such as a medical endoscope, can provide these specific observations. A major limitation to the potential use of an endoscope, however, is the access available on the mummy bundle, as the endoscope would need to enter through existing openings and holes in the textile wrappings to observe the interior.

In 1966, the Fowler Museum at UCLA accessioned a small mummy bundle (X66.1953) into their collections from the "Chile Trade Project" of museum objects between the Fowler Museum and the Museo Nacional de Historia Natural (Santiago, Chile). Based on its small size (12.5 in, (h) 18 in. (w), 25 in. (l)), the assemblage is assumed to contain the remains of a mummified child wrapped with what appear to be three, plainweave warp-faced textiles and bound with plied plant fiber cordage (Figure 1-2). Limited contextual information is available on the mummy bundle. The object list provided by the Museo Nacional de Historia Natural indicates the mummy bundle was excavated from Arica. Other objects from Chile include materials excavated from "Tomb M15" in San Miguel de Azapa of the Arica Valley, which also includes other burial items, such as vegetable fiber mats, baskets, globular vessels and other various objects. The Fowler Museum at UCLA attributes these objects with a San Miguel de Azapa provenance within Arica, Chile; however, the mummy bundle lacks a specific attribution of provenance beyond Arica. Since the time of its discovery, no form of technical study was conducted, and the interior contents and textile technology remain unknown. Small bone fragments including toes, vertebrae and pelvic bones were also accessioned with the mummy bundle, although it is not yet confirmed if the fragments belong to the assemblage (Appendix 9.2). To fully understand the burial and cultural context of the mummy bundle, determine if the separated bones originate from the bundle, as well as establish protocols that will aid in its preservation, the contents need to be examined and known.

Figure 1-2: Child mummy bundle (X66.1953) in diffuse light. Attributed to Arica, Chile. (a) Front (b) Proper right (PR) side. (c) Proper left (PL) side).

## 2 Research objectives and scope

This research aims to determine the assembly, burial context and cultural significance of the Fowler Museum mummy bundle through non-invasive (optical biopsy) and minimally-invasive scientific investigations with the analysis of selected microsamples. The museum is willing to repatriate the mummy bundle back to its respective community, and this research hopes to determine the contents to establish provenance and evaluate the overall condition. A comprehensive materials characterization involving non-invasive and non-destructive techniques of analysis will allow observation of the mummy bundle contents and technical construction of the woven textile wrappings without its disassembly or excessive sampling of material. Through classification of the associated artifacts and textiles comprising the mummy bundle, the context of the individual and what cultural period associates with the bundle can be understood (Peters, Cassman and Gustafsson, 2007). Another objective of this research is to confirm whether the separate bone fragments accessioned with the mummy bundle in 1966 originate from the mummified individual. This may be possible to determine if these specific bones are not detected in the bundle. In addition, identification of all materials and objects present can provide sufficient information on proper environmental storage conditions to aid in the overall preservation of the assemblage.

From the assembly of the outer textile wrappings and plant fiber cordage, the Fowler Museum mummy bundle appears undisturbed, signifying the bundle interior was likely never visually inspected. Non-invasive and non-destructive methods of sampling and analysis were selected to identify the red and blue dye sources in the textile wrappings, as well as to visualize the content in the bundle without disassembly. Computed Tomography (CT) based on the collection of X-ray images taken around a single axis to give a 360° image of the object, was selected for observation of the interior content (Brown and Martin, 2014). The non-destructive X-rays produced are capable of passing through the textile wrappings to capture and compile stackable two-dimensional (2D) grayscale images of the interior contents. These images can then be compiled to create three-dimensional (3D) computer renderings, without the problem of superimposition or geometric distortion that is often common with X-radiography of overlapping materials. Computed Tomography will allow the bundle to remain wrapped to maintain its integrity. The files collected from the CT analysis can be used to digitally isolate and extract items from the bundle for 3D reconstruction and printing to further the conception of the associated cultural style of the funerary objects.

The identification of dyes used in the red and blue sections of the textiles can aid in determining attribution through the identification of plant and/or animal dye sources local to the area of origin for the culture of the mummy bundle. Fiber optic reflectance spectroscopy (FORS) and Raman spectromicroscopy (µRS) are two techniques of non-destructive analysis for the detection of dyes used in the production of historic textiles. µRS is known to be useful in the characterization and identification of dyestuffs. However, the technique can exhibit strong background fluorescence with certain dyes and substrates, such as wool and cotton. Fluorescence can overpower the signal of the dye, making interpretation of the resulting spectrum difficult or even impossible. Therefore, the technique of surface enhanced Raman spectroscopy (SERS) will also be performed to increase the signal of the dyes present in the mummy bundle textiles and reduce the fluorescent background.

# 3 Pre-Hispanic Andean culture, mummies and the processes of natural mummification in the Atacama Desert, Chile

Over successive millennia, various cultures from Southern Peru and Northern Chile intermixed and shared cultural traits, clothing styles, and resources. This causes the archaeology of northern Chile to be studied as a whole (Rodman, 2000). Coastal and altiplano regions are understood to have mixed and shared resources. Through this intermixing, pre-Hispanic cultures of the Andes shared stylistic influences on the production of material heritage, including ceramics and textiles. The expanse of population for the northern Chilean coast and the Atacama Desert primarily begins with the late Formative Period (c. 100 – 400 CE) and last through the Middle Period (c. 400 – 1000 CE) with the Tiwanaku, and spills into the Late Intermediate Period (LIP) (1000 – 1450 CE). Archaeological evidence supports the theory that various cultural groups migrated through the Atacama Desert from the Highlands and settled into coastal locations, such as Arica. The Chinchorro are believed to have originated from the earliest Andean Paleoindians during the Archaic Period (8000 – 1000 BCE), and occupied the region from 7500 to 1500 BCE (Sutter, 2006). From the Chinchorro, other principal inhabitants of the northern and central regions of the Chilean coast include cultures within different periods labeled as the Alto Ramirez (c. 1000 BCE – 350 CE), Cabuza (400 – 100 CE), Tiwanaku (500 – 1000 CE), Miatas Chiribaya (c. 1100 – 1300 CE), San Miguel (c. 990 – 1360 CE), Gentilar (c. 1300 – 1450 CE), Inca (1450 – 1550 CE) and the Colonial Period after European contact (c. 1550 – 1824 CE) (Sutter, 2006; Aufderheide, 2003: 141; Agüerro Pikwona, 2000).

Pre-Hispanic cultures in the modern political boundaries of northern Chile, southern Peru, northwest Argentina and Bolivia comprise a region that was once a single zone of cultural interaction, including travelers, settlers and traders from the influential highland center of Tiwanaku from the Formative Period (c. 100 – 400 CE) until the 11th century CE (Rodman, 2000). The Arica region resides between northern Chile and southern Peru, and is situated in the Atacama Desert, between the Pacific Ocean and the Andes Mountain range. Scholars describe Arica as a multi-ethnic location, and primarily functioned as a coastal fishing region occupied with various cultural groups from the coast, highlands and altiplano regions (Niemeyer and Agüero, 2015; Cassman, 2000a). Fishing along the Pacific coast was a primary method for food sources in Arica. Arica was a place for residence and trade, and flourished with population migration. In the Late Intermediate Period (1000-1450 CE) populations that occupied the region from Arica and the Atacama Desert shared material cultural values and aesthetics (Aguero, 2008). The domestication of camelid species, such as the llama and alpaca, were integrated into the region by the incoming highland cultures, and the camelid wool was used prominently in textile production, followed by cotton (Bonavia, 2008; Minkes, 2005: 36; Rodman, 2000).

Continual occupation over millennia makes the coastal region of the Atacama Desert populated with mummy bundle burials. Allison (1984) reports child mortality in Peru and Chile was very high between 2000 BCE through the early Colonial Period (c. 16$^{th}$ Century CE). During this span of time, nearly 50% of children in most samples died before 15 years of age (Arriaza et al., 1998). An explanation for the high mortality rate for children offered by Allison (1984) is sedentary village life, where crowding and sanitation were more than likely problematic in these regions (Arriaza et al., 1998). In addition, the soils of the Atacama Desert are rich in arsenic (As) and lead (Pb). These heavy metals are commonly found in the analysis of buried Atacama organic materials, such as hair, textile and bodily tissues (Frenais et al., 2015; Salazar et al., 2014; Díaz et al., 2004). As and Pb are toxic with chronic exposure, and potentially resulted in poisoning and a high infantile mortality (Frenais et al., 2015).

Mummy bundles were common funerary practices with cultures local to Peru and Chile, and numerous examples wrapped in textiles and plant cordage are found along the west coast in the Andean region. Many of the deceased are assembled in a flexed position, also often referred to as the fetal position (Figure 3-1). In a tightly flexed position, the elbows are drawn into the torso with the hands placed close to the thorax, and knees are pulled up close to the abdomen with the feet near the pelvis. A semi-flexed position is a less constricted variation of tightly flexed. The elbows have less of a bend, causing the hands to extend outward. A semi-flexed position also has knees that are bent closer to a 90° angle and the feet are positioned slightly further from the pelvis (Byers, 2002). Once positioned, the human remains are wrapped in woven textiles. In many cases, small items, including ceramic vessels, tools, fishing equipment (i.e., nets, fish hooks, etc.), food and other miscellaneous objects associated with the deceased were placed inside the bundle to represent the life and prominence of the individual.

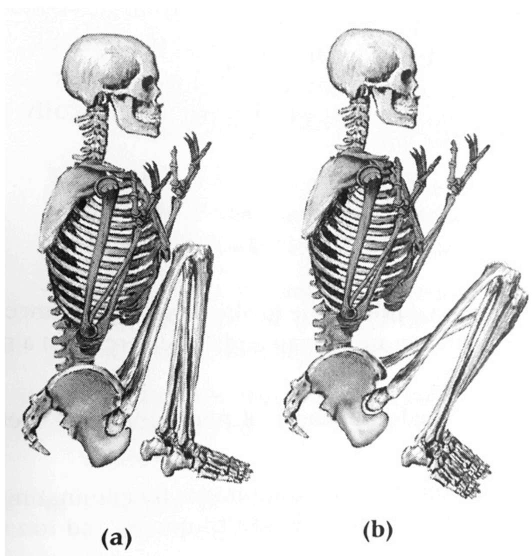


Figure 3-1: Flexed burial position common with pre-Hispanic burials in the Andean region. (a) Tightly flexed. (b) Semi-flexed. Image courtesy of Byers (2002).

Once prepped and wrapped in textiles, the deceased individual was interred in the desert soils. Northern Chile experiences extreme desert conditions with an average of an inch of rain per century, making the Atacama Desert one of the driest places on earth (Meighan, 1980:1). The dry, arid climate and soil content creates a unique desiccating environment that removes moisture from buried organic materials and aids the process of natural mummification (also referred to as spontaneous mummification). The porous soil and sand of the desert promotes desiccation through wicking away water from the body tissues, and accelerates the removal of enzymeladen body fluid from the skin surfaces, which otherwise would liquefy and decay the body (Aufderheide, 2003: 41-44). Burial in these soils promotes preservation of the mummy bundles, and it is immediately following excavation where applied preservation efforts and climate control initiatives are critical for their continued survival.

# 4 Construction and utility of pre-Hispanic Andean textiles

## 4.1 Technology and materials

Andean textiles, such as mummy bundle wrappings from burials in northern Chile, are among the oldest surviving examples of woven fabrics in South America (Niemeyer and Agüero, 2015; Cardon, 2007; Minkes, 2005; Cassman, 2000a). Camelid fibers of llama (Lama glama), alpaca (Lama pacos), the wild guanaco (Lama guanicoe) and vicuña (Lama vicugna), are the major sources of wool sourced in the Andean regions to produce woven textiles (Minkes, 2005: 36). The production technology of textiles in the Andean region involved an iterative operation sequence, starting with the domestication of the camelids and harvesting their wool. Llamas and alpacas are the more common domesticated breads, and were more than likely brought to the Pacific coasts from the Andean highlands after 2000 BCE, and were abundant along the coasts in Peru and northern Chile after 450 CE (Bonavia, 2008: 99, 378).

Once harvested from the camelid, the wool is spun and often plied with a 2-ply-S twist (with each ply spun in a Z direction) in the coastal and highland regions of northern Chile (Rodman, 2000) (Figure 4-1). The yarns were also dyed with natural plant and animal dyes to produce red, blue and yellow hues, or left in its undyed golden-brown or dark brown color (Cardon, 2007; Wallert and Boytner, 1995). The prepped yarns are woven together on a loom, using the warp and weft plainweave techniques to make clothing, blankets and other woven items. Plainweave textiles are the simplest interlacing of warps and wefts, where each weft unit passes alternately over and under successive warp units, and then reverses the pattern with the next woven row (Figure 4-2) (Emery, 2009: 76). Plainweave can be further distinguished with the presence of more warps than wefts, as observed in a warp-faced plainweave textile. When more wefts are present than the number of warps, the textile is referred to as a weft-faced plainweave.

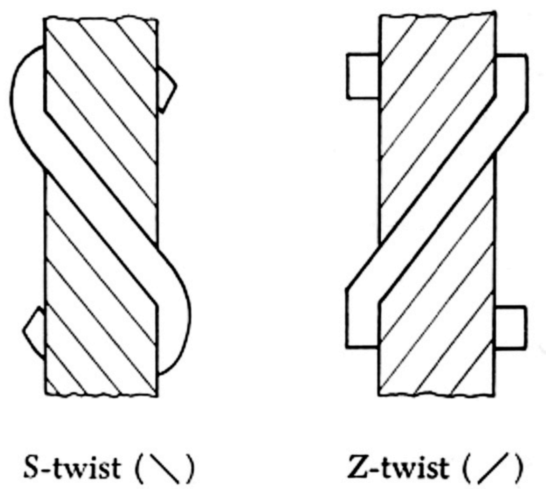


Figure 4-1: Spin direction of plied yarn observd with textiles. (Left) S-twist and (right) Z-twist, based on position of slant of the twisted fibers. Diagram courtesy of Emery (2009: 11).

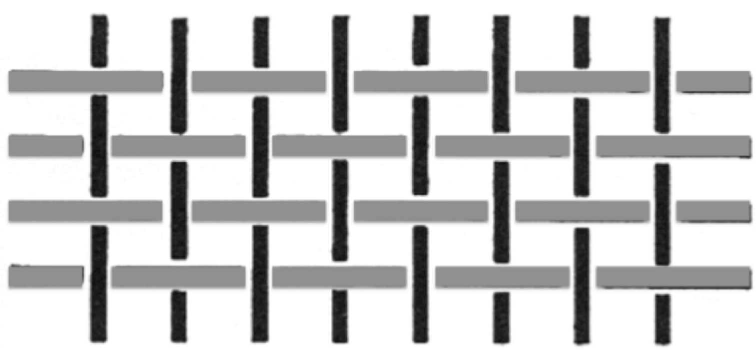

Figure 4-2: Plainweave textile diagram. The black and grey yarns represent the warps and wefts, respectively. Diagram courtesy of Seiler-Baldinger (1994: 87).

Sources of red and blue dyes in Andean textiles are limited. The major red dyes include plant-derived sources belonging to the plant family Rubiaceae. Several species of *Relbunium* (purpurin and pseudopurpurin containing) and *Galium* (alizarin containing) of the Rubiaceae family were used as red dyes with Andean populations (Figure 4-3). According to Niemeyer and Agüero (2015), while there are over 20 species of *Relbunium* in South America, *Galium* and *Relbunium* were more than likely imported into northern Chile from northwestern Argentina, a main location for trade during the Late Formative (c. 100 – 400 CE) and early Middle (400 – 1000 CE) periods. While there are over 20 species of *Relbunium* in the Americas, *Relbunium sp*., *Relbunium ciliatum* and *Relbunium hypocarpium* are some of the most prominent dye sources used extensively with pre-Hispanic cultures (Cardon, 2007; Rodman, 2000; Wallert and Boytner, 1995). Relbunium can be traced to South American textiles from 200 BCE to 1476 CE, making it one of the oldest and extensive sources of vegetable red dyes (Melo and Claro, 2010, Roquero, 2008, Cardon, 2007:162).

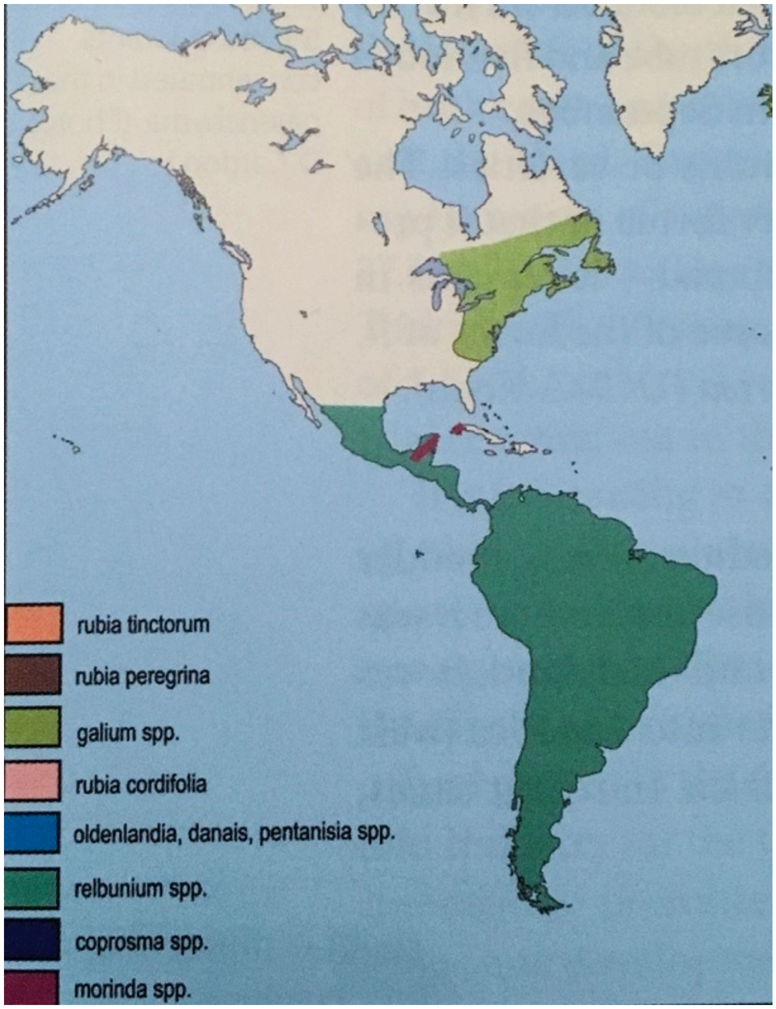

Figure 4-3: Map of *Relbunium* distribution in Central and South America (*Relbunium spp*. indicated in dark green). Map courtesy of Cardon (2007: 107).

The main animal source for red dyes in Andean pre-Hispanic textile production is harvested from female cochineal beetles, *Dactylopius coccus* (Hemiptera: Coccoidea: Dactylopiidae)) (Cardon, 2007: 620 - 624). Cochineal is found naturally in the Andes and parts of Central America, and contains the anthraquinone colorant, carminic acid (Figure 4-4). Sources report that pre-Incan civilizations dating from 500-1100 CE often used cochineal alone or mixed with plant dyes (Relbunium and *Galium*) to obtain red dyes, but is found more prominently in textiles that date closer to the emergence of the Inca Empire, from 1000 to 1476 CE (Melo and Claro, 2010, Cardon, 2007:164). The cochineal insect lives and feeds primarily on the Opuntia cactus, and was more than likely introduced to northern Chile from Peru during the southern expansion of the Huari culture from the Ayacucho area between 600 and 900 CE (Niemeyer and Agüero, 2015; Phipps, 2013: 14; Cardon, 2007).


Figure 4-4: Map of cochineal distribution (indicared in pink) in Central and South America. Map courtesy of Phipps (2010: 13).

Rubiaceae and cochineal are composed of different anthraquinone compounds. Anthraquinone-based components of the dyes include alizarin (1,2-Dihydroxyanthraquinone), psuedopurpurin (2-Anthracenecarboxylic acid), purpurin (1,2,4-Trihydroxyanthraquinone) and carminic acid (Figure 4-5). *Relbunium*, however, lacks alizarin and carminic acid, and cochineal contains carminic acid. The listed anthraquinones have the same molecular backbone of two aromatic six-carbon rings with a quinone group (an aromatic six-carbon ring with a carbonyl group at the 1 and 4 carbons) sandwiched between the rings. The differences in the molecular structure that distinguish the compounds are the number of hydroxyl groups present and the inclusion of a carboxylic acid group. Anthraquinone dyes on their own have a small affinity to bond with the fiber substrate, and are referred to as mordant dyes, *Relbunium*, *Galium* and cochineal require the use of a mordant fixative, such as polyvalent metal cations (i.e., aluminum) and tannic acid, during the dying process to form an insoluble complex with the dye to bind the dyestuff to the fiber (Bernardo, de Faria and Negrón, 2015; Rodman, 2000). Most commonly alum ($Al_2(SO4) \cdot K_2SO_4 \cdot 24H_2O$), iron sulfate ($FeSO_4 \cdot 7H_2O$) and tin chloride ($SnCl_2$) were used (Whitney, Van Duyne and Casadio, 2006).

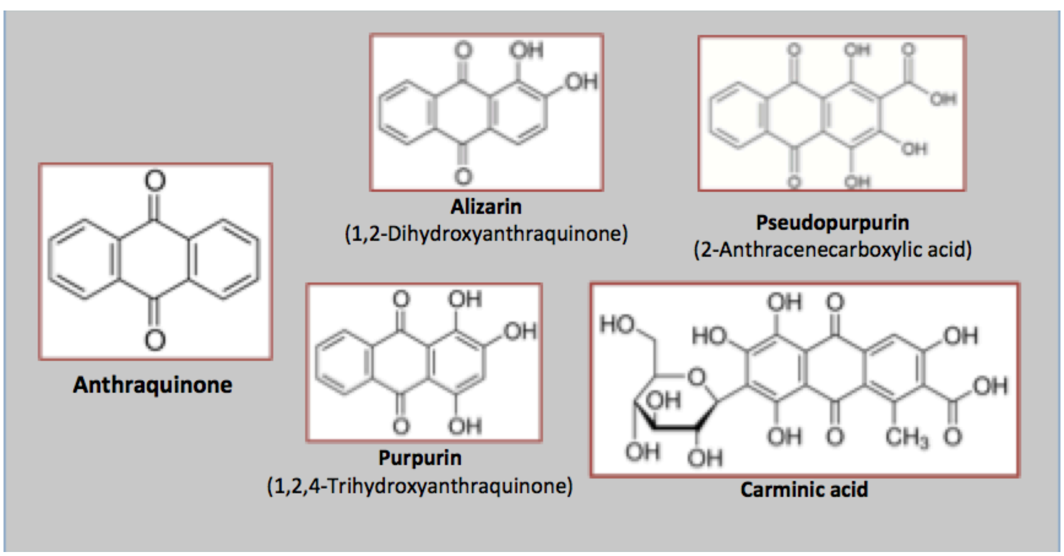


Figure 4-5: Structures of the anthraquinones in typical red dyes of South America. Courtesy of Sigma Aldrich (2017).

The predominant blue dye in South American textiles is indigo extracted from the leaves of the tinctorial plants of the genus *Indigofera* (Fabaceae), *Eupatorium* (Asteraceae) and *Yangua* (Bignoniaceae). *Indigofera* plants, grow naturally along the Peruvian and Chilean Pacific coastline (Figure 4-6) (Cardon, 2007: 337). For pre-Hispanic people in the Atacama Desert region, indigo would likely have been acquired through local harvesting as well as trade with surrounding groups (Niemeyer and Agüero, 2015). Indigo contains the chromophores indigotin and indirubin, and attaches to the wool fibers through an oxidation-reduction reaction (Melo and Claro, 2010). Indigo is water-soluble and considered a lightfast vat dye, where the use of mordants is unnecessary, as the dye is covalently bound to the fibers through van der Waals forces (Bernardo, de Faria and Negrón, 2015). The dye is reduced, or "vatted" in an alkaline solution (usually with sodium dithionite) (Schweppe, 1986). The yarn is soaked in the resulting yellow vat solution and upon removal and exposure to air, re-oxidation of the indigo occurs on the fiber to produce the deep, dark blue color characteristic of indigo. This vat-dying process can produce shades that range from a deep, almost black-blue, to an even lighter, blue-green hue.

Similar to *Relbunium* , *Indigofera* is one of the oldest organic dyes used in South America, with the earliest use by the Ocucaje and Paracas Necrópolis in central coastal valley of Peru, dating as early as 2500-2250 BCE (Splitstoser et al., 2016). Indigo has been used in South American textiles to produce shades of blue and blue-greens, as well as in combination with *Relbunium* or cochineal in mauve and violet fibers from the Andes region.

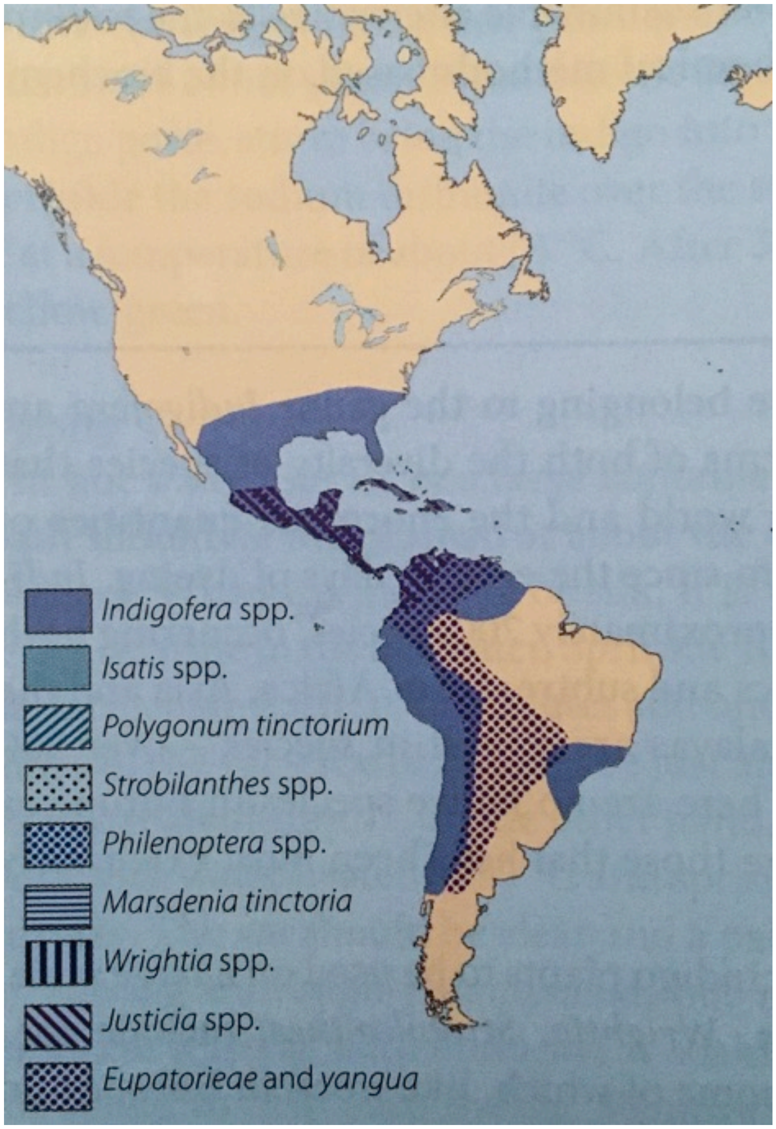


Figure 4-6: Map of indigo species distribution in North, Central and South America (*Indigofera* represented in solid dark blue locations). Map courtesy of Cardon (2007: 354).

Yellow dyes are normally carotenoids and flavonoids, commonly found in different plants (Niemeyer and Agüero, 2015). Yellow dyes are extracted from many South American plants, and their widespread occurrence makes their classification and identification in dyed fibers difficult. Brown dyes were also used extensively and are derived from several tannin species, which also makes their identification in historic textiles a challenge. Peruvian textiles researched by Antúnez de Mayolo (1989) include brown dyes that originate from tannins of the inner bark of the Alnus, jorullensis and Byrsonima chrysophylla plant species. In addition, Wouters and Rosario-Chirinos (1992) used HPLC analysis to identify *Polylepsis incana* in what is described as a brown, pre-Hispanic Peruvian textile sample. In comparison, only a few sources from the Andean region are known to make red and blue dyes, and published information on their identification is more readily available.

### 4.2 Funerary significance

Textiles have been used throughout the Andean region as clothing, methods of storage of goods and to wrap the dead for burial. Cassman (2000b) states that Andean people invested more time and labor into the production of textiles, including woven shirts, belts, tunics and blankets, more than any other grave good. Therefore, textiles, especially in mummy bundle assemblages, are key components to study the provenance technology of a culture. It was very common for the deceased to be wrapped in textiles that may have been worn during their lifetime, and could potentially serve as a significant source of information on the status, provenance and cultural attribution of the mummy (Cassman, 2000b). Extrapolating the status of a child from its textiles can be more of challenge, as child tunics found in burial are rare. Deaths of children were often unexpected events, and funerary textiles were needed for the burial. Pre-Hispanic children in the Andean region were often buried in used or repaired adult garments, more than likely donated by family members (Baitzel, and Goldstein, 2014).

# 5 Materials and Methods

## 5.1 Fiber Materials

### *5.1.1 Mummy textile fibers*

Small pieces of yarn and plant fiber cordage (~ 2 to 5 mm) were sampled from the mummy bundle, with preference to collect from detached yarns. Yarn samples were acquired from locations of red, blue and the light blue-green bands, as well as what appear to be undyed (light and dark browns) sections of each textile.

### *5.1.2 Wool reference standards*

Dyed wool standards from the Saltzman reference collection of South American dyes at UCLA were used to compare the red fibers of the mummy bundle. Plant and animal-based dye sources were collected from Peru and were used to dye llama and cotton fibers. Plant based dyed fibers from the collection and imperative to this study include *Relbunium hypocarpium* dyed wool mordanted with alum (Relbunium #16), and wool dyed with a mixture of *Relbunium ciliatum* and *Galium antuneziae* and also mordanted with alum (*Relbunium* #21). The animal-based dyed fiber, cochineal (carminic acid) dyed wool mordanted with alum (cochineal #18), was also used for analysis to offer a comparative study.

A reference standard of indigo dyed wool was prepared with baby llama wool fiber (100% baby llama wool from Bolivia (Cascade Yarns®)). A vat of synthetic indigo from the Indigo Tie-Dye Kit (Jacquard, Rupert Gibbon & Spider, INC) was prepared with mixing 1.0 g of pre-reduced synthetic indigo, 2.5 g of sodium hydrosulfite (reducing agent) and 5 g soda ash in 757.0 mL of warm water until the indigo bloom formed on the water surface. The llama wool was immersed in water then immersed in the dye vat for ~ 20 minutes, until the fibers turned a saturated yellow-green. The wool was removed and allowed to air dry. The deep, dark blue color characteristic of indigo developed within ~ 20 minutes of drying. The All ingredients in the Jacquard dye kit were manufactured by Dharma Trading Co.

### 5.2 Computed Tomography (CT) Data Collection

The mummy bundle was CT scanned on a Siemens SOMATOM Definition AS (Siemens Healthcare, Forchheim, Germany) using a 64-slice acquisition protocol and a resolution of 0.6mm, where a two-dimensional X-ray image is collected every 0.6 mm horizontally and vertically through the bundle. The bundle was scanned while on a mount made from Ethafoam® and board, and fixed at the isocenter of the Field of View (FOV) with its long axis parallel to the CT gantry along the x-y plane of the detector. Tube voltage was set at 120 kVp with a tube current of 300 mAs. The spiral scanner acquired images at a pitch factor of 0.6 and a rotation time of 0.5 seconds.

### 5.3 Two-Dimensional (2D) Imaging

All images were reconstructed using a filtered back projection (FBP) algorithm with Syngo CT (v2012B, Siemens Healthcare, Erlangen, Germany). Images were reconstructed at 0.6 mm slice thickness with a 0.6 mm increment and a smooth body kernel (B30f). All reconstructions were performed with a FOV of 356 mm and a matrix size of 512x512 pixels.

### 5.4 Three-Dimensional (3D) Imaging

3D renderings were produced from the DCM files of the CT scan using DICOM (Digital Imaging and Communications in Medicine) Imaging Software. The interior contents of the mummy bundle were rendered three-dimensionally with OsiriX MD (Copyright © 2016 Pixmeo) medical image software. Details of the skull were rendered with Horos v2.4.0 (© 2018 Horos Project) using the 3D Volumetric Rendering tool.

## 5.5 Three-Dimensional (3D) Printing

Funerary objects detected with Computed Tomography were 3D printed with a Series 1 Pro printer (Type A Machines, Oakland, CA). The printed objects were rendered from DCM files using OsiriX MD medical image software. The objects were printed to scale and replicated in a Poly-lactic acid (PLA) resin.

## 5.6 Endoscopic Analysis

An Eggsnow HD 720P (Copyright © Topbestsource) USB endoscope with a 5.5mm (diameter) snake camera was used to view the interior of the mummy bundle. The flexible, handheld snake camera comes with six adjustable LEDs and a 1.45 meter long flexible cable. The endoscope camera was inserted into the bundle through existing holes in the textiles and images were captured with a resolution of 720 x 1080 pixels (VGA) using the ViewPlayCap (QCAM) image software for Windows Vista.

## 5.7 Polarized Light Microscopy (PLM)

An Olympus BX51 polarized light microscope was used for fiber identification of the exterior textiles with polarized light microscopy (PLM). A Nikon D90 SLR camera was mounted to the microscope to capture digital images in plane-polarized (PL) light and with the polars of the microscope crossed (under crossed-polarized light: XPL). All analysis was performed with the 50X objective.

#### *5.7.1 Polarized Light Microscopy Sample Preparation*

A single fiber was tweezed out from each sample and longitudinally mounted to separate glass slides with Melt Mount 1.66. A small sample of plant fiber was collected from a detached piece of cordage and longitudinally mounted on a glass slide with deionized water. All mounted samples were covered with a glass cover slip.

### 5.8 Analytical imaging: reflectance and photoluminescence photography (350 - 1000nm)

A Mini-Crimescope® MCS-400 alternate light source (ALS), by SPEX Forensics and a modified (with the hot mirror removed) UV-IR Nikon D90 DSLR with a 60 mm lens were used for non-invasive detection of organic dyes in the red fibers of the polychrome banded textile. The MCS-400 ALS is equipped with a 400 W metal halide lamp, and a fiber optic with two filter wheels enabling the tenability of the light source. The red fibers showed diagnostic features when imaged using UV-induced ($\lambda_{ex}$ max = 300-400 nm) visible luminescence ($\lambda_{em}$ = 400-700nm) and visible-induced (($\lambda_{ex}$ max = 535nm) visible luminescence ($\lambda_{em}$ = 580-700nm). To capture luminescence measurements in the range of 580 nm and 700 nm, a bandpass Peca 916 filter and a Red 25 Tiffen® filter were both placed on the lens of the modified DSLR.

### 5.9 X-ray fluorescence (XRF) spectroscopy

A Thermo Scientific Niton® XL3t GOLDD handheld X-ray fluorescence (XRF) spectrometer equipped with a silver anode and a silicon drift detector was used to non-invasively evaluate the elemental compositions of the textile surfaces and exposed ceramic on the PL side of the bundle. Qualitative information was obtained for various elements with the instrument parameters set to "Soil" and "Mining" modes with acquisition times of sixty and ninety seconds respectively.

## 5.10 Fiber optic reflectance spectroscopy (FORS) in the ultraviolet (UV), visible (Vis), near (NIR) and shortwave infrared (SWIR)

UV-SWIR FORS analysis was performed on all textiles wrapping the mummy and the wool standards, using a FieldSpec3 spectrometer from Analytical Spectral Devices Inc. (ASD) equipped with a contact probe. Data were collected in reflectance mode in a spectral range between 350 and 2500 nm and with a spectral resolution of 3 nm @ 700 nm and 10 nm @ 1400/2100 nm.

## 5.11 Raman spectromicroscopy (μRS)

A Renishaw inVia Raman spectrometer, with a 785 nm laser and Leica confocal microscope interface with 50x objective was used to collect μRS data on the blue fiber samples from the mummy bundle textiles and indigo wool standard. Instrumentation parameters for each sample included 0.1% laser power, 5 accumulations at 10 seconds each, as well as 3 acquisitions and 5 second bleaching to reduce fluorescence from the wool fibers. The sample preparation included securing a single fiber from the blue and light blue-green yarn samples to separate glass slides with a small piece of copper tape on each end.

## 5.12 Hydrofluoric acid (HF) micro-extraction and surface enhanced Raman spectroscopy (SERS)

### *5.12.1 Synthesis of silver nanoparticles (AgNPs)*

Silver nanoparticles (AgNPs) were synthesized using the Lee and Meisel method (1982). 18 mg of anhydrate silver nitrate powder (Sigma Aldrich product 20139 ACS reagent 99+%) and 100 ml of deionized water were combined with 22.4 mg of sodium citrate dehydrate (Fisher Science Education S25545 Lab Grade) in a 1% solution and brought to a boil for an hour. The beaker was placed in an ice water bath to crystallize the nanoparticles. 9.0 mL of the AgNPs colloidal solution was centrifuged using a Fisher brand miniature centrifuge for 15 minutes at 6400 rpm to separate the AgNPs from the solution. After centrifuging, the AgNPs are collected and used for the analysis with a micropipette (VWR Signature™ Ergonomic High-Performance Pipettor, 0.5 – 10 μL). The stock solution of AgNPs were placed in sealed glass jars and kept refrigerated.

### *5.12.2 Fiber sample preparation with HF micro-extraction of red dye*

A singe red fiber from the polychrome-banded textile as well as the *Relbunium* wool standards #16 and #21 were used to aid in the red dye identification. An in-situ micro-extraction was individually performed on each fiber according to the method provided by Leona, Stenger and Ferloni (2006) to hydrolyze the dye molecule from the mordant using HF vapors in a sealed microenvironment. The fiber was placed in a cap cut from a 1.0 mL Epindorff® plastic vial and inserted into a size 00 polyethylene microvial (J.T. Baker™) with a 10 μL drop of HF (49% weight percent) at the cone-shaped section of the vial. The cap of the microvial was closed and pierced with sharp tweezers to allow ventilation during the micro-extraction. The sealed vials were placed horizontally on a glass slide and the fibers remained in contact with the HF vapor for 15 minutes. The samples and their cap holders were then transferred into new size 00 microvials for transport.

### *5.12.3 Fiber sample preparation with AgNPs and SERS Analysis*

Shortly following the HF micro-extraction, the fibers were secured on both ends with a small piece of copper tape on separate glass slides. 0.5μl of AgNPs were deposited directly to the fibers followed by 0.5 μL of 0.2M potassium nitrate ($KNO_3$) (Fischer Scientific®). After five minutes, excess solution of AgNPs and $KNO_3$ was wicked away from the sample with a KimWipe (Kimberly-Clark Corp). The prepared samples were allowed to dry for 5 minutes.

Once dry, the fibers were analyzed at UCLA using a Renishaw inVia Raman spectrometer with the 633nm laser and Leica confocal microscope interface with 50x objective. Instrumentation parameters for each sample included 0.1% laser power, 5 accumulations for 10 seconds each, as well as 3 acquisitions and a bleaching time of 5 seconds to quench fluorescence from the fiber. A spectrum of 0.3 μL of AgNPs was collected and compared to each fiber spectra collected during the Raman session. Analysis of the AgNPs was collected with the same instrument parameters as the dyed fibers.

# 6 Results

## 6.1 Visualization of the interior of the mummy bundle

Computed Tomography (CT) reveals an intact skull and an almost complete skeleton seated in a semi-flexed position (Figure 6-1-6.3). The high energy required for the X-rays to penetrate through the many layers of textile wrappings, organic components of similar radiopacity, including hair and skin, could not be visualized. Two hollow vessels exhibiting a small, circular opening are positioned near each shoulder of the body (Figure 6-1 and 6.2). Also observed on the PL side of the human remains and below the globular-shaped vessel is a cluster of loose, granular material (Figure 6-1). Lastly, five small, top-like artifacts are closely situated together near the top and in the center of the bundle towards the PR side, just below the skull (Figure 6-3).

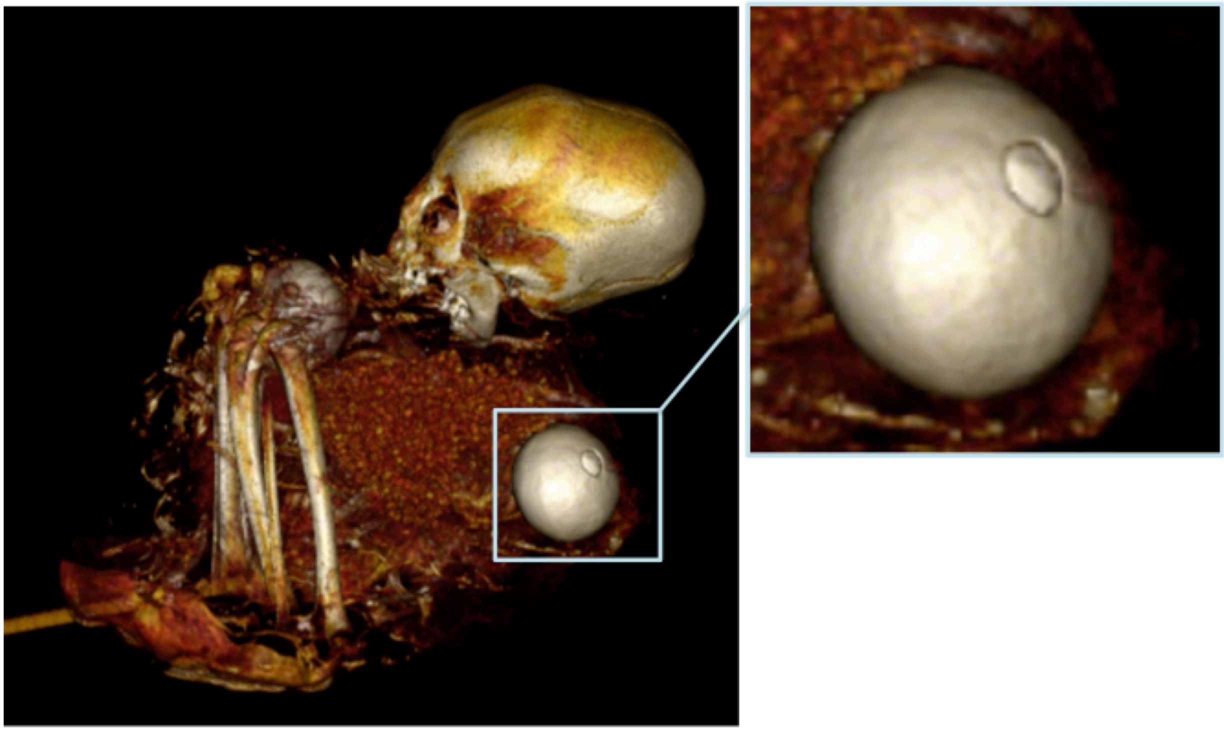

Figure 6-1: (a (left)): Mummy bundle (X66.1953) 3D rendering from CT files, PL side. (b (right)): Detail of globular vessel and pouch holding loose, small granular material on the PL side of the body. Renders courtesy of Jessica Martinez.

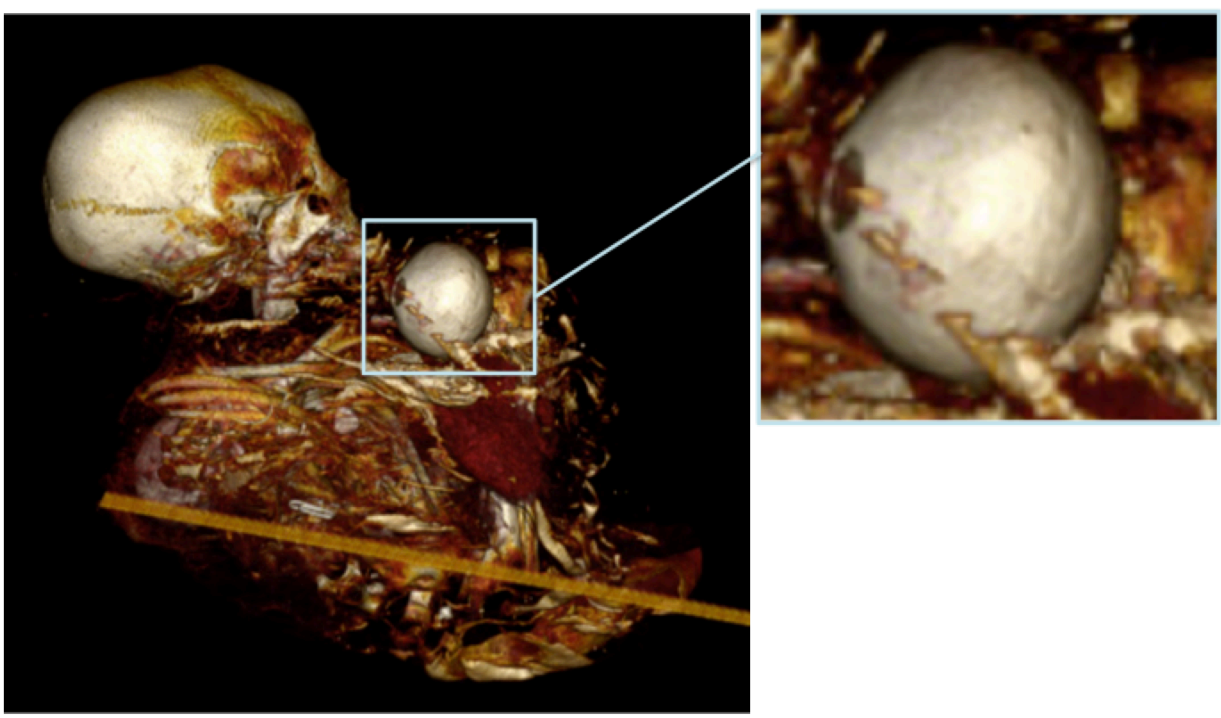

Figure 6-2: (a (left)): Mummy bundle (X66.1953) 3D rendering from CT files, PR side. (b (right)): Detail of globular vessel on the PR side of the body. Renders courtesy of Jessica Martinez.

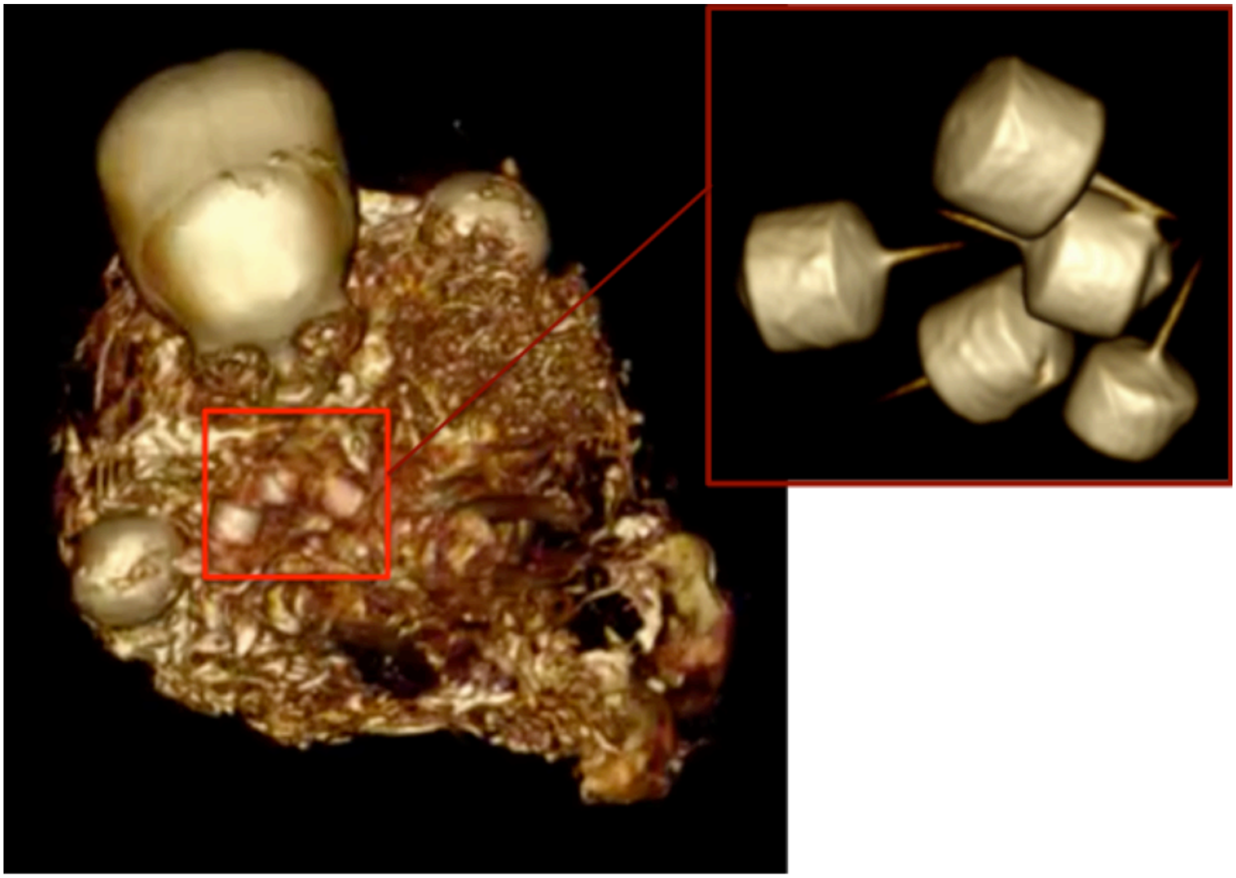

Figure 6-3: (a (left)): Mummy bundle (X66.1953) 3D rendering from CT files, top view. (b (right)): 3D computer renders of the five top-like objects in the center of the mummy, near the top of the bundle. Renders courtesy of Jessica Martinez.

### *6.1.1 Human remains*

The skeleton of the mummy appears mostly complete, with some disarticulation of the bones (Figure 6-4). Seated in a semi-flexed position, with the lower legs oriented vertically and the tibia and fibula facing towards the front of the bundle. The skull also faces anteriorly, with the face positioned towards the front of the bundle. The ribs appear mostly intact and remain in mostly anatomical position near the back of the bundle. Both humeri and the right ulna of the arms are positioned horizontally over the leg bones (Figure 6-5). The left ulna is not observed in the bundle. In slices from the CT scan, Harris lines are observed on both the proximal and distal ends of both femurs and tibiae, near the epiphyses (Figure 6-6(a)). A portion of the articulated left (L) foot is found at the bottom, however the right (R) foot cannot be detected. The vertebral column is not observed in its usual position connecting the skull and pelvis, however, vertebrae are detected near the bottom of the bundle (Figure 6-6(b)). The hands cannot be identified, but many small bones appear to have fallen to the bottom of the bundle. On the skull, the mandible remains articulated, but the mouth has fallen open so the chin rests on the chest. The skull also shows clear evidence of anterior-posterior cranial deformation.

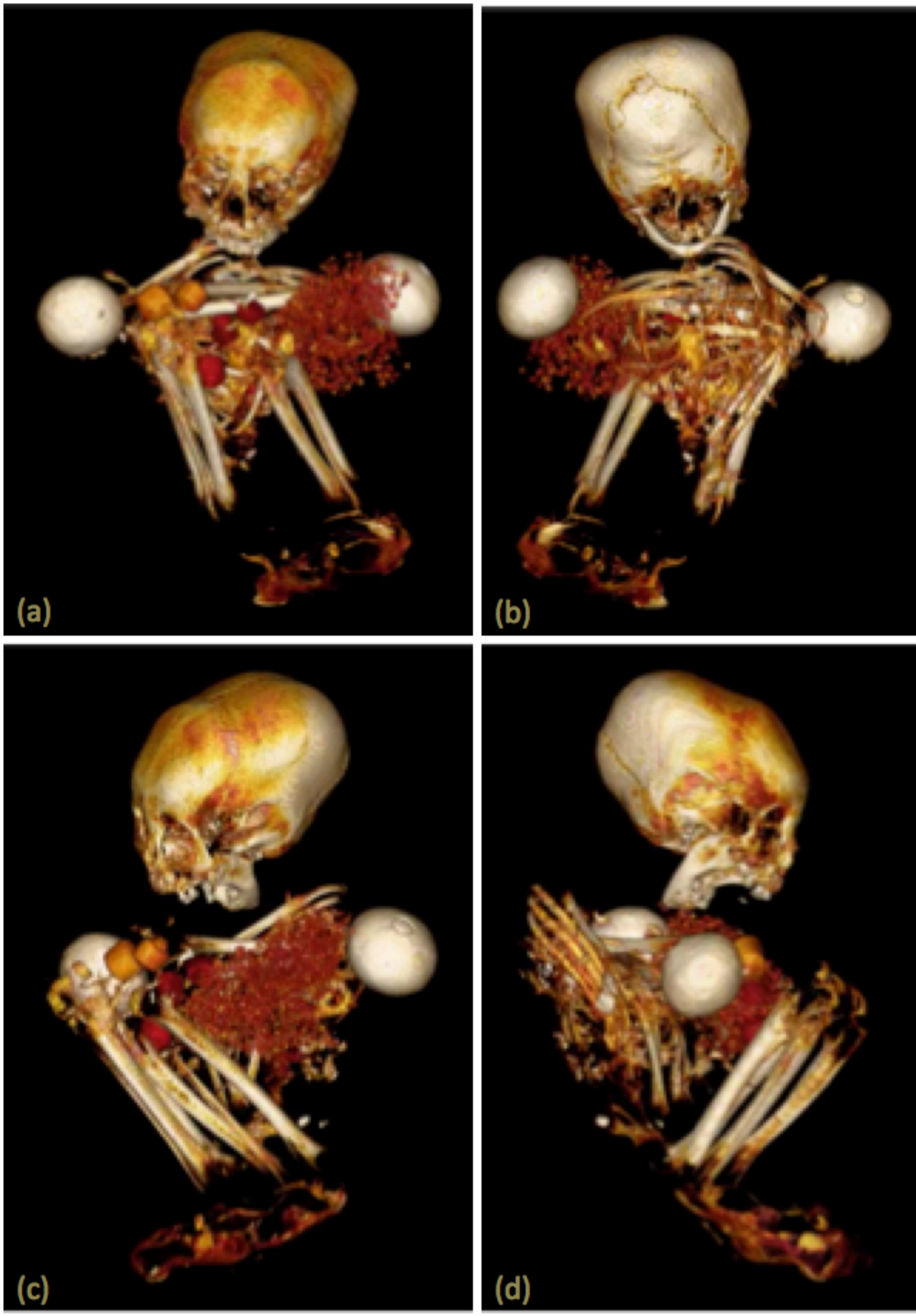

Figure 6-4: 3D computer renderings of the mummy skeleton. (a): Anterior view. (b): Posterior view. (c): PL side view. (d): PR side view. Renders courtesy of Jessica Martinez.

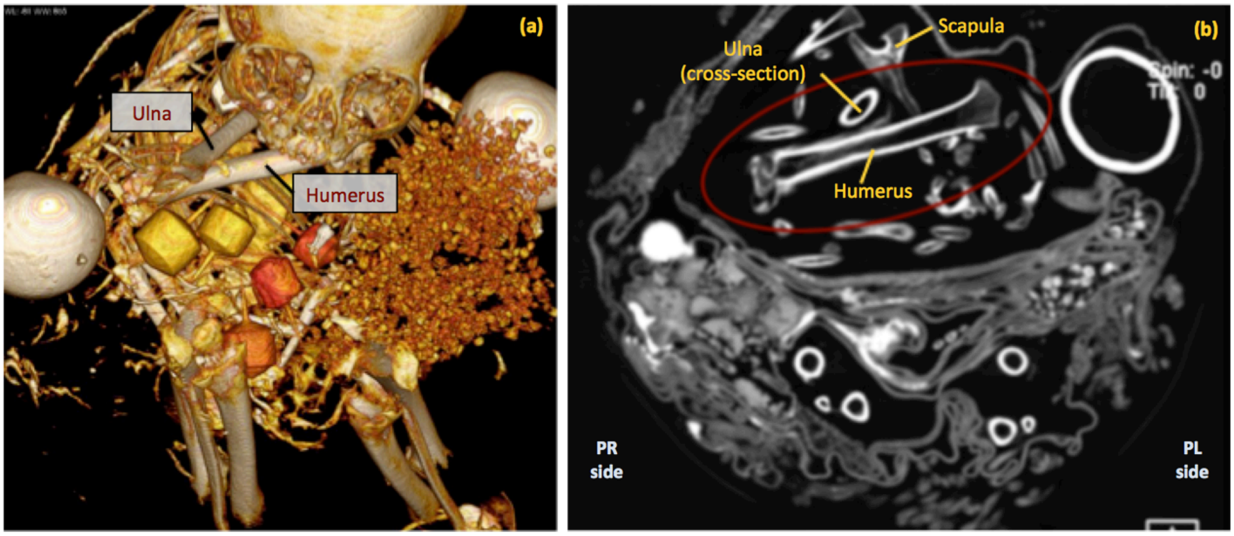


Figure 6-5: (a): 3D rendering of the right ulna over the right humerus. The five top-like objects are distinguished near the arm bones (yellow and red-orange in image). Render courtesy of Jessica Martinez. (b): Two-dimensional horizontal slice showing the longitudinal positioning of the humerus and a cross-sectional view of the ulna.

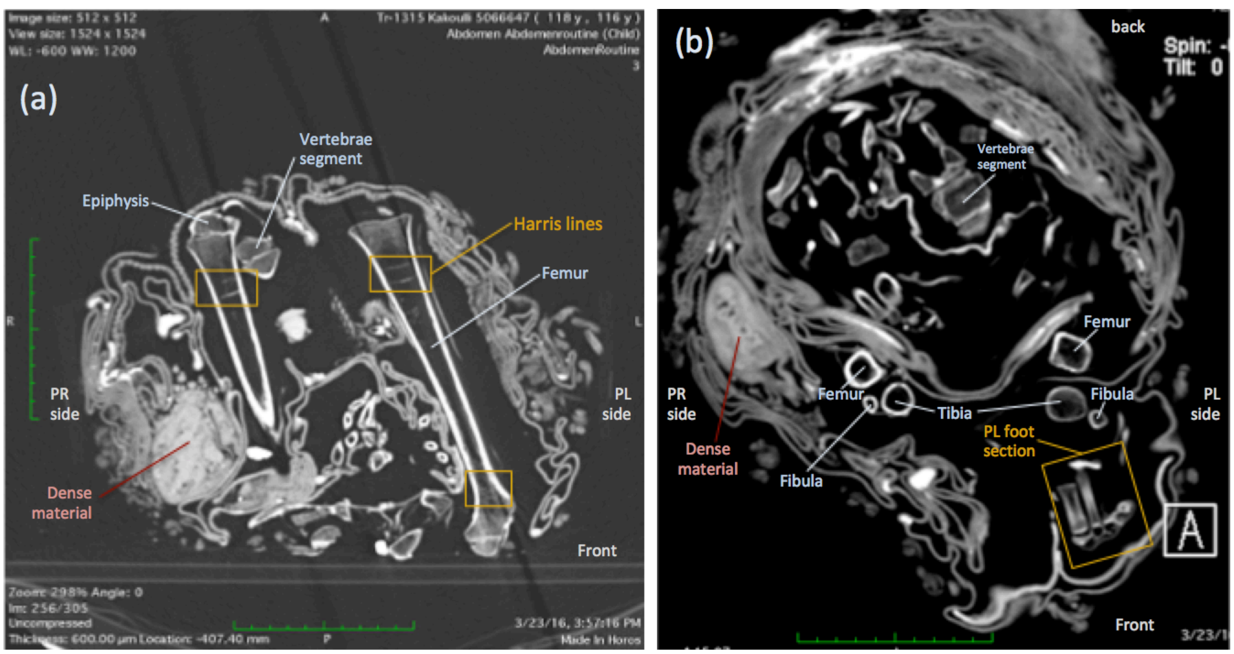


Figure 6-6: (a) Front. sagittal slice of lower limbs, showing Harris lines (stress lines) near both epiphyses on each femur. (b) Top, horizontal slice through bottom of the bundle, revealing articulated toes from the left foot.

Consult the cranium anatomy reference image for cranial bone locations (Figure 6-7).

The maxilla (upper jaw) contains fully erupted second deciduous molars on both sides, and a first deciduous molar on the L side (Figure 6-8). The adult central and lateral incisors, as well as the first permanent molar remain in the crypt of the maxilla and mandible; all in crown complete states and root development has not yet started. Both sets of the first and second deciduous molars have fully erupted through the maxilla and mandible.

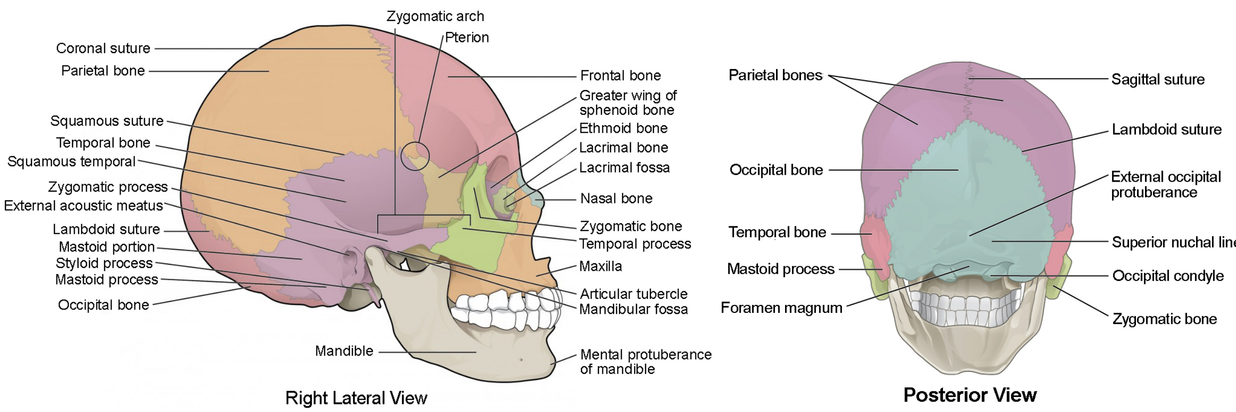


Figure 6-7: Diagram of unmodified skull. (a) Lateral view. Image courtesy of https://tundra.cnx.rice.edu. (b) Posterior view. Image courtesy of https://courses.lumenlearning.com/ap1/chapter/the-skull/.

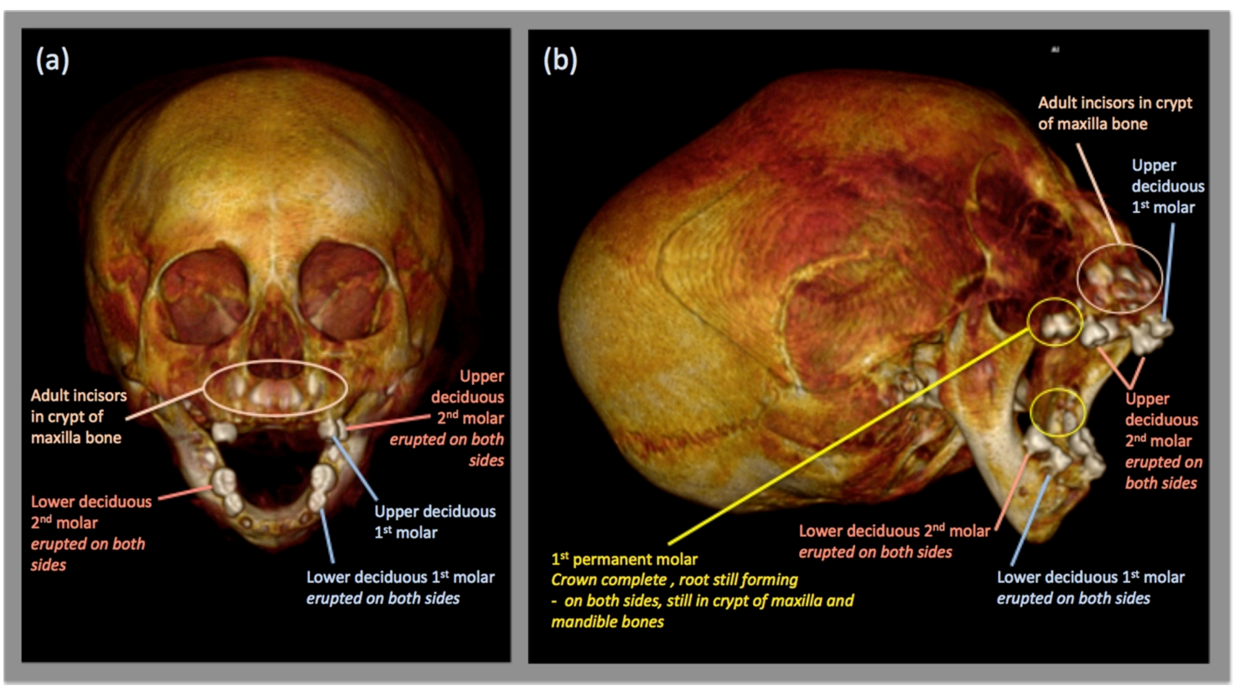


Figure 6-8: 3D rendering of mummy skull. (a) Front. Deciduous molars have erupted and four permanent incisors are crown complete. (b) R side. The first permanent molar is crown complete. Renders courtesy of Jessica Martinez.

The probe of the endoscope could fit through a small hole in the L side of the textile wrapping the head, near the mandible, and captured images of the upper left deciduous molars (Figure 6-9(a)). The majority of the exposed teeth appear yellowed and brown, with white enameled areas on the crowns and between the folds of the roots. Brown stains are also observed on both teeth and the mandible. The yellowed crown of the L first permanent molar is exposed through what appears to be a layer of mummified skin covering the back of the maxilla bone (Figure 6-9(b)).

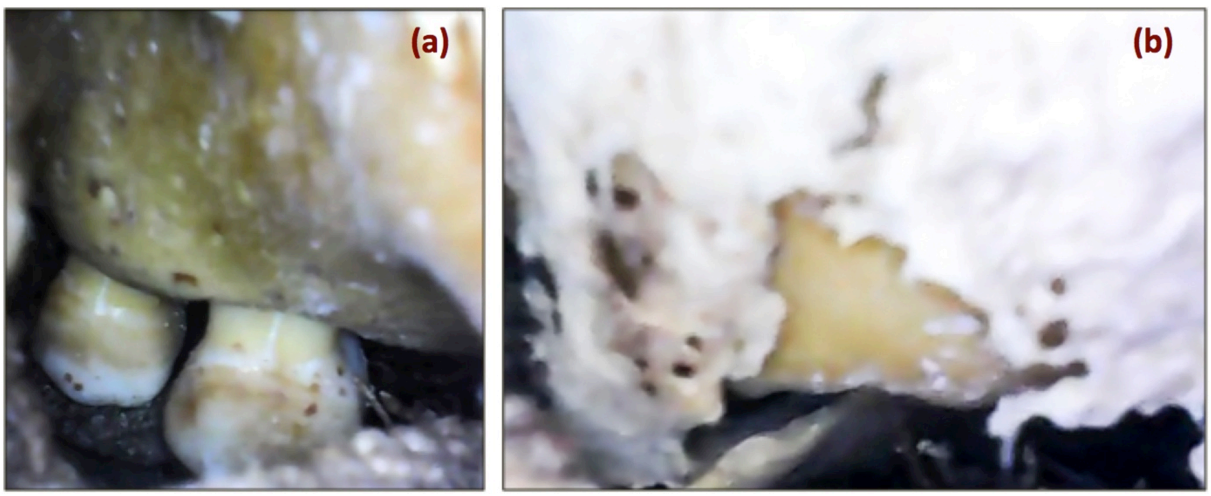


Figure 6-9: Endoscopy of L side of the maxilla, exposing erupted teeth. (a): The first and second deciduous molars. (b): The crown of the first permanent molar covered with mummified skin.

A small tooth was accessioned with the mummy bundle in 1966 (Figure 6-10 (a-c)). The tooth appears intact with a completed shovel-shaped crown with a square mesial aspect that rounds to a slight incline on the distal side, which leads into a yellowed, tapered, and curved single root. The white enamel covers the crown, starting from the cingulum (a bulged and raised area on the lingual surface of the tooth, just below the root neck) down to the bottom edge. Compared to tooth descriptions and diagrams from Bass (2003:279) (Figure 6-10 (c-d)), the separate tooth appears to be an upper deciduous lateral incisor from the L side of the maxilla.

This approximation was made from observation of the pointed corner on the mesial side and the rounded corner located at the distal side. Similar to the deciduous molars observed in the maxilla, a couple of small brown spots are also observed on the detached tooth.

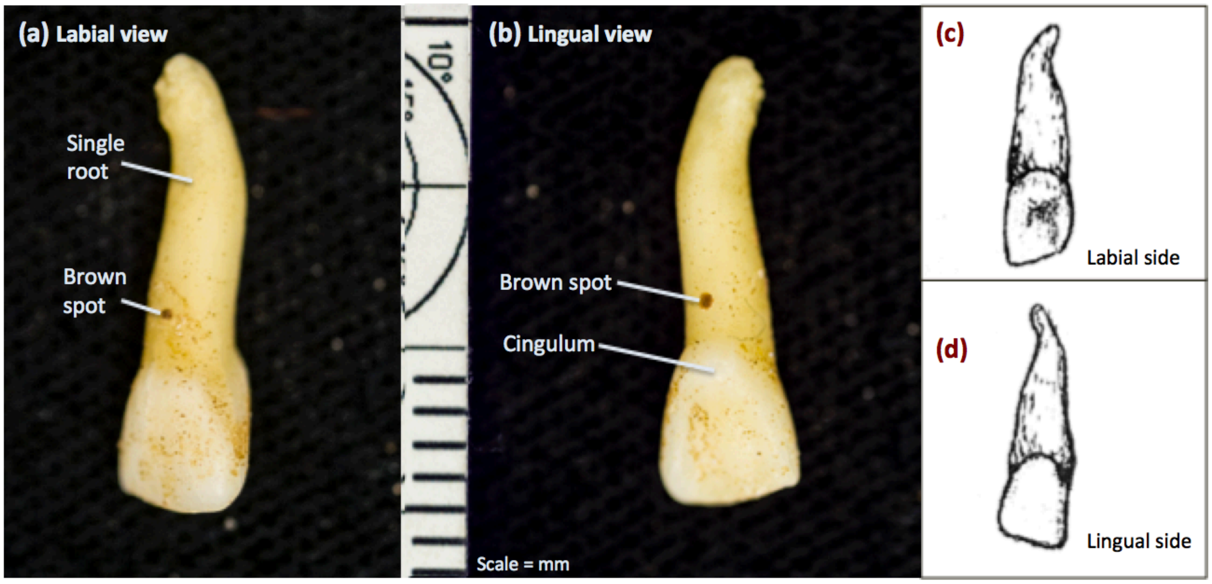


Figure 6-10: Upper deciduous lateral incisor accessioned with the mummy bundle in 1966. (a) Labial (against the lips) side. (b): Lingual (against the tongue) side. (c and d): Illustrations of the labial (c) and lingual (d) sides of a R upper lateral incisor (courtesy of Bass, 2003: 279).

All the cranial bones appear intact and articulated at the coronal, sagittal, lambdoidal and squamosal sutures. A vertical cross-sectional view of the skull shows the frontal and parietal bones have met, the anterior fontanelle has closed, and the bregma has formed with an almost uniform thickness consisting of a defined edge with little thinning of the plates (Figure 6-11). In the same figure, the lambda, where the parietal bones and the occipital bone meet also has a uniform thickness with a defined edge. The shape of the mummy's skull is elongated, with flattened areas located near the forehead and occipital base (Figure 6-12). The frontal bone is angled with an approximate 45° slant that leads to a raised ridge near the coronal suture. The parietal and occipital bones near the base of the skull are also flattened and the back of the skull elongates into a triangular shape. Additionally, two small, circular Wormian bones are observed

(Figure 6-12(d)), with one located on the lambdoid suture and the other at the lambda junction, where the lambdoid and sagittal sutures meet.

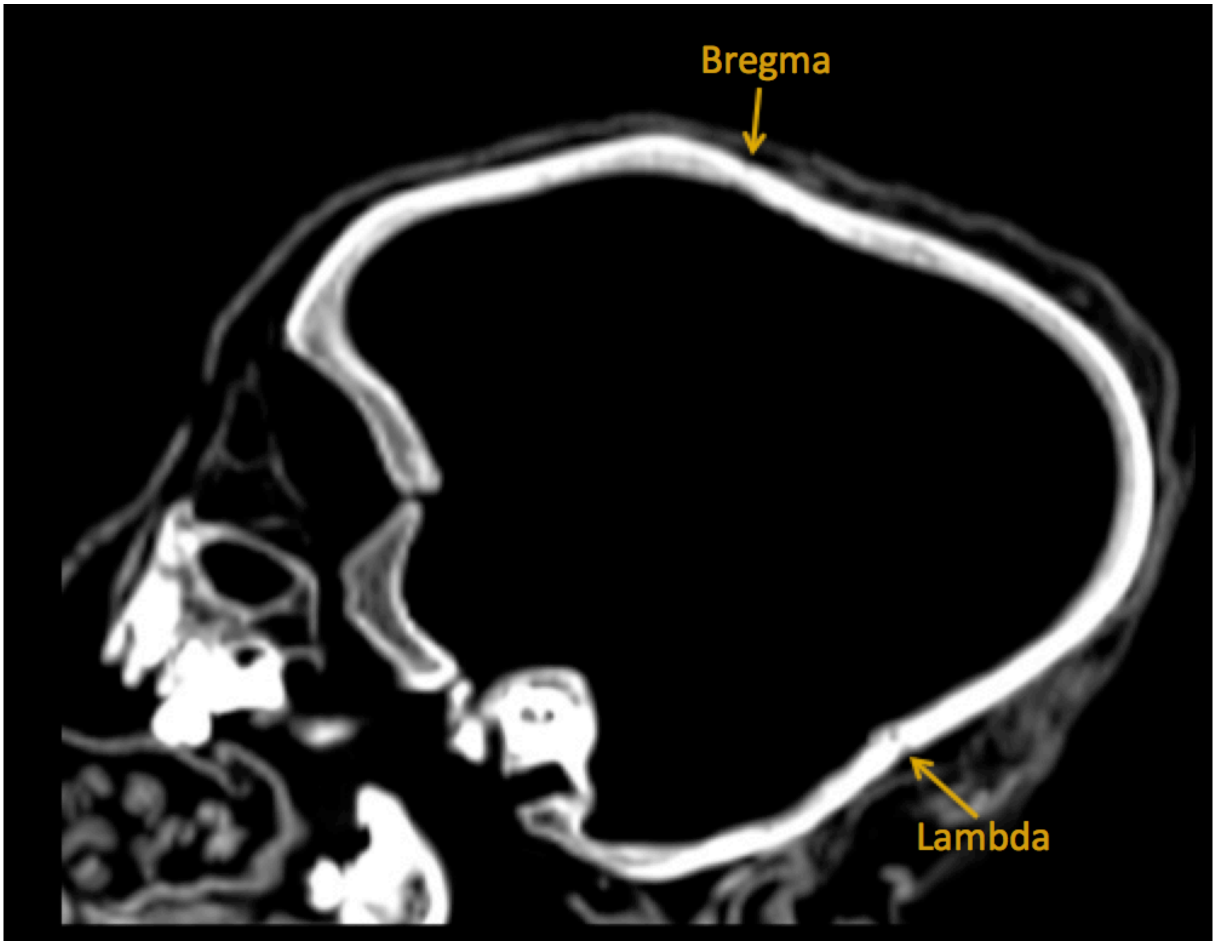

Figure 6-11: Sagittal cross-section of mummy skull showing the bregma and lambda points.

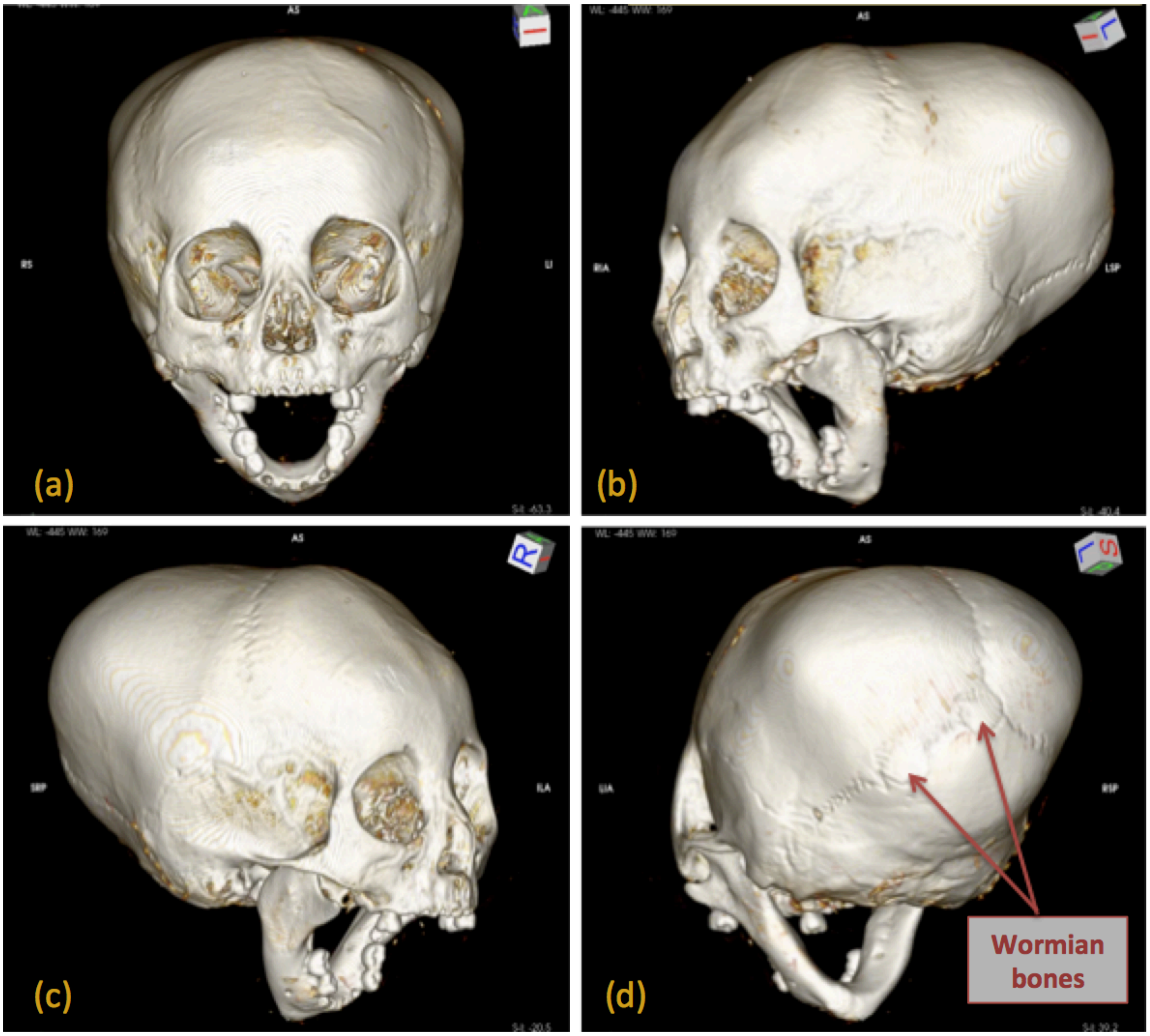

Figure 6-12: 3D rendered series of the mummy skull. (a): Anterior, (b): L side, (c): R side, (d): posterior of skull.

Human hair is noted on the top of the head after careful observation of the interior contents through a small existing hole on the PR side of the textile wrapping the head. Using a wooden skewer to gently hold the split textile open, a small braid (~ 0.5 in. wide) of dark brown-black hair positioned vertically down the cranium was identified, and more than likely confirms the presence of hair on the head of the mummy (Figure 6-13).

Figure 6-13: Detail of a single braid under the textiles on the PR side of the head.

### *6.1.2 Funerary Paraphernalia*

The most obvious objects are two vessels located at the level of the shoulders. Three-dimensional renderings from CT scans reveal the spherical shape of each vessel on the PL and PR sides. Based on the heavy radiopacity, the vessels appear to be made from a dense material (Figure 6-14(a) and 6-14(c)). Cross-sectional slices of the vessels reveal they are hollow inside with a small opening, and exhibit slight irregularly of the wall thickness. A sagittal view of the PL vessel displays a small, tapered fragment near its exterior (Figure 6-14(b)). A sagittal view of the PR vessel reveals a narrow, tapering object inside and extends from its base and through the opening (Figure 6-14(d)). The object also has a similar radiopacity and texture as the object near the PL vessel. The tapered objects associated with the globular shaped vessels are also weaker in radiopacity, possibly suggesting a softer, more organic material. The hollow construction and irregularities in the walls of the vessels are further confirmed when 3D printed and replicated to scale in a plastic resin (Figure 6-14(e)). The 3D printed replicas also provide an accurate and more tangible method for collecting measurements, which reveal how close in shape and size the two vessels are to each other. The PL vessel measures 6.8 cm (d) x 5.6 cm (h), with a circular opening of about 1.7 cm in diameter, and a wall thickness near the opening of about 2.5 to 3 mm. The PR vessel measures 6.2 – 6.7 cm (d) (slightly irregular in spherical shape) x 5.9 cm (h), with a circular opening and thickness similar to the PR vessel.

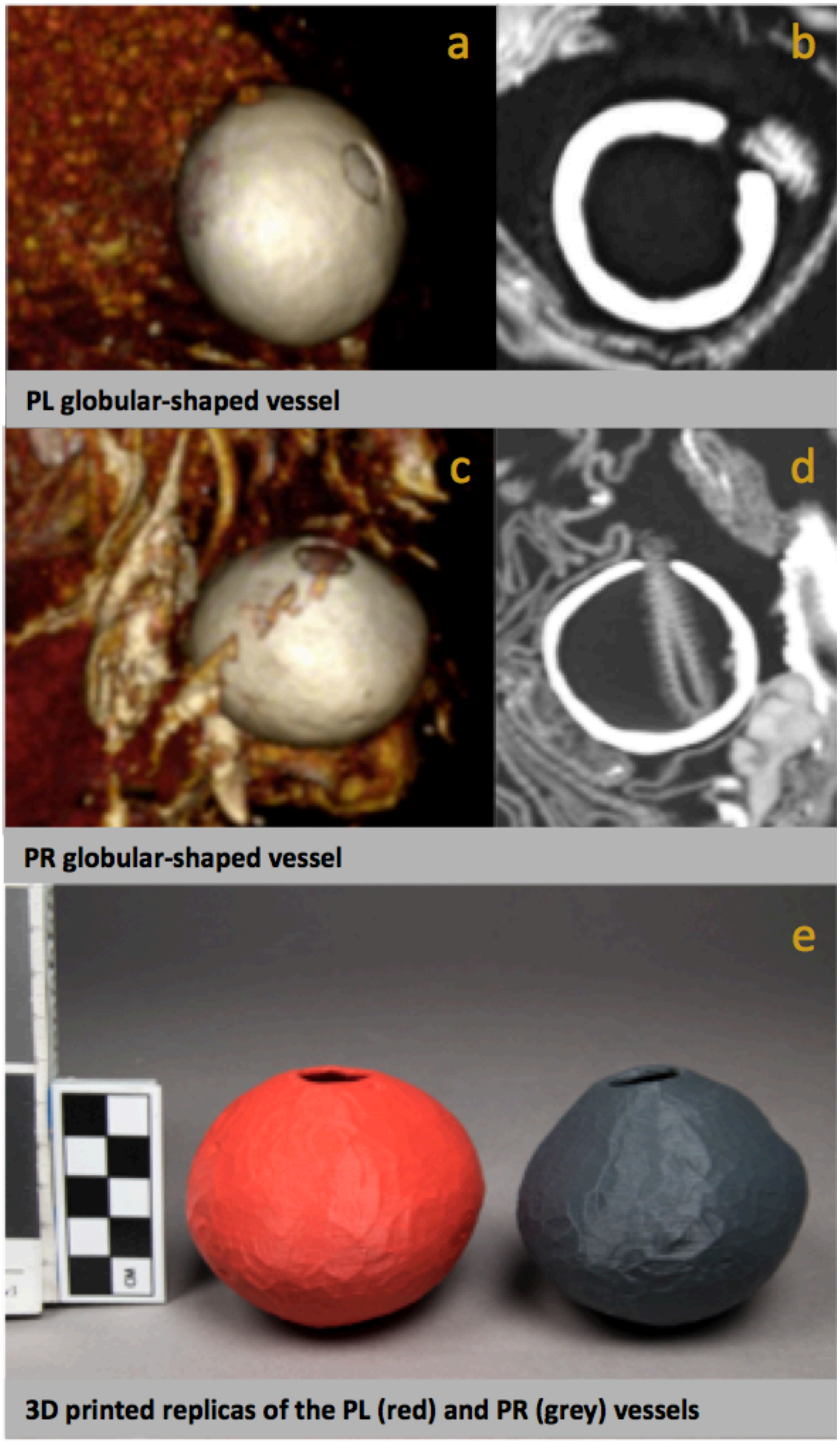

Figure 6-14: (a) 3D rendering of PL globular-shaped vessel with small opening near the top. (b) Cross-sectional view of PL vessel reveals hollow interior and a tapered object near the vessel exterior. (c) 3D rendering of PR vessel showing similar characteristics as (a). (d) Cross-sectional view of PR vessel reveals hollow interior and a tapered object through the small opening. (e) 3D printed vessels. Renders and three-dimensional printing courtesy of Jessica Martinez.

A large split in the thicker, outermost textile on the PL side of the bundle exposes a small portion of the PL globular shaped vessel, including its small circular opening. The vessel appears to have a slightly blacked, pinkish-brown surface color with reflective micaceous, inclusions (Figure 6-15). XRF spectroscopy performed on the exposed area of the vessel detected elevated levels of zirconium (Zr), iron (Fe) and manganese (Mn) compared to analysis of the exterior textiles. These elements appear consistent with an inorganic material. The small, tapered fragment detected with Computed Tomography next to the PL ceramic exterior (Figure 6-14 (b)) is what resembles a small piece of a brown corncob (Figure 6-15 (c)). The same pinkish-brown surface observed on the exterior is also the color of the interior walls of the ceramic, observed with the Endoscope probe placed inside the small circular opening (Figure 6-15 (d)). A small pile of a textured, black-brown residue is found at the bottom of the vessel. This residue was not detected with CT analysis, and is more than likely organic in composition due to its radiopacity. Quite possibly, the pile of residue inside the vessel could be a remnant from the corncob fragment near the exterior side of the vessel.

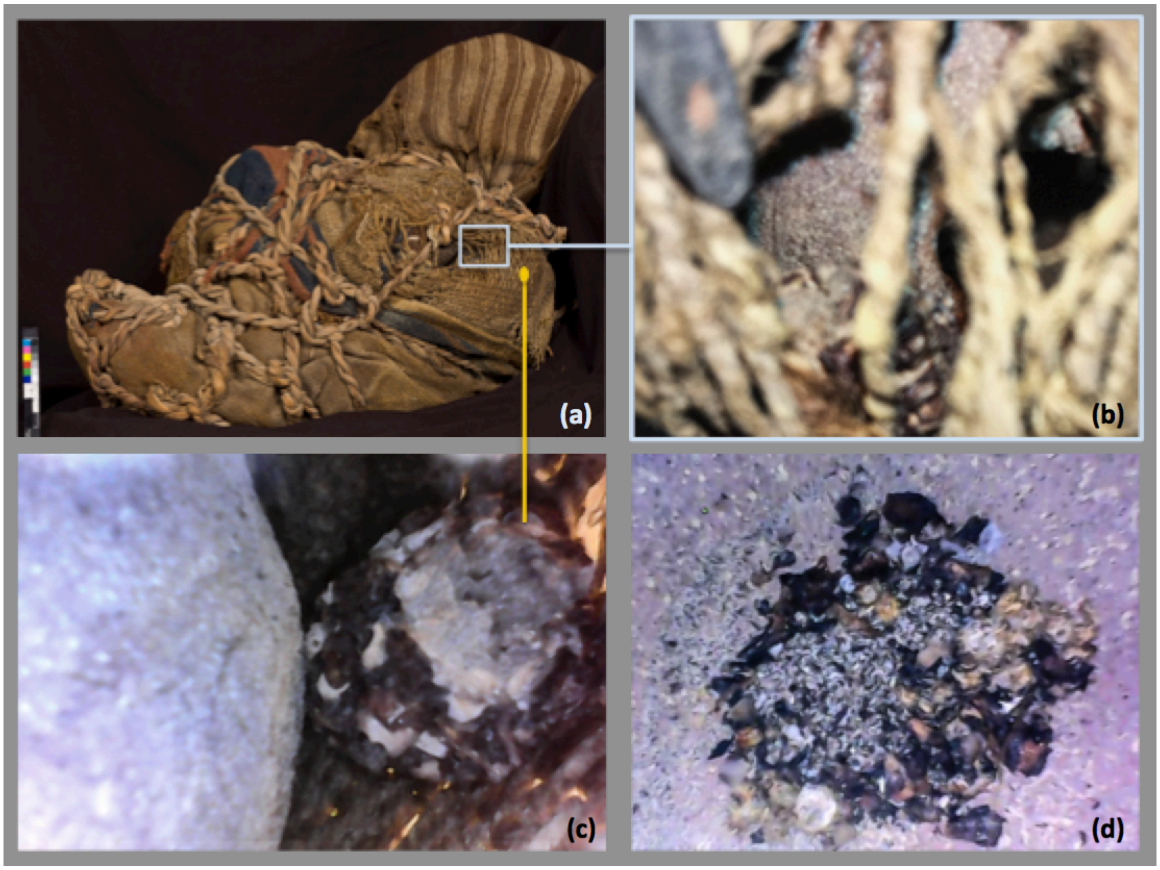

Figure 6-15: (a): PL side of mummy bundle. (b): Detail of the top of the PL globular-shaped vessel, with the circular opening visible. (c): Endoscope image of possible corncob fragment, located next to the PL vessel exterior. (d): Endoscope image of small pile of organic residue at the bottom of PL vessel interior.

The CT analysis also revealed the bundle interior to contain five top-like objects with a bulbous and slightly tapered top and a long-tapered tip at the other end. All five objects are radiopaque, and appear worked, due to irregular notches and flat markings observed in the 3D renders (Figure 6-16 (a)). A horizontal slice shows they are solid throughout (Figure 6-16(b-c)). Their clustered orientation could signal their enclosure in a woven pouch or net, however these organic textile materials are too radiolucent for detection with high energy X-rays.

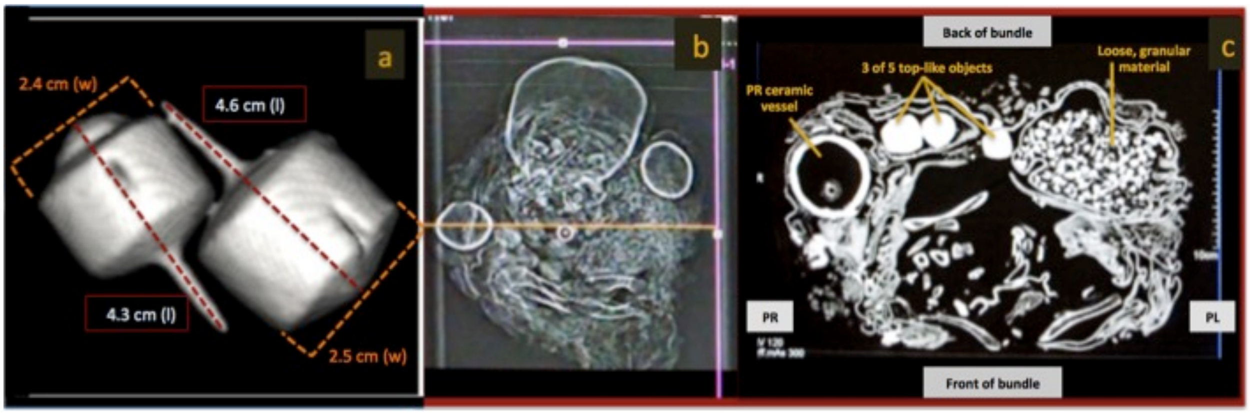

Figure 6-16: (left, (a)): 3D computer rendering of two of the five top-like objects with notches and carving marks. (middle (b)): CT slice location on mummy bundle, defined by the thin yellow horizontal line, showing (c): Horizontal cross-section that reveals three of the five top-like objects (near top of image). Cluster of loose, granular material also visible.

3D printed replications of the five top-like objects to scale better visualize their small size (Figure 6-17). Each rounded body measures between 2.1 – 2.6 cm (l) x 2.0 – 2.6 (w) cm. Only two of the five 3D printed objects were printed with their thin needle-like tips, while they were visible on all five top-like objects in the CT scans and 3D renderings, showing the limits of 3D printing technology. In this case, the 3D renders provided the better method of length measurement, where the top-like objects each measure ~ 4.5 cm in length.

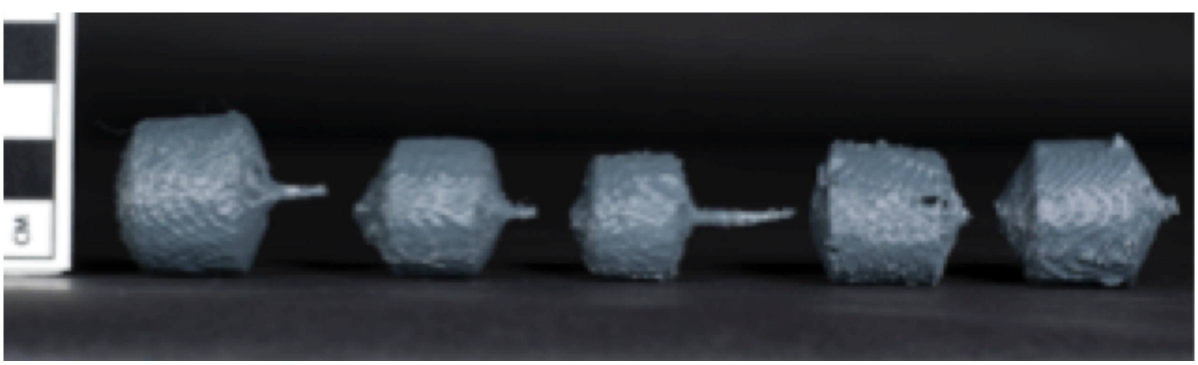
Figure 6-17: 3D printed replicas of the five top-like objects found inside the mummy bundle wrappings.

The five top-like objects located near the top are in close proximity and justified towards the proper right side of the human remains. The top-like objects are also close in size, with rounded, bunt tops and a short, thin tapered point on the other end. Use of the endoscope between the textile folds on the top of the mummy bundle allowed the observation of one of the top-like objects covered in a dark blue net weave material (Figure 6-18). The exposed portion of the top-like object reveals a dark brown surface color. The textile wrappings surrounding the top-like objects were too stiff and secured to proceed further with the endoscope. Therefore, the remaining top-like objects deeper in the bundle could not be observed with this method of optical biopsy.

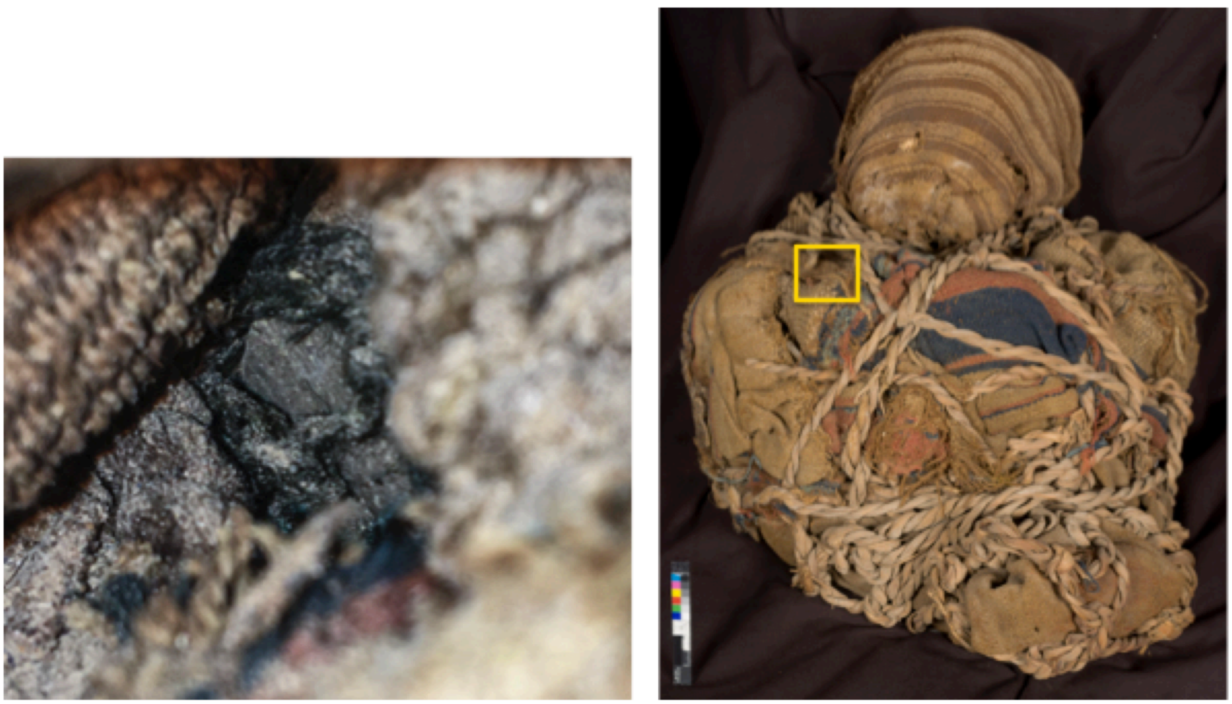

Figure 6-18: (a, left): Detail of top-like object covered with a dark-blue fiber net weave textile (center of image). (b, right): Child mummy bundle, front, with yellow box indicating location of (a).

A bundle of loose, pebble-like material is also observed in the CT scan. With 3D rendering, the small, ovular-shaped material appears tightly packed, and takes the amorphous shape of containment inside a woven pouch (Figure 6-19). These proved to be too difficult to 3D print due to the small size and compact arrangement, and were best observed with three-dimensional imaging.

Figure 6-19: 3D rendering of lose, tightly packed ovular shaped material from the PL side of the mummy bundle.

## 6.2 Characterization of funerary textile wrappings and dyes

### *6.2.1 Child mummy bundle textiles*

At least three distinct textiles were used to wrap the deceased and funerary offerings for the child mummy bundle. All textiles appear to be warp-faced, plainweave textiles with S-plied warp and weft elements. A thin, striped textile with alternating bands of light and dark brown covers the head, and two larger woven textiles wrap around the body and feet. The textile covering the head has a yarn count of eleven warps for every fifty wefts per inch (Figure 6-20). The selvedges are tucked under the other textile wrappings and are bound around the neck with plant-fiber cordage.

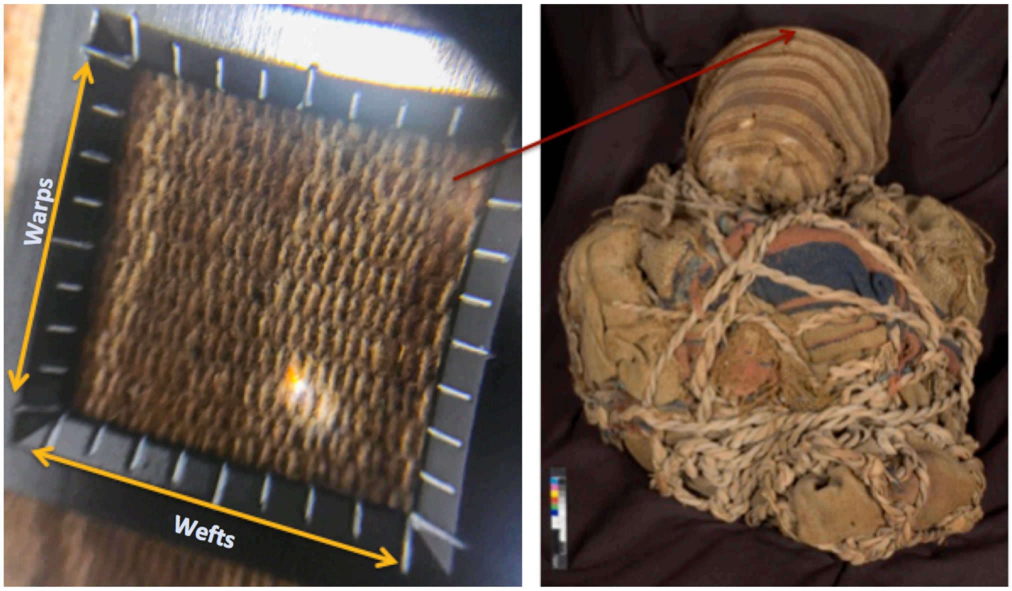

Figure 6-20: Fully striped textile covering head. Yarn count = 50 warps x 11 wefts.

The textile wrapped over the body and feet of the bundle has a section with red and blue bands positioned horizontally over the remains. These are the widest stripes on the textile, and are close to a frayed end of the textile. These could possibly be lateral stripes commonly found at the ends of a textile or sides of a shirt (Minkes, 2005: 45; Cassman, 2000a). Thinner lines of red, blue and a light blue-green are also woven within the neutral brown ground. This polychrome-banded textile has a yarn count of fourteen warps for every sixty-two wefts per inch (Figure 6-21).

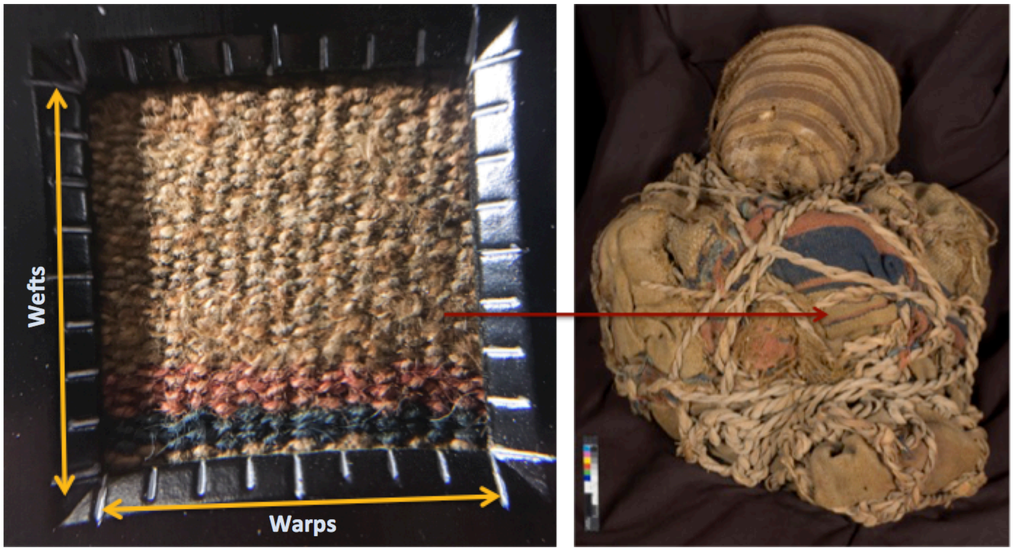

Figure 6-21: Wide striped textile covering body and feet. Yarn count = 60 warps x 14 wefts.

The third and outmost textile wraps the upper back and sides of the mummy bundle. This textile is a think, blanket-like plainweave in neutral brown fibers, and appears to lack any decorative attributes. Rodman (2000) refers to this type of textile as a mantle. The mantle is coarser than the finer woven textiles wrapping the head and body of the mummy. The thicker plied light brown wefts cause the mantle to have a lower thread count of eight warps for every sixteen wefts per inch (Figure 6-22).

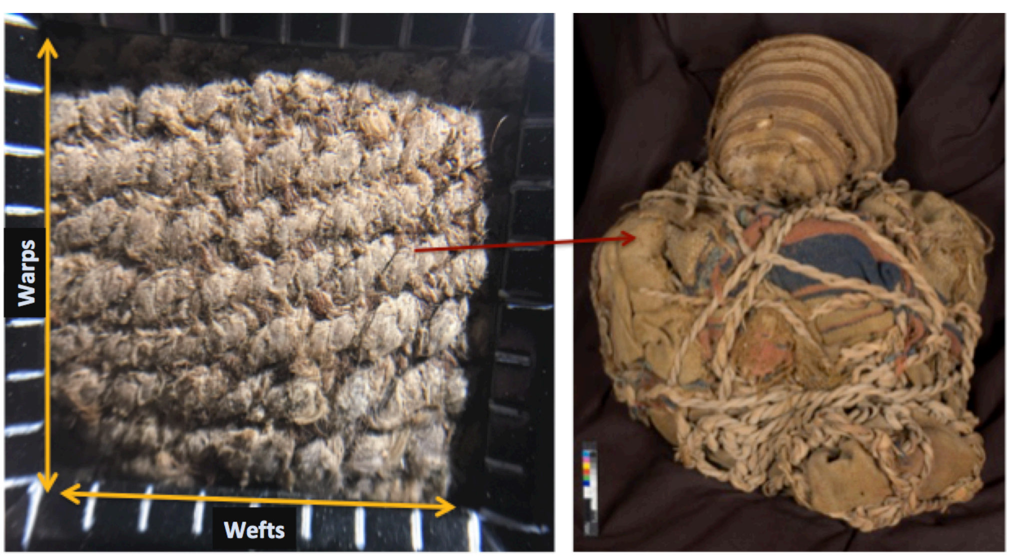

Figure 6-22: Mantle wrapping back and sides. Yarn count = 16 warps x 8 wefts.

### *6.2.2 Textile fibers characterization*

Polarized light microscopy (PLM) of the longitudinally mounted fibers from the three funerary textiles wrapping of the mummy bundle resulted in similar optical characteristics. Almost all fibers studied suggest similar animal origin (Table 6-A, Table 6-B, and Table 6-C). All fibers are birefringent when observed under cross-polarized light and exhibit extinction at 45° rotation of the stage. The fibers from the striped textile wrapping the head and the polychrome-banded textile over the body of the mummy all have observable medullas, in both continuous and fragmented states.

The light brown fiber from the striped textile over the head and the light blue-green fiber from the polychrome-banded textile have fragmented, or interrupted medullas that appear as darkened, tubular fragments in the center of each fiber. The dark brown fiber from the striped textile on the head, the red and dark blue fibers from the polychrome-banded textile, and the light brown fiber from the mantle have continuous medullas. The dark brown fibers from the polychrome-banded textile and the mantle each exhibit a striated appearance without the observation of a medulla. Depending on the species, fineness of hair and location of the body on the animal, fragmented medullas can sometimes appear as small, opaque spots which make them difficult to observe in certain fibers (Langley and Kennedy Jr., 1981; Appleyard, 1972; Gordon, 1931).

<table>
<tr><th colspan="3">Striped textile wrapping head</th></tr>
<tr><th>Fiber</th><th>Plane polarized light (PL)</th><th>Crossed polarized light (XPL)</th></tr>
<tr><td>Light brown fiber</td><td>


</td><td>
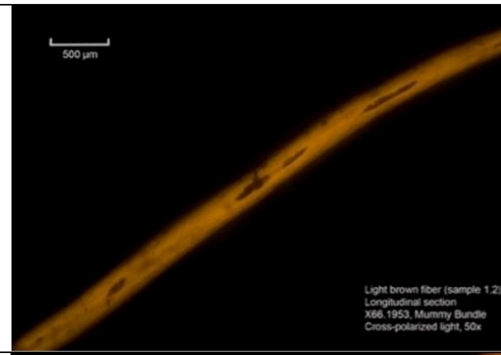

</td></tr>
<tr><td>Dark brown fiber</td><td>
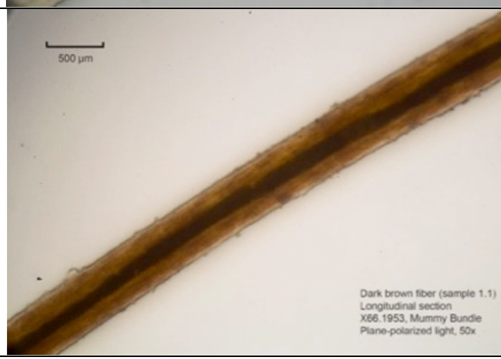

</td><td>


</td></tr>
</table>

Table 6-A: Polarized light microscopy (PLM) of the brown striped textile covering the head of the mummy. Light brown and dark brown fibers were analyzed in plane polarized light (PL) and crossed-polarized light (XPL).

<table>
<tr><th colspan="3">Polychrome banded textile wrapping body and feet</th></tr>
<tr><th>Fiber</th><th>Plane polarized light (PL)</th><th>Crossed polarized light (XPL)</th></tr>
<tr><td>Red fiber</td><td>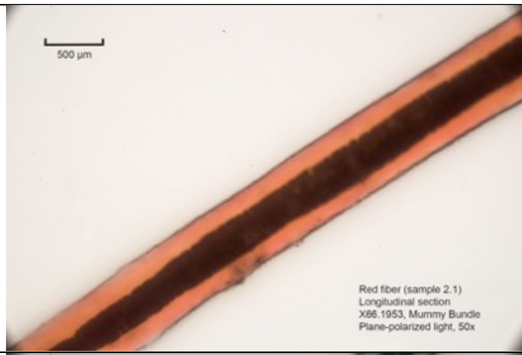</td><td>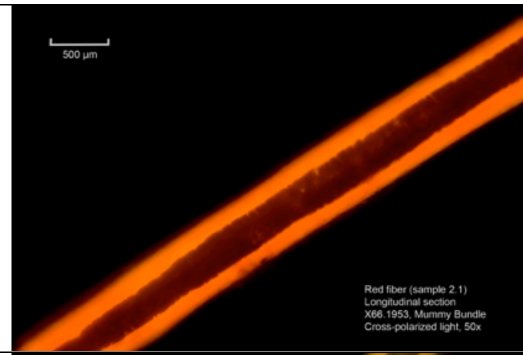</td></tr>
<tr><td>Blue fiber</td><td></td><td></td></tr>
<tr><td>Light blue-green fiber</td><td></td><td>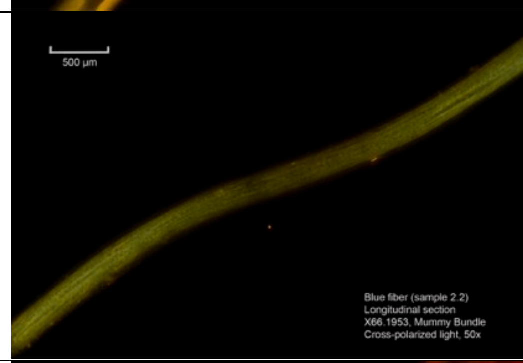</td></tr>
<tr><td>Dark brown fiber</td><td></td><td>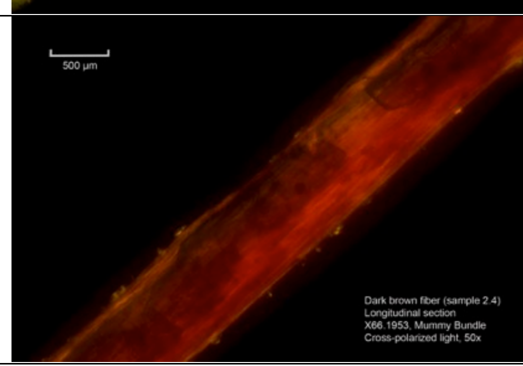</td></tr>
</table>

Table 6-B: Polarized light microscopy (PLM) of the dyed and undyed fibers from the polychrome banded textile covering the body of the mummy. All fibers were analyzed in plane polarized light (PL) and crossed-polarized light (XPL).

<table>
<tr><th colspan="3">Mantle wrapping back and sides</th></tr>
<tr><th>Fiber</th><th>Plane polarized light (PL)</th><th>Crossed polarized light (XPL)</th></tr>
<tr><td>Light brown fiber</td><td>
</td><td>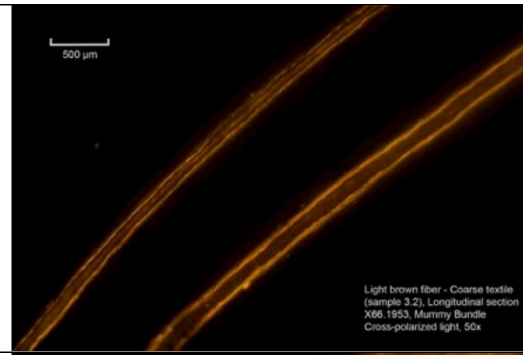
</td></tr>
<tr><td>Dark brown fiber</td><td>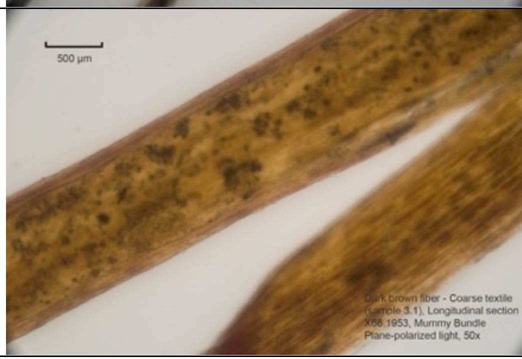
</td><td>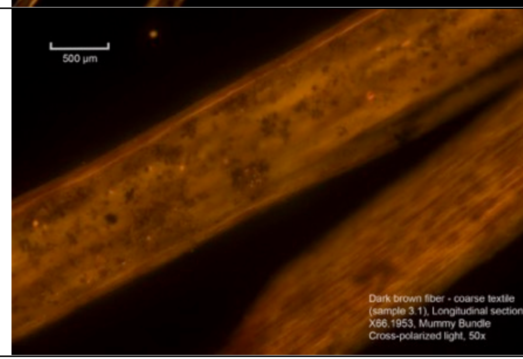
</td></tr>
</table>

Table 6-C: Polarized light microscopy (PLM) of the fibers from the mantle wrapping the back and sides of the bundle. The light and bark brown fibers were analyzed in plane polarized light (PL) and crossed-polarized light (XPL).

XRF detected strong signals for sulfur (S) on the textiles, as well as iron (Fe), calcium (Ca), and potassium (K). The S signal in the textiles may support the presence of animal fibers from the sulfide linkages of cystine ($– CH_2SSCH_2–$), a large amino acid found in the α-keratin of animal hair (Timar-Balazsy and Eastop, 2012: 48). Although, the presence of S as a contaminant from the burial environment cannot be excluded. Ca, K and Fe may also come from a variety of contexts such as salts from burial.

FORS data from fibers analyzed from several areas of all three textiles (Figure 6-23, analysis location map) showed fingerprint markers characteristic of wool (Figure 6-24), composed mainly of polypeptide keratin, which is built on 18 different amino acids. Absorptions at ~1420nm (O-H stretch, first overtone), ~1500 nm (N-H stretch, first overtone), ~ 1905-40 nm

(O-H combination bands) and ~2180 nm (N-H combination bands) are observed in all the fiber types, and correspond to the carboxylic acid and amino groups in amino acids (Canazo-Cayo et al., 2012; Workman Jr. and Weyer, 2008). Absorption bands observed at ~1700 nm and ~1740 nm refer to C-H (stretch, first overtone) and S-H (stretch, first overtone), respectively, and correspond to lipids and fatty acids in the wool substrate (Canazo-Cayo et al., 2012; Workman Jr. and Weyer, 2008; Gishen and Cozzolino, 2007). A trend worth noting is the decrease in reflectance with the increase in wavelength, which is due to the strong absorptions of water and other molecular groups (i.e., amino acids, amides, etc.) in the mid-infrared region.

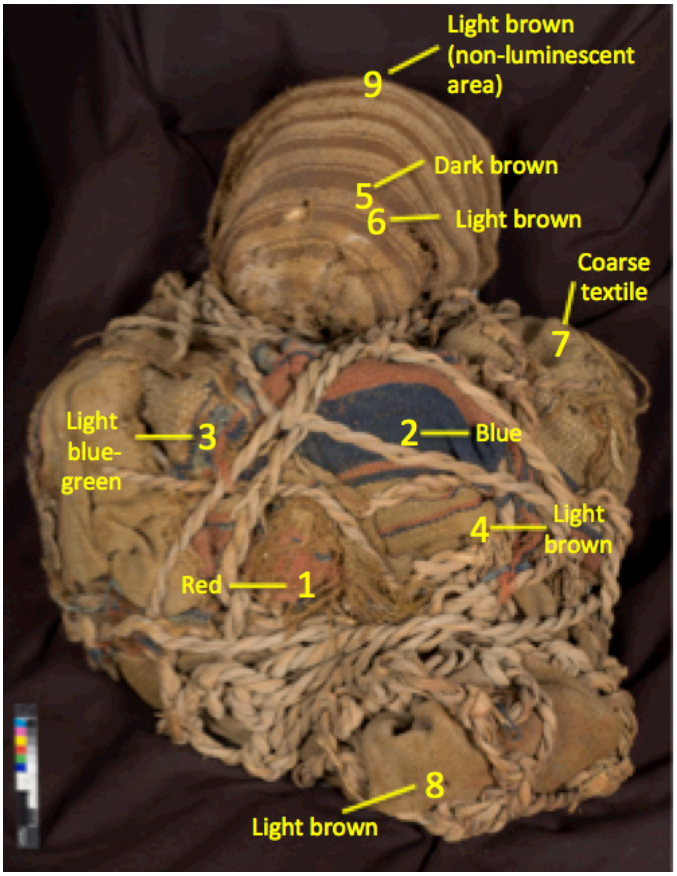


Figure 6-23: vis-NIR FORS analysis map. Numbers indicate locations in contact with the fiber optic probe for analysis.

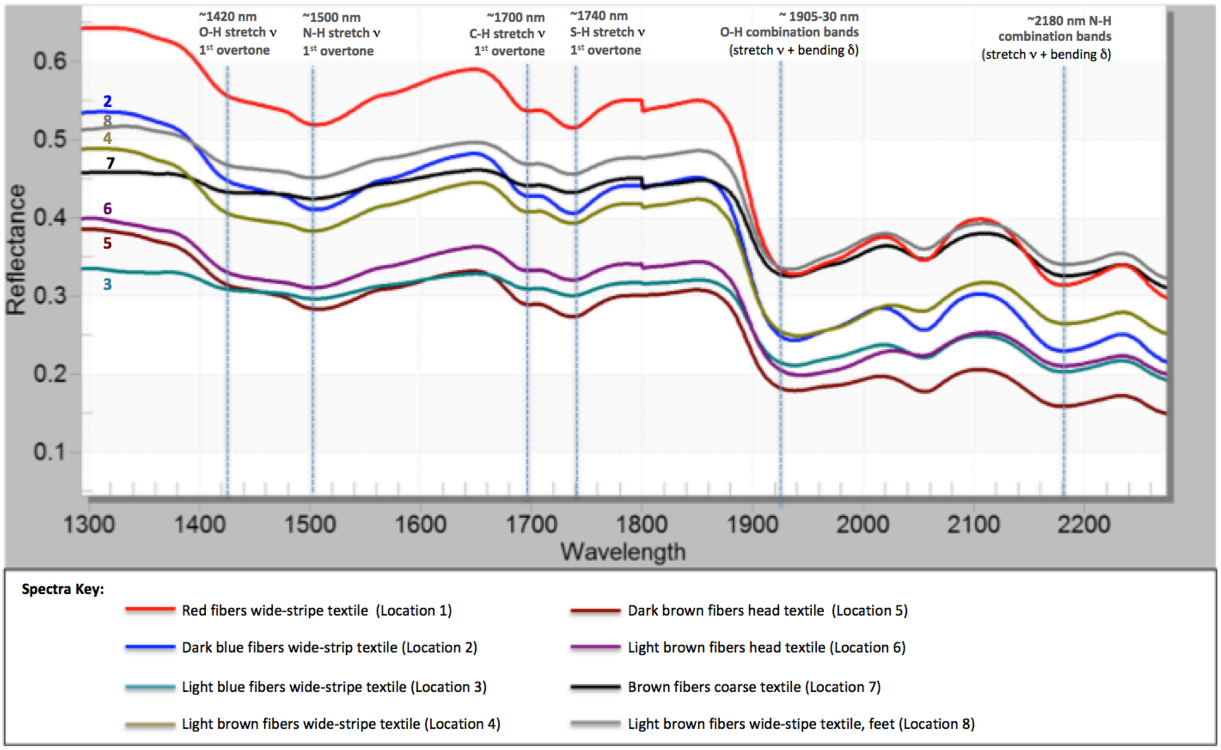


Figure 6-24: FORS (detail, 1300 – 2280 nm) of all neautral brown fibers in the polychrome banded textile, mantle and the textile covering the head. All spectra show similar overtones and combination bands that reflect the molecular composition of wool.

### *6.2.3 Cordage*

Plant fiber cordage was used to wrap the funerary textiles and bind the assemblage together, from the neck of the mummy to the feet. The plant fiber cordage of the mummy bundle was first prepared with several plant fibers spun into a plied Z configuration, followed with plying two spun fibers together to make cordage with a 2-ply S structure. Several elements of cordage are knotted together in various places on the mummy bundle, creating a net-like structure. A longitudinally mounted sample collected from a detached fragment of plant fiber cordage displays a dark brown coloration as well as a striated pattern with transmitted, plane polarized light (Table 6-D). The striated, or linear patterning of the fiber can be interpreted as sclerenchyma bundles composed of groups of uniform cells, running parallel to the length of the fiber; a salient characteristic for monocot leaves (Florian, Kronkright and Norton, 1990: 45). The striated patterning of the sclerenchyma bundles is emphasized with cross-polarized light, where a strong birefringence is also observed throughout the sample.

<table>
<tr><th colspan="3">Plant fiber cordage</th></tr>
<tr><th>Fiber sample</th><th>Plane polarized light (PL)</th><th>Crossed polarized light (XPL)</th></tr>
<tr><td>Plant fiber</td><td>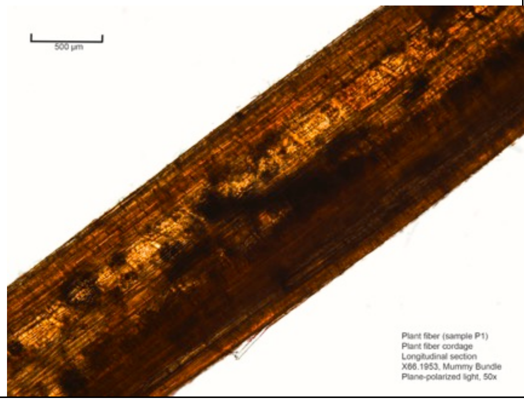
</td><td>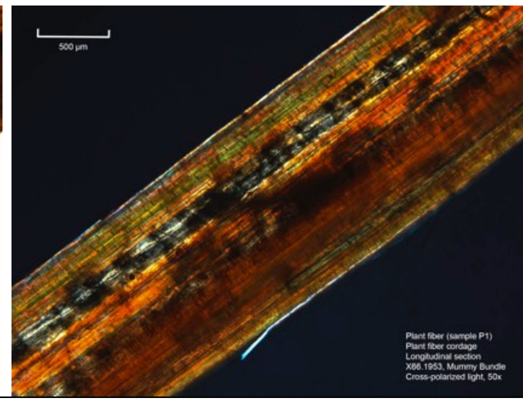
</td></tr>
</table>

Table 6-D: Polarized light microscopy (PLM) of a fiber from the mummy bundle plant fiber cordage in both, plane polarized light (PL) and crossed-polarized light (XPL).

## 6.3 Dyes

### *6.3.1 Red Dye*

Photoexcitation of the red dye with $\lambda_{ex}$ max = 535 nm and capturing at $\lambda_{em}$ max = 580-700 nm, recorded the luminescence in the red-tinted fibers of the polychrome banded textile (Figure 6-25). The same imaging settings also captured a luminescence in the lower portion of the textile wrapping the head, and in contact with the face of the mummy. The plant fiber cordage also exhibits variations of luminescence with these imaging settings.

Figure 6-25: (a) Mummy bundle in normal diffuse light. (b) Mummy bundle with visible induced (λex = 535 nm) visible luminescence (580-700 nm). The red fibers fluoresce with excitation at 535 nm. Luminescence also observed on lower portion of the textile on the head at these settings.

FORS of the red bands and cluster of loose red yarns showed a major absorption in the visible with two sub-bands at ~509 and ~543 nm (Figure 6-26). These bands fall within the characteristic absorptions range 510-515 nm and 540-550 nm of red dyes-rich in purpurin from plants of the Rubiacae family (Gulmini et al., 2013, Kakoulli et al., 2017; Clementi et al., 2008, Grazia et al., 2011). The cochineal wool standard #18 showed the characteristic reflection between ~415 and ~435 nm and absorptions at ~525 nm and ~564 nm, which are red-shifted form the mummy fiber dye absorption and does not correlate with the red mummy fiber FORS (Gulmini 2013, Comelli 2010, Clementi, 2008, Wallert and Boytner 1996). The FORS spectra from the red fibers were further compared to the FORS spectra of the *Relbunium* wool standards (section 5.1) (Figure 6-27). The absorptions at ~509 and ~543 nm correlate best with the *Relbunium hypocarpium* (*Relbunium* wool standard #16).

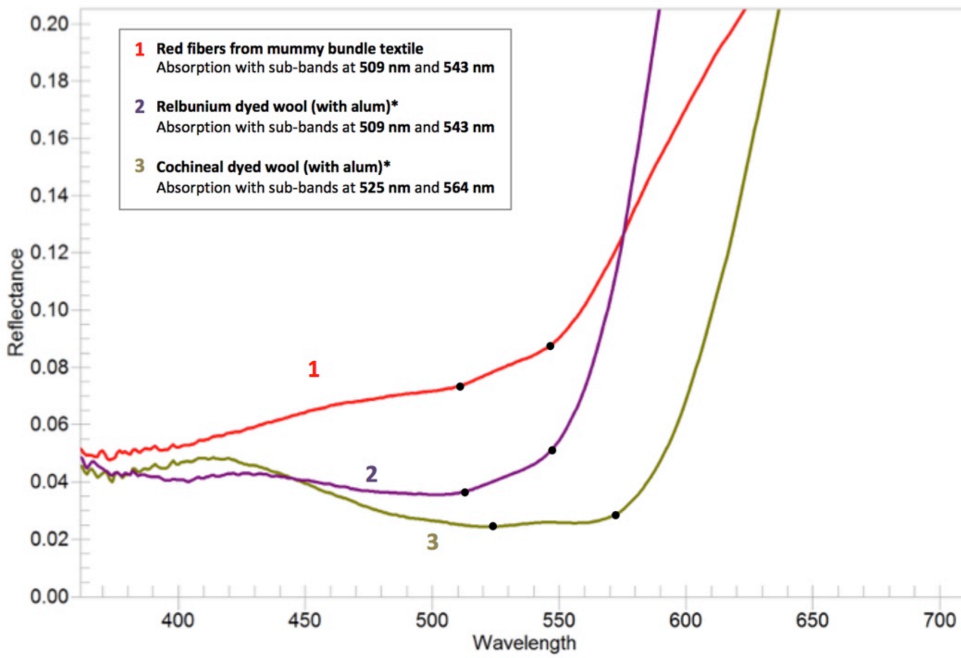


Figure 6-26: FORS spectra with characteristic absorption and reflectance features of the red fibers on the polychrome banded textile (red, 1), *Relbunium* ref. #16 (purple, 2) and cochineal ref. #18 (yellow, 3).

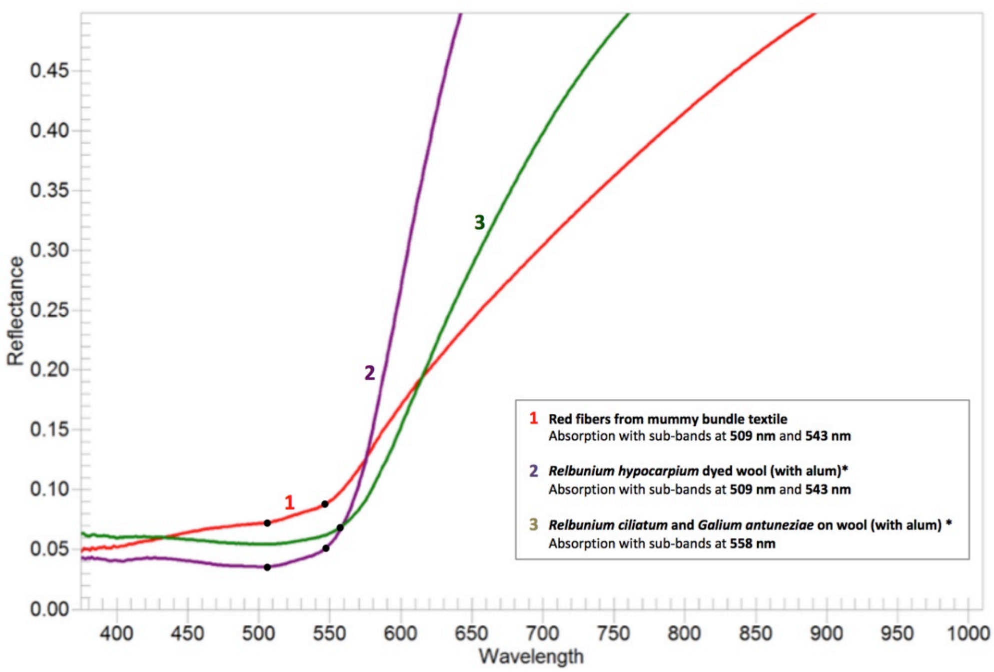


Figure 6-27: FORS spectra (350 and 1000 nm region) showing characteristic absorption and reflectance features of the red fibers on the polychrome banded textile (red, 1), *Relbunium* ref. #16 (purple, 2), and *Relbunium* /*Galium* ref. #21 (green, 3).

To confirm the results from the imaging and FORS, an ultramicroscopic sample from a red fiber was exposed to HF vapors and analyzed using SERS. *Relbunium* wool standards #16 and #21 were also analyzed using HF-SERS for comparison. SERS data from the mummy red fibers matched the spectrum of *Relbunium hypocarpium* (ref. #16), with the characteristic pseudopurpurin and purpurin peaks (Table 6-E) (Figure 6-28) (Rambaldi et al. (2015) and Leona, Stenger and Ferloni (2006)). The *Relbunium ciliatum* and *Galium antuneziae* wool standard (ref. #21) displays peaks that correspond to alizarin (Table 6-E), a prominent anthraquinone present in *Galium* species of dyes. Individual spectra for each fiber can be found in Appendix 9.3.

| **RED FIBERS** | | | **Rambaldi et al. (2015)** | | | **Leona, Stenger and Ferloni (2006)** | |
|---|---|---|---|---|---|---|---|
| **Red mummy fiber** | ***Relbunium hypocarpium* (Ref. #16)** | ***Relbunium ciliatum* and *Galium antuneziae* (Ref. #21)** | Pseudopurpurin | Purpurin | Alizarin | Purpurin | Alizarin |
| | | 1621 | | | 1627 | | 1628.0 |
| 1584 | | | 1585 | | | | |
| | | 1552 | | | 1554 | 1558.2 | 1553.5 |
| 1469 | 1471 | | | 1466 | | 1475.9 | |
| 1444 | | 1447 | 1445 | | 1449 | | 1451.1 |
| | 1437 | | | 1438 | | | |
| 1402 | 1400 | | 1400 | | | 1389.0 | 1406.1 |
| 1334 | | | | | | | |
| | 1326 | 1326 | | 1326 | 1326 | 1320.8 | 1323.8 |
| | | 1182 | | | 1186 | | 1188.8 |
| 1159 | 1159 | 1161 | 1155 | 1158 | 1158 | 1157.8 | 1162.5 |
| 1068 | 1067 | | | 1064 | | 1066.2 | |
| 1039 | 1038 | 1038 | 1036 | | | 1032.1 | |
| 968 | 967 | 967 | | 969 | | | |
| 650 | 649 | | | 651 | | 650.4 | |
| 460 | 461 | | 462 | | | 464.1 | |
| | | 451 | | 455 | | | 451.7 |
| | | 341 | | | | 340.0 | 343.1 |

Table 6-E: Surface Enhanced Raman Spectroscopy (SERS) band assignments (units of $cm^{-1}$) following pretreatment with hydrofluoric (HF) acid vapor. Fibers include the red fiber from the mummy bundle textile, and *Relbunium* wool standards #16 and #21. The results are compared to peaks collected for pseudopurpurin, purpurin and alizarin found by literature sources.

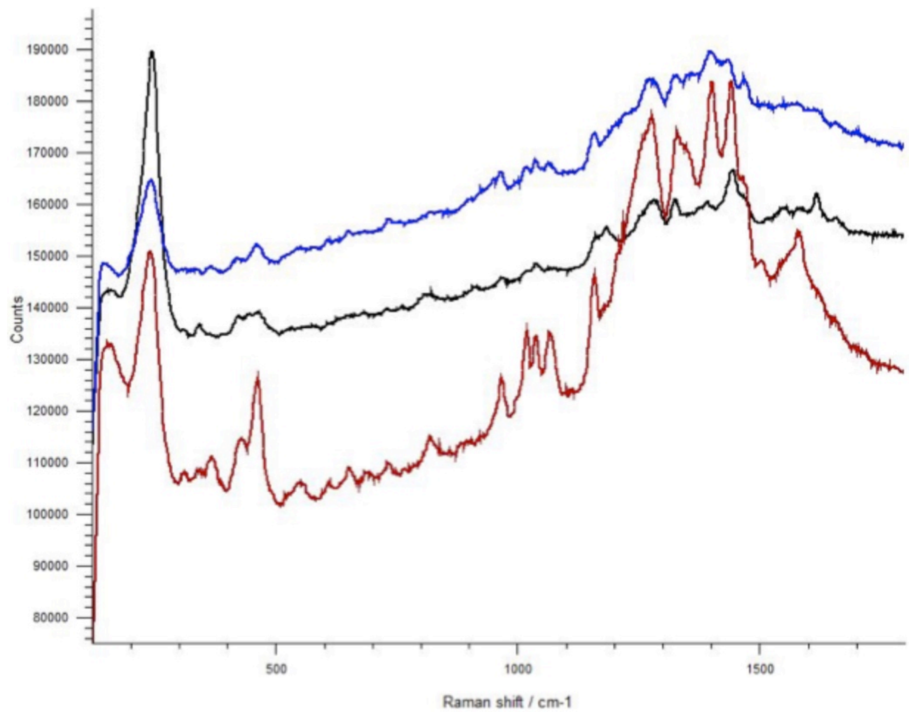


| Red mummy fiber | *Relbunium hypocarpium fiber* * | *Relbunium ciliatum* with *Galium antuneziae fiber* * |
|---|---|---|
| | | 1621 |
| 1584 | | |
| | | 1552 |
| 1469 | 1471 | |
| 1444 | | 1447 |
| | 1437 | |
| 1402 | 1400 | |
| 1334 | | |
| | 1326 | 1326 |
| | | 1182 |
| 1159 | 1159 | 1161 |
| 1068 | 1067 | |
| 1039 | 1038 | 1038 |
| 968 | 967 | 967 |
| 650 | 649 | |
| 460 | 461 | |
| | | 451 |
| | | 341 |

Figure 6-28: Surface Enhanced Raman Spectroscopy (SERS) of the Red mummy fiber (red), *Relbunium* wool standards #16 (blue) and #21 (black). SERS collected on each fiber after pretreatment with hydrofluoric (HF) acid vapors.

### *6.3.2 Dark and light-blue color dyes*

Reflectance spectra of the dark blue and the lighter blue-green yarns of the blue bands in the polychrome banded textile reveals a strong sub band absorption at 660nm, and characterizes the presence of indigo (Figure 6-29) (Gulmini 2013, Melo and Claro 2009, Aceto et al., 2014). The small sub band expected at 350 nm also observed but not as intense as the absorption at 660 nm. Results from FORS show the variance in the color hue of each blue exhibited on the funerary textile is not due to a difference in the chemical identity of the dye. The light and dark blues appear to be the same dye component, based on the same absorption characteristics.

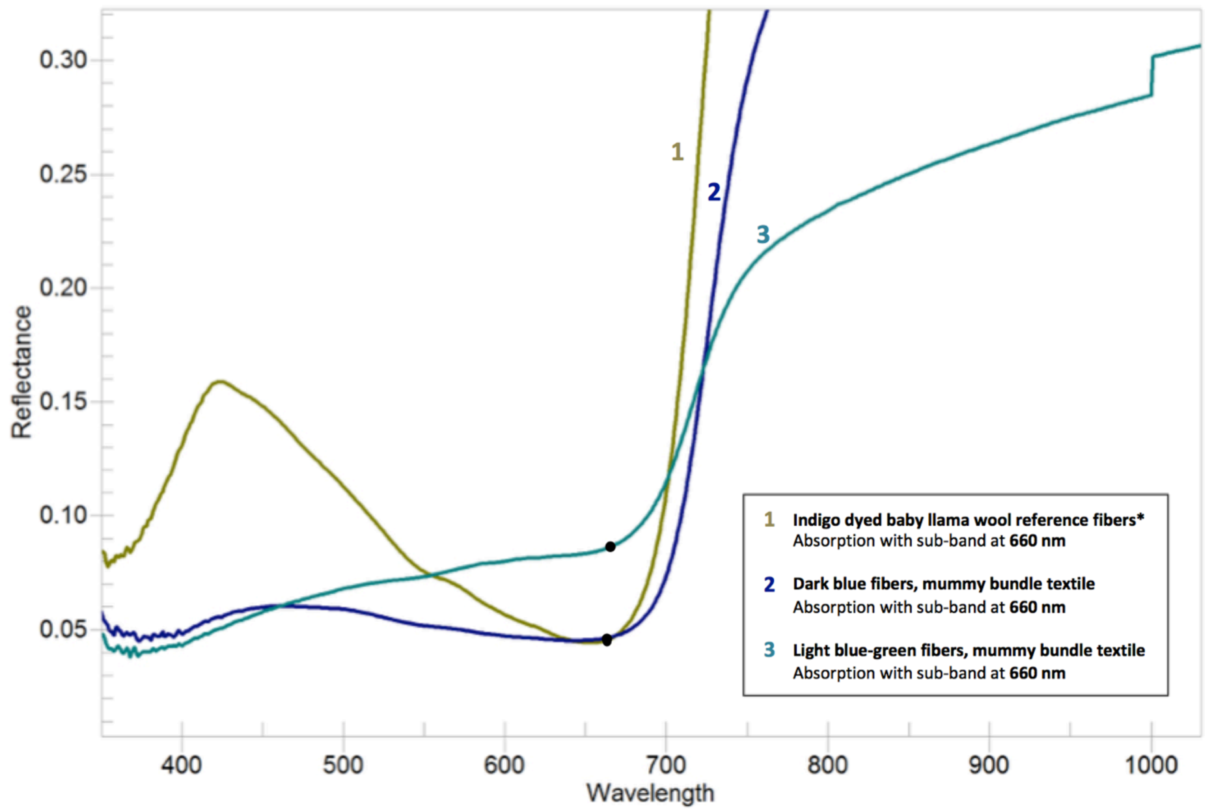


Figure 6-29: FORS (detail, 350 – 800 nm) of the indigo wool standard (yellow, 1) with the dark blue (blue, 2) and light blue-green (turquoise) fibers of the polychrome banded textile. All have absorptions of 660 nm, characteristic of indigo.

μRS of a single fiber from both hues of blue were compared to the indigo wool standard dyed with indigo. All three fiber samples exhibit a doublet at 1574 $cm^{-1}$, which is characteristic of indigo and represents the in-phase stretching of the C=O bond with the central C=C bond, and stretching vibration of the six-member carbon ring (Figure 6-30) (Leona et al., 2004). The two blue mummy bundle fibers share similar broad peaks at 1638 $cm^{-1}$ (blue fiber) and 1630 $cm^{-1}$ (light blue-green fiber) and potentially correspond to the vibration of the protein, amide I, in the wool fiber. The amide I protein is susceptible to structural changes, and with degradation, can reduce in peak intensity compared to contemporary wool fibers (Bernardino, de Faria and Negrón, 2015). Peaks found at approximately 1482, 1461, 1365, 1312, and 1220 $cm^{-1}$ on the dark blue and light blue-green mummy textile fibers are also observed, and correspond to important bands of pure indigo (Andreev et al., 2001). While absent on the dark blue fiber spectrum, the light blue-green fiber observes minor peaks at 776 $cm^{-1}$, 654 $cm^{-1}$, 600 $cm^{-1}$ and 561 $cm^{-1}$.

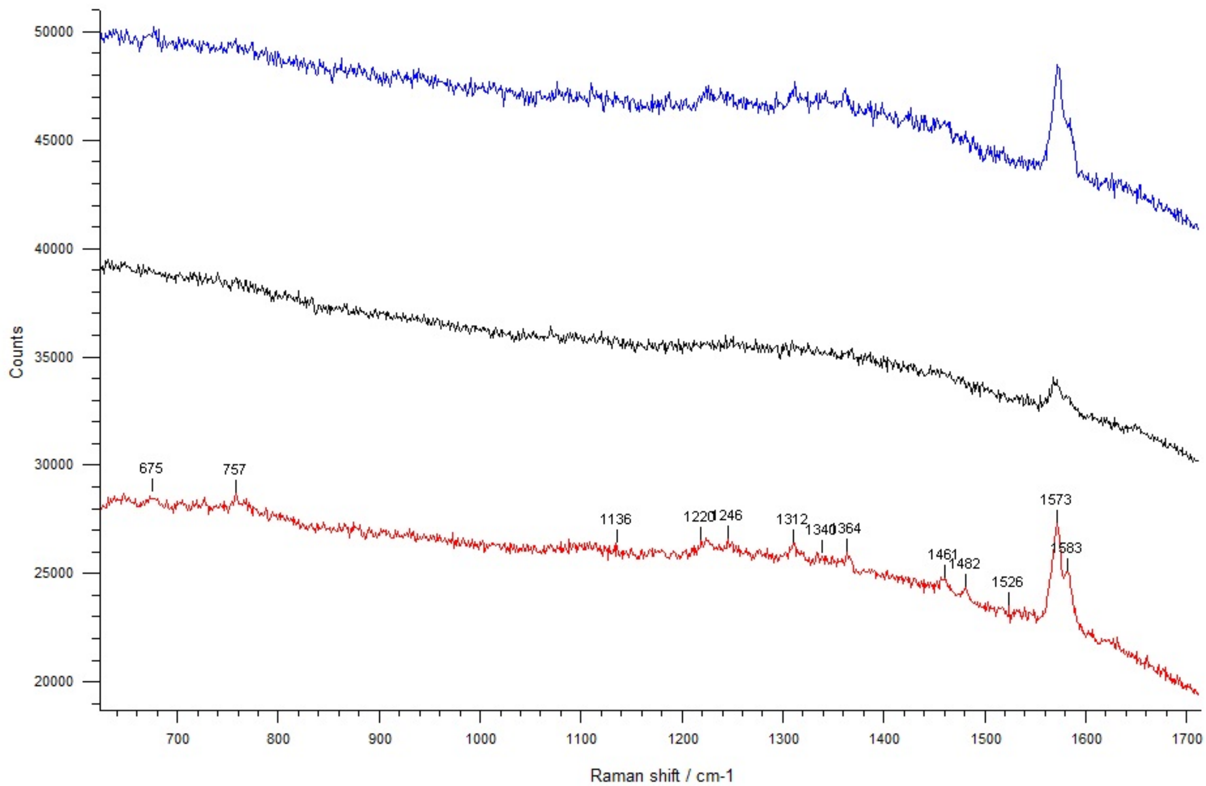


Figure 6-30: μ-Raman spectroscopy of dark blue (red) and light-blue (blue) fibers from the polychrome banded textile, compared to a fiber from the indogo wool standard (black).

### *6.3.3 Dark and light-golden brown fibers*

FORS spectra of dark and light brown areas of all three textiles display absorptions characteristic of amino acid and lipids, which correlate the fibers as animal in origin (Figure 6-31). The second derivative of all brown fiber reflectance spectra match with similar absorption properties, and correlate with the absorptions in the NIR reflectance spectra. In addition, a comparison of the second derivative spectra of the brown fibers from the three textiles does not exhibit any significant differences for the fiber substrate. These similarities appear to suggest the fibers are of the same composition.

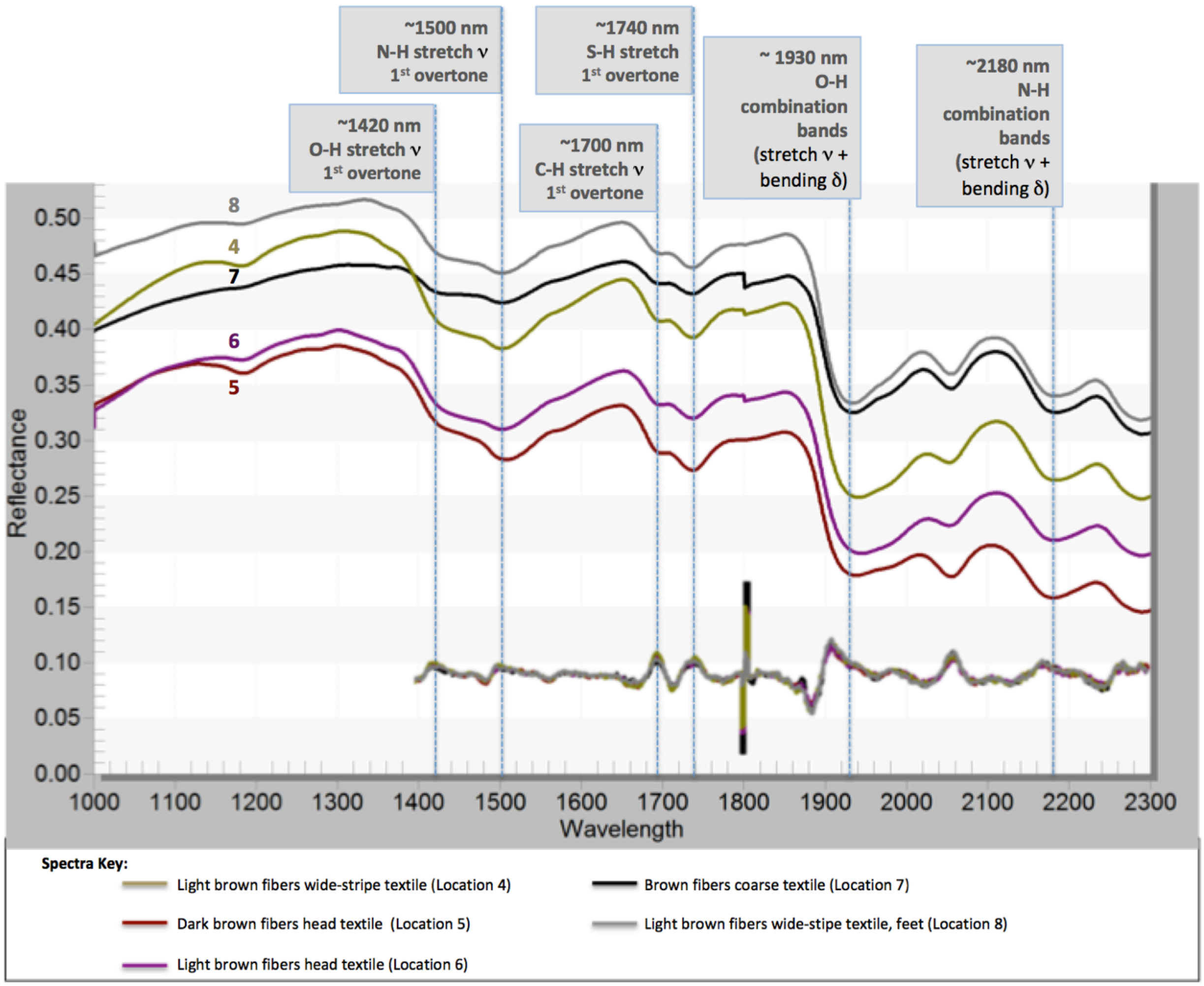


Figure 6-31: FORS (1000 – 2300 nm) of brown fibers in all three textiles have similar overtones and combination bands. Likewise, the second derivative FORS (~1400 nm – 2300 nm) of the brown fibers (below reflectance spectra) are also similar.

Luminescence on the lower portion of the fully striped textile over the face of the mummy (see Figure 6-25(b)) with a $\lambda_{ex}$ max = 535 nm and capturing at $\lambda_{em}$ max = 580-700 could be indicative of an organic residue, or possibly a dye. FORS of both, the light and darker brown bands in the area of luminescence on the striped textile were compared to the undyed brown fibers at the top of the head, which did not exhibit luminescence with photoexcitation. For all brown fibers, including the two luminescent areas, the FORS spectra did not show a specific absorption in the visible region (see Figure 6-32). This more than likely confirms the fibers are naturally brown from the camelid species used for the fiber production, rather than the color originating from a dye.

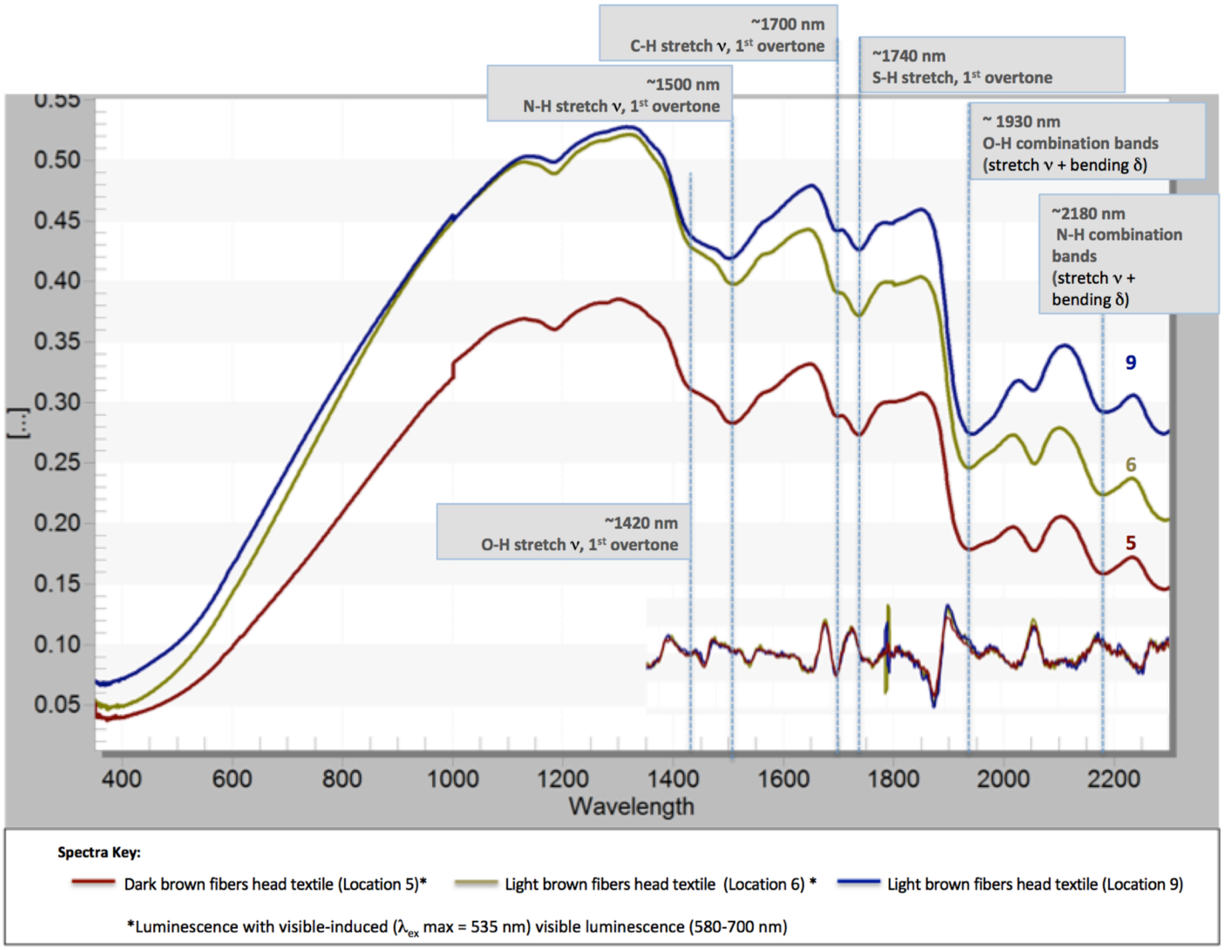


Figure 6-32: FORS (400 – 2300 nm) of the dark and light brown fibers that luminesce with visible-induced ($\lambda_{ex}$ max = 535 nm) visible luminescence (580-700 nm), compared to a non-luminescent area (top of the head). Similar overtones and combination bands are observed. Likewise, the second derivative FORS (~1400 nm – 2300 nm) spectra of all brown fibers (below reflectance spectra) are similar.

# 7 Discussion

## 7.1 Use of Computed Tomography to observe contents of the mummy bundle

Computed Tomography was beneficial to the study of the mummy bundle interior, allowing mostly unobstructed visualization of the human remains and funerary objects through the layers of textiles. Observation of the skeletal remains did not detect a left ulna, right foot or a complete pelvis. In addition, several small bones, such as the vertebrae, are scattered at the base of the bundle. The separate bones accessioned with the mummy bundle in 1966 include a left ulna, the toes of the right foot, vertebrae, an upper deciduous lateral incisor and portions of the pelvis (i.e., sacrum and right ischium), as well as a possible epiphysis (Figure 9-1 – 9-7). As the bundle appears to lack these specific bones, the separately accessioned bones likely belong to the human remains wrapped inside the mummy bundle.

Dense and radiopaque materials such as bone, ceramic and wood were detected, and in some cases, construction methods were indicated with CT analysis. The globular vessels appear to be shaped, hollow objects and the top-like objects are carved based on the flattened surface areas and cut marks in the surface. Less dense materials that are more radiotranslucent with X-radiography, such as organic materials, were not as prominently observed with CT. The high energy of the X-rays required to penetrate through the textile wrappings also passed through the skin and hair of the mummy, which were not observed with the CT. The endoscope provided the best method to view these softer, less dense organic components. However, analysis with the endoscope was limited to locations with pre-existing holes in the textiles that are large enough for the camera to enter. The single braid of dark brown hair observed on the right side of the head, confirms the presence of hair on the mummy, and there are more than likely several other small braids. Cassman (2000b) reports that both genders were commonly found with braided hair, and while females are commonly found with lateral braids, men have a variety of complex braided styles, possibly suggesting that men held a variety of social roles and positions.

The distance of 0.6 mm between X-ray slices was sufficient to distinguish the presence of bones and the larger, dense funerary objects inside the bundle. However, the distance between X-rays appears too large to capture the surface features and textures of the vegetal material. The tapered objects inside the PR vessel and near the PL vessel are more than likely corncobs, which are common artifacts found in funerary bundles and burials, especially with small spherical ceramic vessels (Arriaza Torres, 2016; Uribe Rodrigues; 2016; Bird, 1943). However, only their faint, tapered outline was observed with CT, and the analysis did not reveal distinguishing surface features, such as kernels on the cob. The loose granular material was also difficult to interpret, as it appears as a cluster of loose material (more than likely corn) and creates an amorphous dense feature within the bundle.

## 7.2 Human remains interpretation

### *7.2.1 Age Approximation of Mummy at Time of Death*

To determine the age of the child mummy at the time of his or her death, the teeth and bones of the skull are reliable sources for an age approximation (Bass 1995; Ubelaker 1978). Teeth formation begins with enamel formation at the crown cusps and then progresses outward towards the root (Byers, 2002: 199). With this in mind, the amount of tooth calcification and eruption can be translated into approximate age ranges of a child up until about 12 years of age (Bass, 1995: 303). When compared to teeth development description by Byers (2002: 209), Bass (1995: 303) and Schour and Massler (1941), the teeth of the child mummy appear to match dental characteristics observed in a child of three to four years of age. This approximation of age is supported further by a comparison with tooth development charts provided by Ubelaker (1978) and published in Bass (1995: 303) (Figure 7-1).

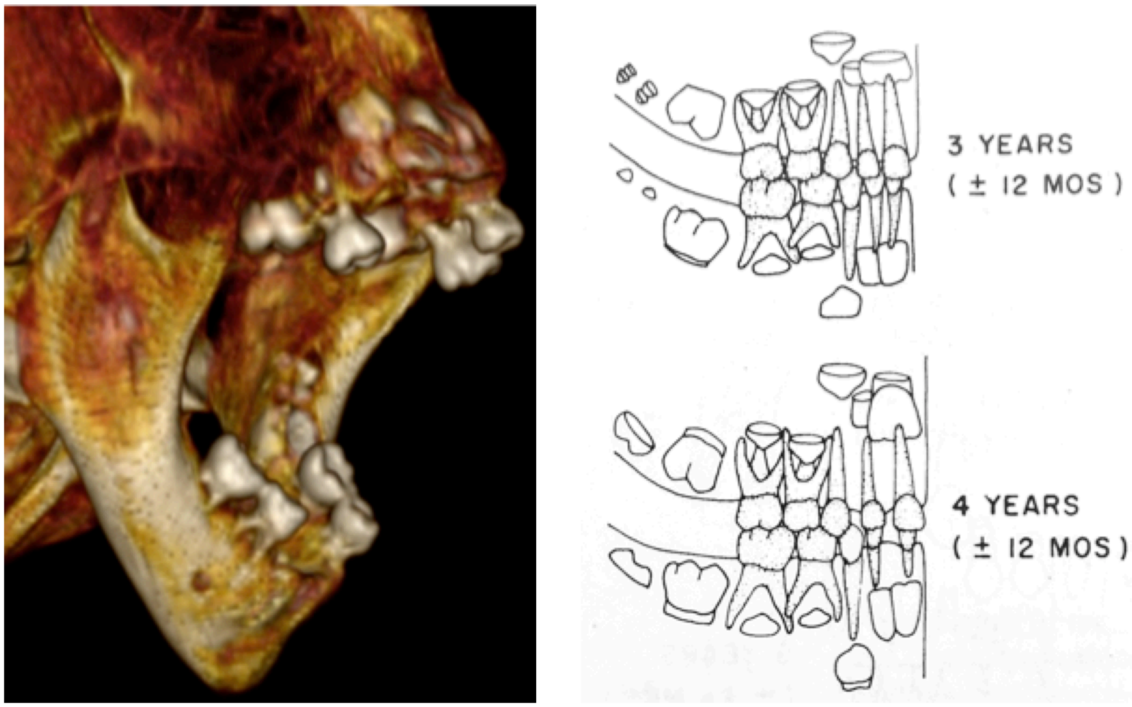


Figure 7-1: Tooth formation and eruption comparison with tooth development charts of the formation of teeth in a three year old (upper right) and four year old (bottom right) child. Tooth diagrams courtesy of Bass (1995: 303).

The first and second deciduous molars of the child are crown complete with root development, and have erupted from the maxilla and mandible. The complete formation of deciduous molars, including root development and eruption, occurs by approximately three years of age. The first permanent molars remain crown complete in the crypt of the maxilla and lacks root development. Root development on the first permanent molar begins when the individual is around 4 years of age, and erupts from the crypt around six years of age (Bass, 1995: 303). The first permanent molars in the maxilla of the mummy lack root development, but are crown complete. Based on the dentition formation of the mummy, the child appears to have been just over three years of age but not more the four years old at the time of death. The developmental stages of the adult incisors in the crypt of the maxilla are crown complete with a possible initiation of root growth. Tooth development charts indicate adult incisors begin root development also around 4 years of age, and begin to emerge out of the crypt around six to seven years old (Byers, 2002: 209). The crown complete state of the adult incisors remaining in the crypt further supports the approximate age of the child in the mummy bundle between three and four years of age.

The development of the cranial bones appears to further support the three to four year-old age approximation of the child. The frontal and parietal bones have merged along the coronal suture, and the anterior fontanelle (commonly referred to as an infant's "soft spot") is closed, which typically occurs at approximately 18 months to 2 years of age (Stanford Children's Health, 2018). The point at which the frontal and two parietal bones of the skull meet along the coronal suture, also referred to as bregma, is observed with CT analysis as closed with a uniform bone thickness. This area is thin when the anterior fontanelle first fuses around two years of age, and reaches a thickness consistent with the frontal and parietal bones by three years of age (Cunningham, Scheuer and Black, 2016:102-109). A CT sagittal cross-section of the skull shows bregma of the child mummy is only slightly thinner than the plate thickness. This indicates the area surrounding bregma was nearing a total uniform thickness, and could further support an age closer to the three to four year approximation of age at the time of death.

## 7.3 Textile technology, dyeing and significance

### *7.3.1 Textiles/fibers' origin*

Microscopic analyses supported by PLM and FORS suggested that most fiber samples from the funerary textiles of the mummy bundle are of animal origin, most likely camelid hair; the llama, alpaca and *vicuña* are closely related and have similar hair characteristics (i.e., fine and smooth fiber, with a narrow, fractured and/or opaque medulla), making a specific determination often difficult (Appleyard, 1972; Gordon, 1931). Compared to the other textile fibers, the dark brown fibers from the mantle are shorter, and under magnification, appear to lack any indication of a medulla but are also birefringent. In some cases, camelid medullas are not visible, even with transmitted light (Langley and Kennedy Jr., 1981; Appleyard, 1972). Therefore, the absence of a medulla does not disprove the possibility of the fiber being camelid. Another possibility is the fiber could originate from a plant. Cotton is a very common plant source for textile production in the Andean region, and grows naturally along the Peruvian and Chilean coasts. Similar to the dark brown fiber sample, cotton is also birefringent with XPL, and has a flattened, ribbon-like structure observed with magnification (Florian, Kronkright and Norton, 1990: 41). Indigenous cotton comes in a variety of hues due to photosynthesis the moment the seed opens, and can result in shades of white, off-white, lilac-tinted grey and even a light, rusty dark brown (Minkes, 2005: 38). Rodman (2000) mentions similar thicker woven textiles found at Caserones in northern Chile. The textiles are similar to the mantle, where they are rarely decorated, have coarse and thicker yarns, and also have a lower warp count than camelid fiber textiles. According to Rodman, these textiles are made with cotton, or a combination of cotton and camelid fibers.

Plied camelid, or mostly camelid burial textiles are common in the region from the Osmore valley in Peru, to the San Pedro de Atacama and Azapa Valley in northern Chile (Rodman, 2000). Mixtures of cotton and camelid are also encountered, but less frequently. Andean cultures in this region may have preferred camelid wool textiles for clothing and ritual, and reserved cotton for domestic use (Rodman, 2000). The polychrome bands of red and blue on a mostly neutral brown ground and use of camelid wool are very characteristic of Late Intermediate Period people in the Arica region, which include the Cabuza  Maitas, San Miguel, Loreto Viejo, and Regional Development (Agüerro Piwonka, 2000; Cassman, 2000a). These societies were not sequential, but represent overlapping ceramic styles that distinguish different cultures within the same group of people living in Arica from 900 – 1400 CE (Cassman, 2000a).

The cordage binding the mummy bundle appears to be a monocot leaf structure based on the striated pattern observed in the longitudinal sample. Most commonly, plant fibers used in the production of materials used in textiles and cordage are sclerenchyma bundles and vascular bundle sheaths of monocot leaves and phloem fibers of herbaceous dicot stems (Florian, Kronkright and Norton, 1990: 45). The fibers are removed from the plant and processed to create workable fibers that are then spun, or "plied" together for additional strength. The cordage in bound over the mummy bundle creates a net-like structure from the neck to the feet. Bird (1943) refers to the plant fiber cordage wrapping the mummies found in his excavations as "tortora rope". Tortora (Schoenoplectus californicus ssp.) is a type of sedge monocot plant commonly found in South America, including northern Chile, and a likely identity of the plant fiber cordage binging the mummy bundle.

### *7.3.2 Pre-Hispanic red dyes in Chile*

Analysis of red dyed textiles of the mummy wrappings did not identify alizarin, but did confirm the presence of the two anthraquinones: pseudopurpurin and purpurin. These are two major constituents of *Relbunium* plant species, rather than *Galium* plant sources, which contains more alizarin (Degano and Colombini, 2009).

The distinction of Rubiaceae from carminic acid with luminescent photography was made due to the luminescence observed in the red bands. *Relbunium* and *Galium* are expected to exhibit a characteristic luminescence between 600 and 615 nm, while carminic acid quenches and does not emit a luminescence within this range (Comelli et al, 2011). FORS further confirmed the red bands of the mummy bundle textile to contain absorptions characteristic of Rubiacae, rather than cochineal.

SERS successfully identified the dye in the red mummy fibers as *Relbunium hypocarpium*, which match similar literature studies of *Relbunium* dye detection with SERS. Whiteny, Van Duyne and Casadio (2006) found they could distinguish between the purpurin and alizarin from certain marker bands consistent to each respective dye with the SERS technique. They suggest to use marker bands centered at 366, 606, 970, 1020 and 1401 $cm^{-1}$ for the identification of purpurin, and 473, 900 and 1157 $cm^{-1}$ for alizarin. Results from the SERS analysis of the red mummy fiber revealed significant peaks at 366, 968, 1019 and 1402 $cm^{-1}$, while lacking all but one (1159 $cm^{-1}$) marker bands characteristic for alizarin. These findings appear to resemble the marker bands for purpurin rather than alizarin, which further supports the use of a *Relbunium* species of madder dye rather than the alizarin containing species, *Galium*. Furthermore, the bands from the SERS analysis of the red mummy fiber are most similar to the SERS bands produced by the *Relbunium hypocarpium* wool standard (see Figure 6-28).

The identification of *Relbunium hypocarpium* is consistent with the source of other red-dyed funerary textiles from the Atacama Desert region in northern Chile, particularly from San Pedro de Atacama (SPA). It is also listed as a most common plant source for red dyes in the Andes of the Middle and Late Intermediate Periods, and more than likely the only source of *Relbunium* in Chile (Wallert and Boytner, 1995; Wouters and Rosario-Chirinos, 1992). Niemeyer and Agüero (2015) detected purpurin without alizarin on all red-dyed fibers in their study from the Middle Period (c. 400-1000 CE) and Late Intermediate Period (c. 1000-1450 CE) SPA textiles using high performance liquid chromatography with a diode array detector (HPLC-DAD). No traces of cochineal-based dye were detected in any of these Middle to Late

Intermediate Periods, which occurs in later time periods closer to the Inca Period. Therefore, the identification of *Relbunium hypocarpium* as the red dye source strongly supports the mummy bundle attribution as Late Intermediate Period of northern Chile.

### *7.3.3 Pre-Hispanic blue dyes in Chile*

Andean provenance was further supported with the identification of *Indigofera* as the blue dye source in the polychrome textile of the mummy bundle. A major benefit of using FORS and μRS for the identification of indigo in the textiles was that the two forms of analysis did not require the need to sample and destroy as much as 5 mm of fiber, a common requirement for other dye analysis methods, such as High Performance Liquid Chromatography (HPLC).

Some μRS peaks of the blue mummy fibers and indigo wool standard seem to vary from literature sources discussing the Raman spectrum of pure indigo. According to Leona et al. (2004), different microenvironments surrounding the indigo molecule can modify the electronic structure of the indigo molecule, resulting in diverse spectral characteristics. This alteration suggests the indigotin has altered, more than likely from the vat-dye process. The chemical alterations from the dying process as well as the addition to a wool substrate appear to have caused Raman inactive vibrational modes to become Raman active. FORS confirmed the absorptions of ~ 350 nm and ~ 660 nm in both, the lighter blue-green and darker blue hues in the stripes of the funerary textile over the body of the bundle. This result demonstrates both hues of blue are the same, chemically, confirming the presence of indigo. The difference of color intensity between the lighter blue green and the darker blue hues could be attributed to other factors of manufacture, such as the degree of oxidation, number of dye intervals and time of immersion of the indigo dye process. Even the color of camelid wool selected (i.e., ivory, tan, orange, brown or black) could affect the resulting coloration of the dyed fiber.

Andean textiles with blue fiber components are commonly found to contain indigotin and indirubin, confirming the use of indigo as the organic blue dye (Rodman, 2000). The presence of indigo as the only blue dye source in Middle and Late Period funerary textiles from the Atacama Desert are confirmed in various studies (Niemeyer and Agüero (2015; Salazar et al., 2014; Cardon, 2007).

### *7.3.4 Tannin brown dyes*

From the lack of absorptions in the visible and near-Infrared regions of the FORS spectra, the brown fibers do not appear to contain a dye. They are more than likely undyed, natural camelid wool. Llamas and alpaca wool can range in color: ivory, brown, red-orange and black hues.

## 7.4 Cultural and funerary context

### *7.4.1 Cranial deformation*

The elongated, conical shape of the skull is a purposeful result of binding the head during the first year of the individual's life. The degree of elongation is best observed with cross-sectional slices through the head using Computed Tomography. The CT analysis reveals the conical structure of the cranium, with the occipital base forming a rounded point (Figure 7-2). This purposeful alteration in the cranial shape is referred to as artificial cranial modification (or deformation) (ACM), where the skull of an infant is bound with textiles wrapped tightly around the head, and most commonly with the addition of wooden boards (Gerzten, 1993).

Located on the lamdoid suture and the lambda junction of the mummy skull are two circular ossification sites. These inclusions are referred to as wormian bones, and are defined as isolated ossicles of variable size and shape within the cranial sutures and at the fontanelles, and usually grow to the thickness or be slightly thinner than the surrounding cranial wall (El-Najjar and Dawson, 1977). While wormian bones can develop in unmodified skulls, they are often found in skulls with ACM. The wormian bone at the lambda junction of the mummy skull is a common trait of modified skulls from South America and is referred to as the Inca bone (Figure 6-12(d)) (Fujita et al., 2002). A theory proposed by El-Najjar and Dawson (1977) suggests wormian bones form to fill in gaps in modified skulls during the binding phase, when the pressure is exerted on the skull to cause the fontanelles to shift and change shape.

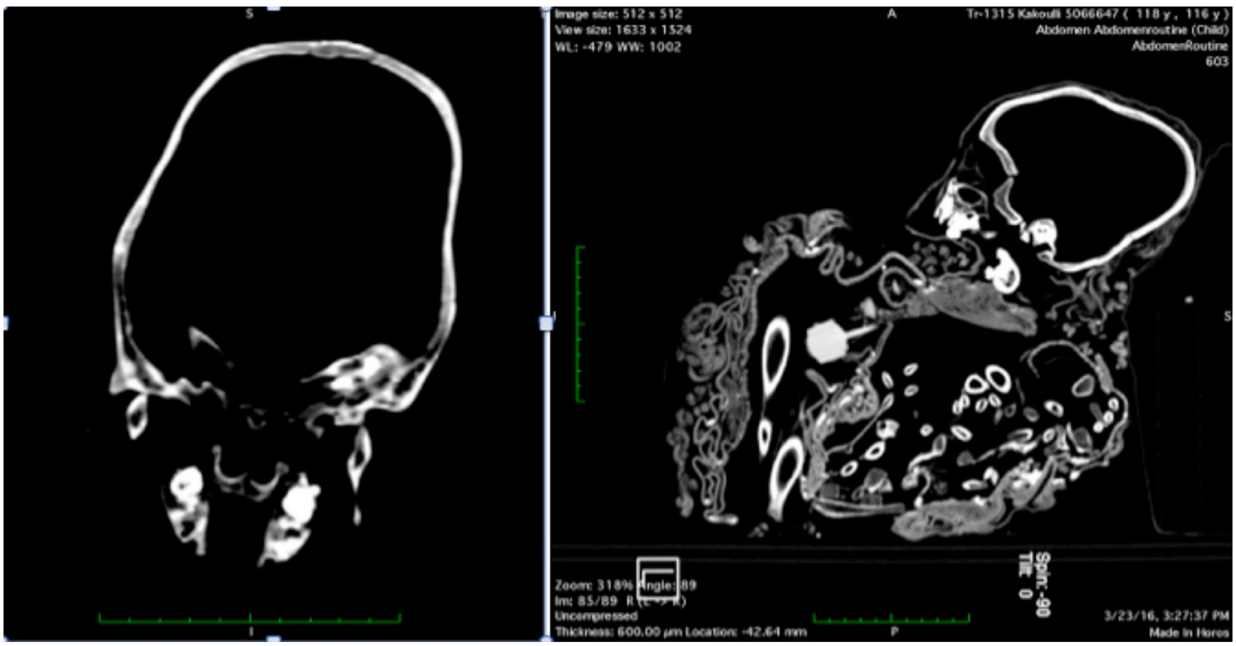


Figure 7-2: Computed Tomography slices (cross-sections) detailing the annular style of artificial cranial modification. (Left) CT slice horizontally through the base of the skull. (Right) Sagittal CT slice of mummy bundle.

In accordance with research presented by Torres- Rouff (2002), the mummy skull appears to have an annular style of modification, which is characteristic of Tiwanaku influence of northern Chile (400-100 CE) from the Bolivian Highlands. Also referred to as the “bandage only” method of ACM, the skull lacks severely flattened areas, which rejects the idea that wooden boards were incorporated into the bandages (Gerzten, 2005). Instead, the head is continuously cone-shaped with a rounded, convex nature. This ACM technique is known as the annular style as wrapping the infant's head tightly with woven textiles, or "bandages" to direct the skull into a conical, elongated form, and neglects the use of wooden boards (Figure 7-3) (Gerzten, 2005; Rouff-Torres, 2002). The annular style was used by fewer cultures, and is notable in establishing the provenance of the mummy bundle. The annular form was a predominant style of ACM with the San Miguel in the coastal fishing villages of northern Chile during the Late Intermediate Period (Sutter, 2006).

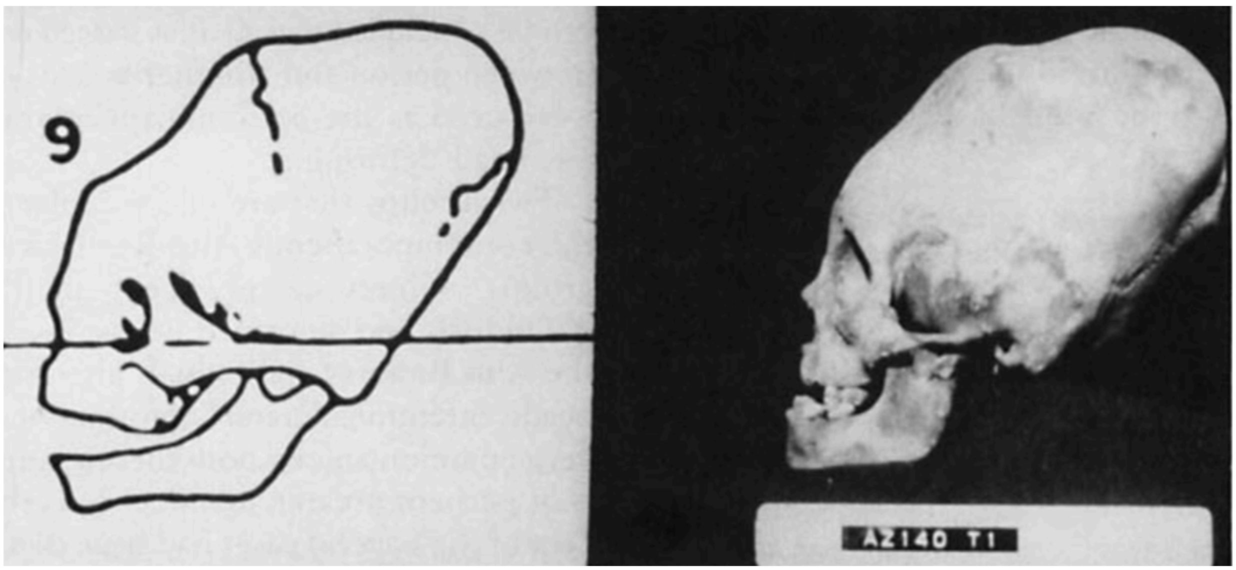

Figure 7-3: Bandage method of artificial cranial modification (ACM), also referred to as the annular style. Images courtesy of Gerzten (1993).

Artificial Cranial Modification (ACM) was a common practice for Andean cultures, beginning with the Chinchorro (6000 BCE) in Arica. The practice of altering the shape of the cranium occurs during infancy while the brain develops and the skull is soft ((Torres-Rouff, 2002). Gerszten (1993) studied 415 skulls representing 7,000 years of habitation (starting with the Chinchorro) in the Azapa Valley. The approximate ages of the individuals range between infants to over 60 years, and include both, male and female. The study found that 88.9% of the skulls studied were altered purposefully, with an even distribution between male and female. The study presented by Gerszten (1993) found no correlation to social status or gender, but found certain trends that followed specific cultural groups and time periods. He further hypothesizes that that ACM was decided by the parents of the child and performed as a function cultural identity and acceptance of social influence.

### *7.4.2 Funerary textile wrappings*

To summarize, the majority of the child mummy bundle is wrapped in a large textile with polychrome bands of red and blue on a brown ground. A thicker, coarser brown woven mantle wraps the back and sides of the body. An alternating dark brown and light brown striped textile covers the head and tucks into the textiles covering the body and is most fragile and damaged with several splits and holes. Bird (1943: 228) notes the use of "raged scraps" of wool cloth to cover the faces of mummies found in the Arica region, and describes its inclusion on a child mummy bundle found during his excavations. In a study by Cassman (2000b) on Arica funerary textiles, no style of tunics and wrappings were found between male and female burials, however finer quality fabrics with minimal decoration were generally associated with females.

All textiles are finely constructed with camelid fiber and woven with a 2-ply S-twist (with each ply spun in a Z direction) (See Figure 4-1-5), all characteristic of Andean highland textile production that is also observed in the coastal regions of northern Chile (Rodman, 2000). Aguero (2008) reports textiles from Arica are similar to those from the Pica Tarapaća style, where trapezoidal tunics with curved and straight warp borders and warp face decorations organized in polychrome lateral bands are often encountered. Tunics are long woven shirts worn by men and women in South America, and usually have an opening at the top for the head to pass through, allowing the tunic to drape the body. The cordage wrapped under the head of the mummy bundle makes the top of the red and blue banded textile difficult to observe. However, its size is large enough to wrap almost the entirety of the bundle, as well as the inclusion of the decorative lateral red and blue bands appear to support the original purpose of the textile as a tunic. Given its large size, more than likely the polychrome banded textile was not originally worn by the child during its lifetime, and was donated by someone older and close to the child.

### *7.4.3 Funerary paraphernalia*

The high radiopacity of the round bottom vessels on the PL and PR side of the mummy support their construction as a dense, inorganic material, such as ceramic or stone. The irregularity of the vessel walls, however, is a strong indication of hand-build construction from fired clay, rather than stone. The hollow and wide globular shape would be very difficult to execute through such a small opening if carved from stone, whereas soft clay can be shaped and built up readily by hand. Therefore, it seems appropriate to state the two globular vessels are fired ceramics, small ollas (Meighan, 1980). The presence of mica (i.e., complex silicates) further supports the vessel material as ceramic made from fired clay, as mica is a common natural component found in clay (Reycraft, 2005). In addition, the elevated levels of Zr, Fe and Mn are characteristic elements in northern Chilean clays (Pardo, Jordan and Montero, 2018; Flewett et al., 2016; Centeno et al., 2012). The two ceramic vessels are similar to other ollas commonly found in burials of Peru and northern Chile, and could either be used for drinking and to hold water, or made as an offering to the deceased (Meighan, 1980; Bird, 1943). The small size of the vessels correlates to what a child might use to drink, or were included in the bundle as an offering. The globular style is a common shape with San Miguel ceramics, and could support the mummy bundle originating from this cultural period (Rivera, 2008; Meighan, 1980).

In a report documenting excavations in Arica, Bird (1943: 212) describes the inclusion of small, spherical vessels inside infant and child burials mummy bundles in the Arica and northern coastal locations Playa Miller and the Playa de los Gringos Cemetery. Bird describes objects found in a mummy bundle of a small child, which includes “two spherical jars, approximately 8 cm high with very narrow openings…the vessels are unpainted and are a pinkish-brown ware” (Bird, 1943: 219). Another spherical vessel of “reddish pottery with a faint black line decoration” in another child mummy bundle, which measures 4.5 cm (h) x 5.5 cm (diameter) with a small opening 1.1 cm across. The descriptions and images of the globular/spherical shaped ceramic vessels provided by Bird are very similar to the globular vessels in the Arica child mummy bundle from the Fowler Museum (Figure 7-4).

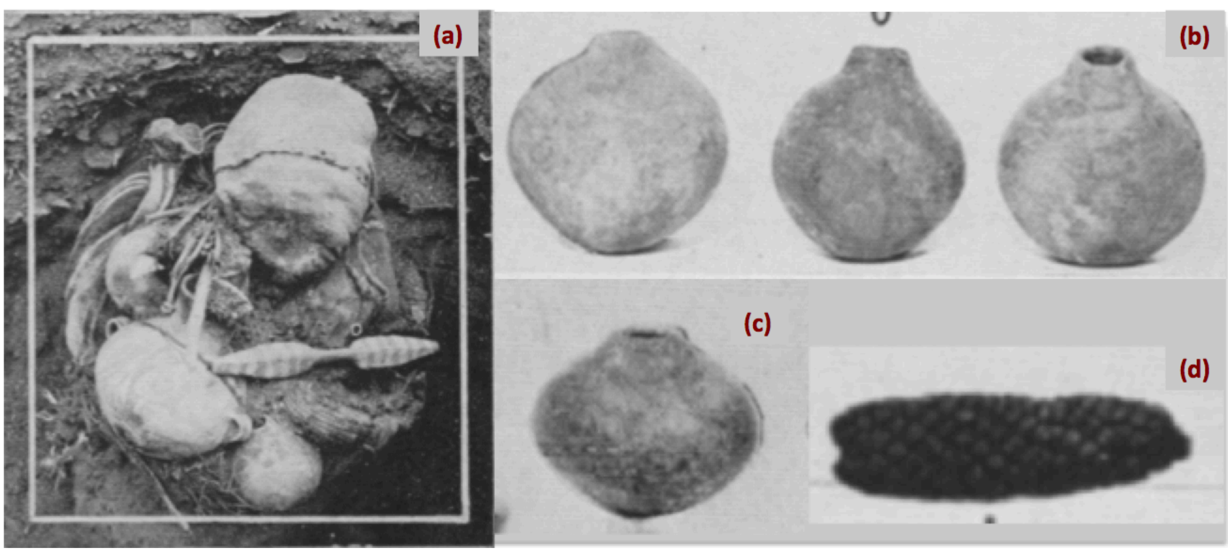

Figure 7-4: Mummy bundle with globular-shaped ceramics and corncobs found by Junius Bird in 1943 Arica excavations. (a): Child mummy burial at Playa Miller. (b): Three globular-shaped ceramic vessels found with Playa Miller child mummy bundle. The vessel in the middle is observed in (a), near the base of the mummy bundle. (c): Globular shaped ceramic vessel found inside child mummy bundle from the Playa de los Gringos Cemetery. (d): Corncob found inside the Playa de los Gringos child mummy bundle. All images courtesy of Bird, 1943.

The CT scan and resulting three-dimensional volumetric rendering and printed ceramic vessel replicas provided a tangible method to visualize and study the vessels, including their exact shape and measurements. What appear to be corncobs were also detected with Computed Tomography, revealing the PR vessel contains a piece that extends from the bottom of the vessel through the opening, and the endoscope further confirmed the presence of a corncob fragment near the PL vessel. The organic pile of residue inside the PL vessel was only observed with the endoscope, and based on its dark brown color and raised texture, could be a remnant from the corncob fragment near the exterior side of the vessel. In a correspondence with Mauricio Ivan Uribe Rodriquez (June 1, 2016) and Bernardo Arriaza Torres (May 10, 2016), both Chilean archaeology experts state it is common for Late Intermediate Period 900-1450 CE) mummy bundles to be buried with small vessels (also referred to as "conquitos") plugged with corncobs as a "tapa", or lid. In addition, Bird (1943) also documents the pairing of small, globular-shaped ceramic vessels with corncob remnants in mummy bundles and burial sites in Arica. His excavation reports provide several examples of corncobs of the red variety, as well as loose corn kernels found in mummy bundles excavated from Arica.

The five top-like objects found clustered together in the child mummy bundle remain unclear in terms of their purpose. 3D computer rendering of the CT scans reveal notches and slight carving marks indicative of shaping with a tool (Figure 6-16 (a)). This could indicate that the objects are potentially made from a dense, carvable material, such as wood, bone, shell or stone s. The number of top-like objects and their placement in a net-like enclosure woven with dark blue fibers is consistent with other documented examples of the mysterious artifacts from other excavations in coastal sites of Arica. Bird (1943) describes these artifacts found with other mummy bundles, including from children burials from Arica (Playa Miller and Playa de los

Gringos) as “top-like objects” (Figure 7-5). Bird states they were usually found in groups of 4-5, with most carved from wood or at times, bone. His descriptions also include they are often found together in a small, open-weave bag or net (Bird, 1943: 208). Some are said to have remnants of “red paint” on the surfaces. Bird offers no interpretation to the purpose or meaning of the top-like objects within a burial context. He notes slight surface differences in the objects’ construction between the two sites. Bird describes the Playa Miller top-like objects as “smooth”, whereas he found the ones from Playa de los Gringos to be “roughly cut” and “crudely whittled”.

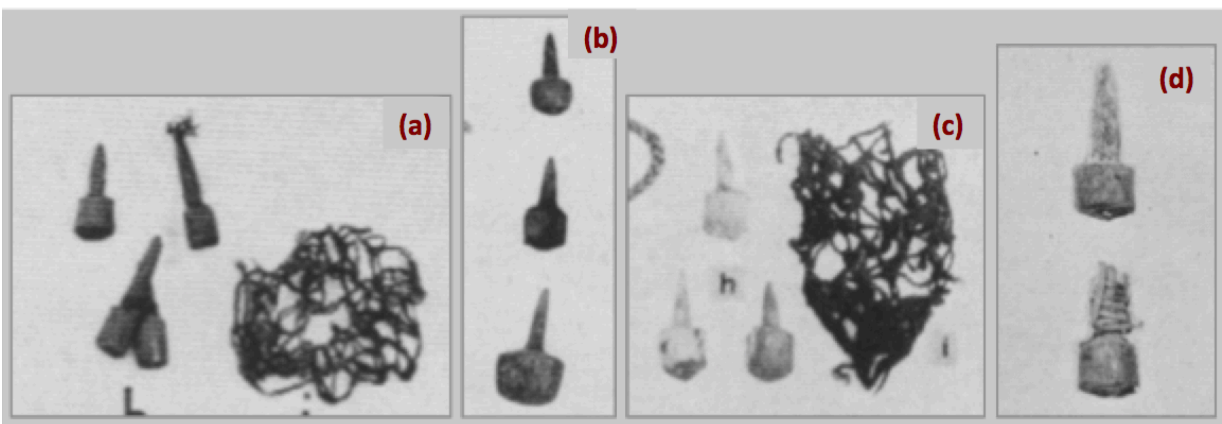


Figure 7-5: (a): Four wooden top-like objects with smoothed surfaces found enclosed together in a netted cord enclosure from a child mummy burial in Playa Miller, Arica. (b): Three of five top-like objects found in another Playa Miller Midden burial. Four are carved wood, one is carved whalebone. (c): Three “roughly cut” wooden top-like objects with red paint from a netted cord pouch found in Playa de los Gringos child burial. (d): Two top-like objects with red paint found in another Playa de los Gringos child burial. The lower object has a strip of rush wound at the stem. All images courtesy of Bird, 1943.

## 7.5 Issues of preservation

### *7.5.1 Human remains and funerary paraphernalia*

Observation with CT shows the skeletal structure of the mummy appears mostly complete, with some disassembly of certain bones from their original position, which are now at the bottom of the bundle interior. This signals the fragility of the skeletal assembly, and movement of the bundle should be minimized to prevent further detachment. The separate bones accessioned with the bundle were confirmed as original to the mummy bundle, which indicates a possible hole in the bundle. This hole might be near the bottom of the bundle. Therefore, the mummy bundle should not be removed from the mount to prevent further loss of material.

The most problematic agents of deterioration for human remains are extreme and inconsistent temperature and humidity levels, especially with repetitive fluxuation (Cassman and Odegaard, 2007: 105). Delamination and cracking of the bone occurs with low humidity (40-45% < 65%), and high humidity (RH > 65%) can cause mold growth, usually observed as white spots (Bowron, 2010). Temperatures of 50-100°C can reactivate bacteria and enzymes in the skin tissues, which can begin to decay the body and become severely problematic in the preservation of the mummy (Aufderheide, 2003: 48). Daylight is another main agent of deterioration for human remains, as it contains Infrared (IR) and ultraviolet (UV) (wavelengths lower than 400 nm) light, which produce heat and high energy wavelength, respectively. While damaging to bone, daylight is most harmful to organic components, which would include the hair and soft tissue of the mummy (Cassman and Odegaard, 2007: 117).

The CT scans and observations made with the endoscope appear to confirm the ceramic vessels lack any structural issues (i.e., cracks, holes, breaks, etc.). The PR 3D printed vessel replica printed with a small, irregular hole on the side, however this is more than likely a result of the 3D printed process, rather than a condition issue on the actual artifact. It is unclear if the vessels contain soluble salts, such as chlorides ($Cl^-$) and nitrates ($NO_3^-$), within the ceramic body. Contamination by salts can occur during burial, especially in coastal archaeological sites, where chlorides are usually present in a substantial quantity and contribute to the formation of soluble salts (sodium chloride is carried inland from the sea in the atmosphere) (Paterakis, 1987). Ceramics can absorb these salts, which migrate and recrystallize with changes in relative humidity and temperature. This phenomenon creates structural instabilities in the ceramic material, such as efflorescence (powdery-white surface accretions), spalling (loss of surface), and structural instability overall.

The top-like objects are more than likely carved from wood and/or potentially bone. Wood is susceptible to softening, expansion, splitting and biological attack (i.e., mold, fungus, insect and pest activity) when exposed to high humidity. Certain invasive insects that use wood as a food source, such as termites and wood boring beetles, pose a thread to wood. Wood boring beetles are commonly associated with wooden artifacts, and are found in panel paintings, books, sculpture, etc. They do most damage at the beetle larvae stage by feeding on the wood interior, creating channels, and emerge through round exit holes when they reach the adult stage (Lewis and Seybold, 2010). In addition to the wooden materials, organic vegetal material, including the corncobs, loose granular material (more than likely corn kernels), and plant fiber cordage, is susceptible to insect and pest activity.

### *7.5.2 Textiles*

The textiles are covered with a layer of light brown dust and soiling. Insect activity can be heightened with materials coated in dust, which is hygroscopic and provides the additional moisture needed by many insects for optimum metabolic and reproductive conditions (Florian, Kronkright and Norton, 1990: 176). XRF analysis detected signals for heavy metals arsenic (As) and lead (Pb) on the surface of the textiles. These are considered carcinogenic and gloves should be worn at all times when handling the mummy bundle. It is also unclear if the mummy bundle was treated with a pesticide to prevent insect activity.  Wool is a prominent food source for insects attracted to proteinaceous materials. Some insects that digest proteinaceous materials and encountered with museum artifact infestations include the clothes moth and carpet beetle. The larvae of these moths and beetles will attack proteinaceous organic materials, putting the mummy hair and wool textiles at risk (Museum Conservation Institute, 2006). If insect activity is observed on the mummy bundle in the future, it is strongly recommended to freeze the mummy bundle as an insect pest eradication strategy, rather than apply chemical treatments, such as insecticides. The bundle is composed of dry adsorbent organic material (i.e., desiccated mummy, textiles, etc.), and application of harmful chemicals can result in toxic byproducts and pose health hazards to the museum (Florian, 1990).

The textiles appear mostly intact, but are fragile, stiff and the light brown areas are slightly yellowed in several areas. This is all indicative of photochemical deterioration from light radiation, which results in both, fading, yellowed discoloration and changes to the mechanical properties of wool (Timar-Balazsy and Eastop, 2012: 51). Photochemical degradation arises with UV radiation exposure, which can occur from natural and artificial light sources. The amino acids within wool that are susceptible to photochemical degradation include histidine, tryptophan, tyrosine, methionine, cystine and cysteine (Timar-Balazsy and Eastop, 2012: 51). These molecules form free radicals with UV light, which weaken the structure overtime through cleavage of the peptide chains, creating shorter molecules and weakened structure, leading to breakage. High levels of humidity can also be adverse for textiles, and can promote dimensional changes, catalyze chemical reactions and promote biological attack (Landi, 1998: 18).

Holes are exhibited in several locations. Many small holes are observed in the textile covering the head (a larger split on PR side, holes in front and two on the PL side), exposing pulled, frayed and broken warps and wefts of the textile. Some of these holes are large enough to expose the bone material of the skull and hair to collect dust and other environmental particulate. The polychrome banded textile covering the body and majority of the bundle exhibits a large split in the on the PL side, exposing a small portion of the ceramic and woven pouch containing loose organic material. The woven structure of the textile in this area is very loose and contains many exposed warps and broken wefts. The proximity of the hole to the heavy ceramic is a concern, and could likely be a contribution to the mechanical damage observed in the textile. This area of the textile should be stabilized and supported with an external support. If left untreated, the hole could potentially get larger, causing the ceramic to dislodge from the bundle. The mantle covering the back and sides of the bundle is also very frayed and brittle.

### *7.5.3 Environmental condition standards*

The mummy bundle comprises several different types of materials; the mummy (bone, skin, hair), ceramics, wood, plant material and wool (with possibly cotton elements) textiles. As the human remains, wood, plant materials and textiles are hygroscopic (ability to absorb water), the materials are sensitive to the environment, and the assemblage should be stored according to the recommended parameters for organic materials. A stable RH without extreme fluxuation should be maintained between 45-65% (not drop below 45% and not exceed 65%) to prevent embrittlement and mold growth of the bone (Boersma, 2013: 33-35; Bowron, 2010). Similarly, these RH parameters will also satisfy the top-like objects, possibly made from wood. An RH lower than 40-45% will cause wood to warp, and if a painted surface is present (Bird notes some top-like objects are found with a red painted surface), cupping and detachment of paint from the wood can occur. RH values over 65% can cause the wood to swell and split, and in high RH environments can develop mold (Stolow, 1987: 8).

As the materials are susceptible to photodegradation, most notably, the exterior textiles, the mummy bundle should be kept in a cool (68 - 72°F) space away from UV and IR light sources to prevent cumulative damage, such as embrittlement and fading of the wool fibers. It is recommended to not exceed 50 lx (below 5 footcandles) in an extended period of time (Philadelphia Museum of Art, 2018; Boersma, 2013: 33-35; 50-51; Brill, 1980: 189-190). Likely the mummy bundle will not be on display, and in that case, should be kept inside the housing with the lid on at all times. This will block harmful UV light as well as protect from dust, debris some pests.

### *7.5.4 Materials appropriate for collection housing*

The mummy bundle is currently on a suitable mount made from polyethylene foam block (Ethafoam®) covered with polyolefin (Tyvek®) and secured with a cotton twill tape strap horizontally over the bundle. Tissue (acid free, unbuffered, pH 7) loosely covers the mummy, which is kept on the mount in a custom box made from foam board (Foam-Core) with a lid that secures with Velcro on the exterior. According to Cassman and Odegaard (2007: 115-116), these are approved materials for the housing of human remains, and the mummy bundle should continue to be housed on the support and kept in the foam-core box while in collections. The tissue should be changed often, as it can absorb acidic environmental components, lowering the pH of the tissue (Kilby, 1995).

Cassman and Odegaard (2007: 115-116) provide a list of approved materials for storage supports to house human remains:

Boards

- <u>Polypropylene board (Coroplast®, Corex™)</u> – a lightweight, rigid corrugated sheet.
- <u>Blue/greyboard</u>. – A corrugated lignin –based paper inner layer sandwiched by smooth acid-free paper.
- <u>Acid-free foam board (Foam-Core, Gatorboard®, ArtCore®)</u> – a lightweight, rigid material made with extruded polystyrene backed with paper or plastic sheet.

- Acid-free cardboard – a corrugated sheet with a single or double ply.
- Acid-free blotter – a porous, absorbent paper made from cellulose for use as a barrier.

Film/Sheets

- Polytetrafluorethylene (PTFE) (Teflon™) – a smooth, low static charge film used as a wrap or barrier. Material sticks to itself.
- Polyethylene sheet – a smooth, translucent film. Make sure it is not recycled polyethylene, which can contain harmful contaminants.
- Polyester (Mylar®) – a clear, inert semi-flexible film. Used to encapsulate and create barriers between materials.
- Acid-free tissue, unbuffered – a lightweight smooth paper made from cellulose with a neutral pH (7). Used for interleaving, covering, wrapping and padding materials.
- Polyester tissue (Hollytex) – a fine, nonwoven sheer material for interleaving and wrapping materials.
- Polyolefin (Tyvek®) – a non-woven, spun-bounded polyethylene olefin used for wrapping and lining.
- Polyethylene/metal (Marvelseal® 360) – an aluminized polyethylene and nylon barrier film. Heat-sealable and used as a method of passive humidity and pest control.

Foams and Paddings

- Polyethylene (Ethafoam®) – stable, open-cell foam used for lining, supporting, mount making and cushioning. Available in different densities.
- Polyethylene (Volara®) – a soft and stable, flexible closed-cell foam used for lining and cushioning materials. Moldable with heat, and available in different densities and thicknesses.

- Polypropylene (Microfoam™) – stable, open-cell foam.
- Polyester batting – polyester (100%) needle-punched material. No resin bonding or flame retardants added is preferred. Used for cushioning.

Fabrics

- Stockinette – a smooth, soft and seamless tubular knit fabric. Used to cover supports and make cushioning supports.
- Cotton fabric (Muslin) – an unbleached cotton used to wrap, cover and create a barrier between materials. Always wash before use to remove finished and sizing.
- Cotton tie (Twill tape) – a soft and strong cotton twill weave tape used to secure artifacts in packing.
- Polyester fabric – a smooth, soft and strong fabric.

Unsuitable materials

- Bubble pack
- Cotton batting (contains lignin)
- Ester and ether-based urethanes
- Starch packing peanuts and polystyrene packing peanuts
- Polyvinylidene chloride (PVDC, Saran® wrap).

#### *7.5.5 Cultural and ethical considerations for South American human remains*

After a discussion with Wendy Teeter, the Curator of Archaeology at the Fowler Museum, it was decided ethically best to not 3D print any of the human remains. This decision was made due to the lack of a cultural provenance associated with the mummy bundle and therefore, the inability of modern descendants to provide consent or guidance. This lack of a primary source makes it impossible to answer if 3D replicas of the human remains would be acceptable, or discourteous to the living descendants to which the bundle culturally belongs. To ensure that the integrity of the mummified individual is maintained, only associated objects detected in the bundle were replicated three dimensionally to better visualize the shape, size and condition of the objects in the mummy bundle.

# 8 Conclusion

The goals of this study were to determine the Fowler Museum mummy bundle assembly, burial context and cultural significance through non and minimally-invasive scientific techniques. The study confirms the inclusion of mummified child human remains with an arrangement of associated artifacts wrapped together in woven textiles and tied with plant fiber cordage. Based on the results, the origin of the mummy bundle is in the coastal region of Arica, and proposes a cultural provenance of the San Miguel cultural period (990 – 1350 CE) in the Late Intermediate Period (LIP) (1000 – 1450 CE). In addition, the separate bones originally accessioned in 1966 with the  mummy bundle appear to originate from the human remains inside assemblage.

The interior of mummy bundle was CT scanned, and 3D visualization of the bundle contents with high dimensional accuracy was achieved. The CT data provided a means to reconstruct the mummy bundle as a whole, as well as 3D render the objects and skeletal remains individually to assist study, and not interfere with the integrity of the mummy. The results determined the bundle to contain the remains of a child of approximately 3-4 years old at the time of death. Positioned around the mummy are two globular shaped ceramics, five top-like objects possibly carved from wood, corncobs and a bag of food (more than likely corn). The globular shaped ceramics, or ollas, as well as the artificial cranial modified (ACM) skull, correlate to mummy bundles from the LIP.

CT analysis was successful in the visualization of dense materials, but softer, more radiolucent materials such as skin and hair were incapable of observation with this form of analysis. The high energy X-rays required to penetrate through the textile wrappings to observe the denser materials inside passed through the skin and hair of the mummy, as well as the net holding the top-like objects. The incorporation of the endoscope in the assessment of the mummy bundle interior provided the ability to view softer, less dense organic components, and confirmed the mummy exhibits some preserved skin and laterally braided hair on the skull. The combination of CT and the endoscope were complementary techniques to observe all types of materials present in the bundle as well as assess the condition. No major structural instabilities of the assemblage were observed. The PL ceramic, however, is in close proximity to the large split in the mantle. It is highly recommended to stabilize this split to prevent the ceramic from falling out of the bundle. Internally, the bundle looks stable, overall. To ensure its continued preservation, it is imperative the mummy bundle be kept in a cool storage environment without excessive humidity.

Study of the mummy bundle textile technology resulted in identification of camelid fiber for all three textiles wrapping the mummy, with the possibility of the dark brown fiber from the mantle as cotton. The incorporation of camelid predominant fiber-based textiles is common with northern Chilean burials, and the ollas and top-like wooden (and/or bone) objects are also found with other coastal bundles from the Arica region (Rodman, 2000; Bird, 1943). The polychrome textile covering the majority of the body of the mummy bundle was identified to have the plant-based dyes *Relbunium hypocarpium,* as the red dye source in the red fibers, and *Indigofera* as the blue dye source in the dark blue and blue-green fibers of the horizontal banded design. These are two prominent dyes used in textile production in the Andean region, including northern Chile from the Formative Period until cochineal became the more prominent dye source during the Inca Period. The aesthetics of the red and blue stripes with a neutral light brown background of the polychrome textile and the alternating dark and light brown fully striped textile covering the head are both characteristic of textiles found with mummy bundles in the LIP of Arica (Cassman 2000a, 2000b).

The Fowler Museum mummy bundle correlates with other examples from the coastal regions of Arica (Bird 1943; Agüerro Piwonka, 2000; Cassman, 200a, 2000b). Therefore, the attribution to Arica, Chile provided by Chilean Trade Project object list is confirmed. A distinguishing feature that attributes a specific cultural provenance is the annular style of artificial cranial modification (ACM), where the head of an infant is bound with textiles without the addition of wooden boards. The annular style of modification was a common practice with the San Miguel period of northern Chile, and supports the mummy bundle provenance to this cultural group within the LIP coastal region of Arica (Sutter, 2006). Based on the results presented, further study into the anthropological aspects of the child mummy bundle to solidify the cultural provenance as San Miguel is encouraged. This should also include research into the purpose of the top-like objects and their distribution in northern Chile, which would help to determine the importance of their inclusion in a mummy bundle.

# 9 Appendices

## 9.1 Condition assessment

Note: The front of the mummy bundle is designated as the side with the horizontal red and blue stripes of the polychrome-banded textile and the feet of the mummy bundle facing forward. The mummy bundle is supported on a mount made from Ethafoam®, Teflon® Relic Wrap™ and acid-free unbuffered tissue. The mummy was never removed from the mount during examination, documentation and analysis procedures due to the fragility of the assemblage. Therefore, the bottom and back portions of the bundle were not examined.

#### *9.1.1 Textiles and cordage*

From observation of the exterior, the mummy bundle assemblage appears mostly intact and stable, overall. All three textiles appear secure in their placements and held in place with the wrapped plant fiber cordage. Breakage is exhibited in a few locations of the cordage (PR side, front and PL side), but the broken ends are held in place by subsequent layers of wrapped plant fiber cordage. The cordage is also fraying and exhibits broken fibers in several locations of the piled sections. The textiles are fragile and embrittled. Splits are observed as groupings of broken warps and wefts in all three textiles. Holes are found as pulled and/or missing warps and wefts in several locations. The largest hole is in the mantel on the PL side. This hole exposes many broken warps and wefts, and uncovers a portion of the ceramic and pouch containing loose organic material. The textile covering the head has a large split on the PR side, and several other small holes in the front and PL side. No holes appear to be present on the PR side of body textiles (polychrome textile and mantle.

Mottled yellowing is observed throughout the light brown fibers, and the red and blue dyes appear muted, as if they are faded. The mummy bundle is covered in a layer of soil, dust and other debris (i.e., feather barbules, fibers, etc.). XRF detected a signal for sulfur (S), which can be interpreted as either the sulfide linkages of the cysteine in wool, a mineral in the burial soil, or both. XRF also identified calcium (Ca), strontium (Sr), potassium (K), iron (Fe), manganese (Mn), and titanium (Ti). Trace amounts of other elements were also detected: arsenic (As), zirconium (Zr), Rubidium (Rb), gold (Au), zinc (Zn), copper (Cu), barium (Ba) and thorium (Th). These elements more than likely originate from the Chilean burial environment, especially As could be attributed to the arsenic-rich soils of the Atacama Desert (Díaz et al., 2004). Lead (Pb) was only detectable at a level of 9.14 ppm on the PL shoulder of the bundle, and registered at below the limit of detection (LOD) in other locations of analysis.

The detection of the heavy arsenic and lead signify the presence of toxic heavy metals on the funerary wrappings. Daily ingestion of 3-4 mg of As can result in long-term toxicity, and an acute ingestion of 1-3 mg/kg may be lethal (Seifert et al., 2000). Gloves should be worn at all times when handling the assemblage. Lastly, a patch of white surface debris is located on the textile covering the head, but only in the lower portion of the front of the face, and slightly justified towards the PR side. The white debris is strongly adhered to the textile surface, and could be salts from burial.

### *9.1.2 Mummy bundle interior*

The bones of the mummy skeleton are mostly intact. CT analysis allows observation of the bones, revealing information on their location and structural condition. The mandible has dropped, leaving the jaw to hinge open. The skull is also slightly slumped towards the PL side of the bundle, but is contained within the textile. A front incisor has fallen from jaw and trapped between the folds of the textile around neck. Analysis of the CT scans reveals that several small bones, including ribs, vertebrae, bones from the hands and others have fallen to bottom of bundle. The leg and arm bones, as well most of the ribs are in their original locations within the semi-flexed position of the mummy.

Analysis of the CT scans did not indicate any structural issues (i.e., breaks, cracks, etc.), but was limited in determining surface conditions of the bones. Endoscope analysis through existing holes in the textiles provided means to observe portions of the jaw. The teeth that remain in the mandible and maxilla are yellow with white and brown deposits on the surface. The skin appears mostly intact on the skull, however, seems absent on the lower PR side of skull, such as in the mandible area. The skin observed is thin and a light tan-brown color, as observed on the portion of the right foot separately accessioned with the mummy bundle  In addition, observation with the endoscope through a split on the PR side found a small lateral braid of dark brown hair. The section of hair was smooth and held securely within the braid, which could be an indication of additional hair on the head, possibly in a similar condition.

Based on observation of the CT scan, the ceramic vessels appear structurally stable, with no indication of cracks, holes or loss of material. The small portion of the ceramic exposed through the hole in the mantle revealed a stable surface without evidence of salt efflorescence. However, this is only a small portion of the ceramic that can be studied, and beyond the information provided with CT, the remainder of the vessel surface condition remains unclear. What looks like a small pile of organic material, possibly a corncob remnant (based on the raised texture), is located on the bottom of the PL vessel interior. A larger remnant of a corncob (possible topper for the vessel) is observed near the hole in the mantle and next to the ceramic. Both, the ceramic and corncob fragment are in proximity to the weakened area of the mantle, and where the large hole in the textile exists.

Under a flap of textile on top portion close to the PR side of the bundle a portion of one of the top-like objects is observed in a woven blue fiber net. The object seems secure in its placement, and the surface is hard and smooth, and dark brown in color. The other top-like objects are too far into the bundle to be observed. In addition, the organic loose material in the woven pouch on the PL side in the bundle interior cannot be observed with the available methods of analysis. Based on the CT results, the material appears to be tightly contained. A small portion of the woven pouch is visible through the large hole in the mantle, and has a thin red stripe with a thick purple-mauve colored band. A white yarn binds a portion of the pouch, which seems secure in its placement.

## 9.2 Separate bones accessioned with the mummy bundle

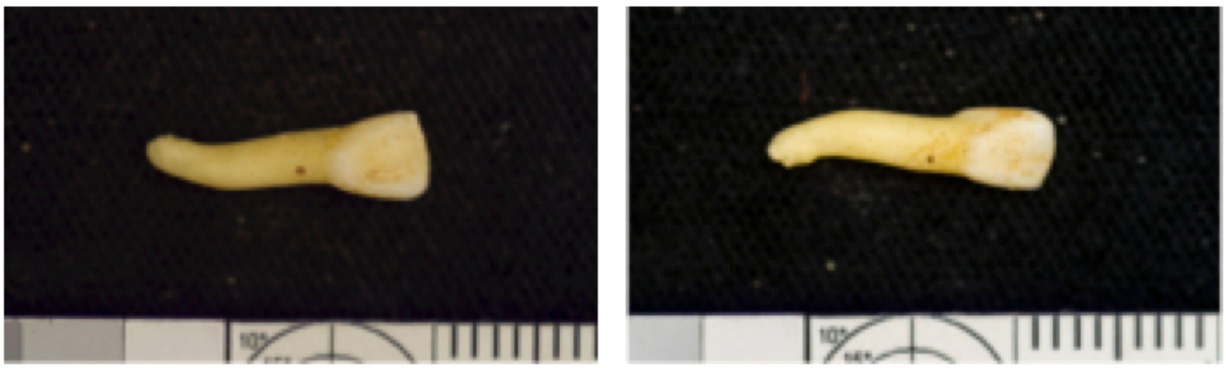

Figure 9-1: Upper deciduous lateral incisor. (Left): Labial (against the lips) side of the incisor. (Right): Lingual (against the tongue) side of the incisor.

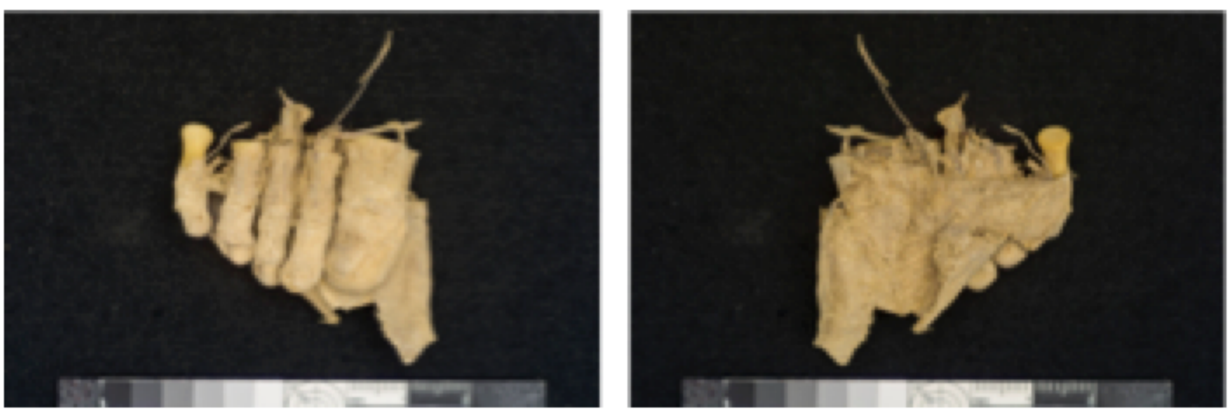

Figure 9-2: Portion of the right foot containing all five toes. (Left): Top of toes. (Right): Bottom of foot and toes, with mummified skin folded over toes.

Figure 9-3: “Sacrum” labeled on polytheylene ziptop storage bag. (Left): Side 1. (Right): Side 2.

Figure 9-4: “Right ischium” labeled on polytheylene ziptop storage bag. (Left): Side 1. (Right): Side 2.

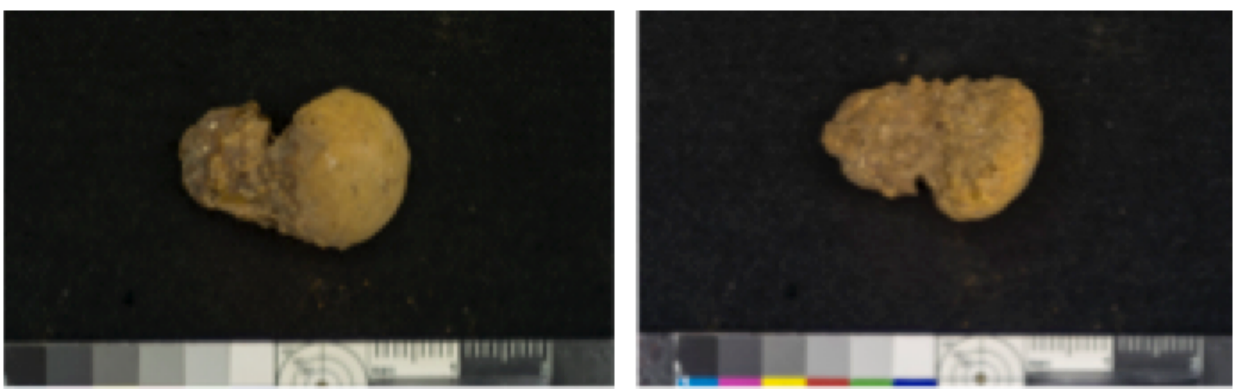

Figure 9-5: Unlabeled bone, possibly an epiphysis. (Left): Side 1. (Right): Side 2.


Figure 9-6: “Left ulna” labeled on polytheylene ziptop storage bag. (Left): Side 1. (Right): Side 2.

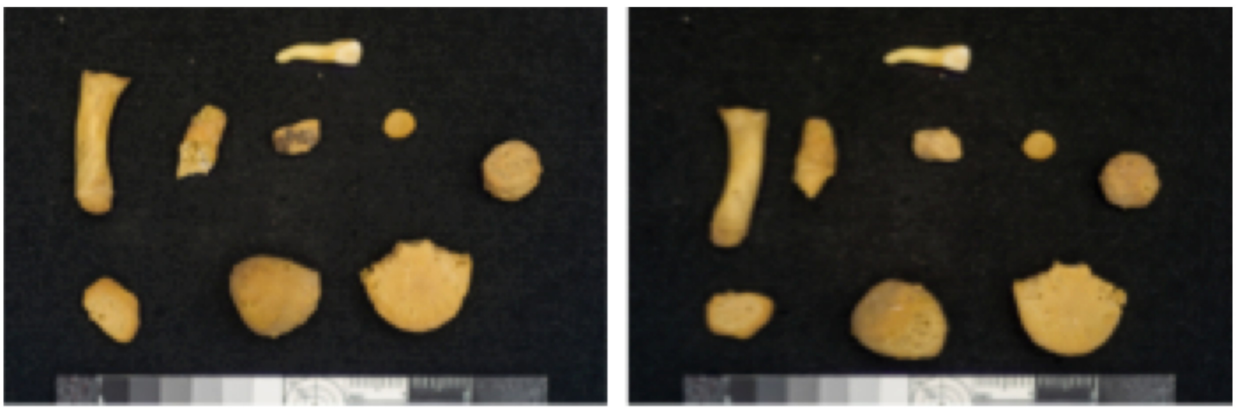

Figure 9-7: Unlabeled bones, compiled into a single polytheylene ziptop storage bag. The bones in the row closest to the scale could possibly be vertebrae. (Left): Side 1. (Right): Side 2.

## 9.3 Surface Enhanced Raman Spectroscopy (SERS) Spectra – Red Fibers

The silver nanoparticles (AgNPs) in this study were synthesized with the Lee and Meisel method (1982) by Moupi Mukhopadhyay and Xuanyi Wu, graduate students with the UCLA Materials Science and Engineering Department. Wu also performed the microextraction with HF vapors on the red mummy fiber, the *Relbunium hypocarpium* and *Relbunium ciliatum*/*Galium antuneziae* fibers in the Molecular and Nano Archaeology Lab at UCLA.

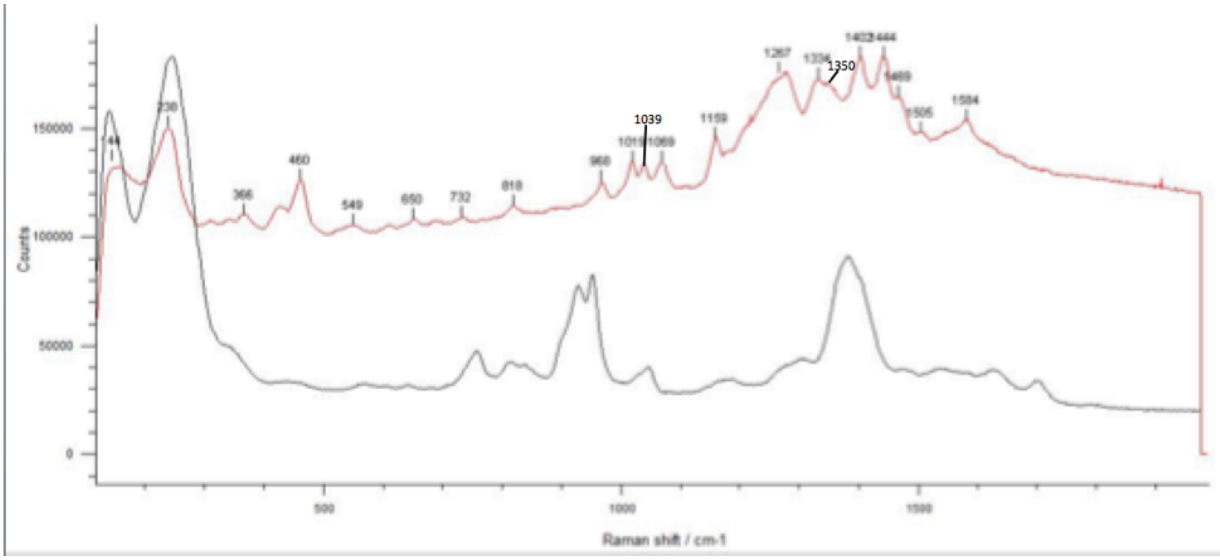


Figure 9-8: Surface Enhanced Raman Spectroscopy (SERS) of the red mummy fiber (red) and μ-Raman spectrum of the silver nanoparticles (AgNPs) used for analysis on all red fiber SERS spectra. SERS spectrum of the red mummy fiber was collected after pretreatment with hydrofluoric (HF) acid.

## 9.4 Analysis, Sampling, Imaging and Three-Dimensional Printing Permission

Wendy Teeter, Curator of Archaeology at the Fowler Museum at UCLA, and Christian de Brer, Head Conservator of the Fowler Museum at UCLA, both approved the use of all analysis performed and permission to sample fibers from the mummy bundle for fiber and dye identification. Wendy Teeter approved the use of Computed Tomography and two and three-dimensional rendering of the mummy bundle in its entirety, including the human remains and associated funerary objects. Approval was granted by Wendy Teeter to print replicas of the funerary objects, and it was requested that no human remain components of the mummified child be replicated with three-dimensional printing. This decision was made on ethical principles and respect for the mummified individual as well as the lack of a cultural provenance associated with the mummy bundle and therefore, the inability of modern descendants to provide consent or guidance. As a result, the present-day ancestors are unknown and a consultation requesting permission is not possible. This lack of a primary source makes it impossible to answer if 3D replicas of the human remains would be acceptable, or discourteous to the living descendants' ancestors to which the bundle culturally belongs. To ensure that the integrity of the mummified individual is maintained, only associated objects detected in the bundle will be replicated three dimensionally to better visualize the shape, size and condition of the objects in the mummy bundle.

# 10 Bibliography

Aceto, M., Agostino, A., Fenoglio, G., Idone, A., Gulmini, M., Picollo, M., Ricciardi, P. and Delaney, J.K. 2014. Characterization of colourants on illuminated manuscripts by portable fibre optic UV-visible-NIR reflectance spectrophotometry. *Analytical Methods* 6: 1488-1500.

Aguero, C. 2008. The use of trapezoidal tunics with curved warp borders as a means to define the Pica Tarapacá cultural group of Northern Chile (900-1200 AD). *Textiles as Cultural Expressions*. Textile Society of America 11th Biennial Symposium, 24-27, September 2008.

Agüero Piwonka, C. 2000. Las tradiciones de tierras atlas y de calles occidentales en la textileria arqueológica del calle de Azapa. *Chungara: Revista de Antropología Chilena* 32(2): 217-226.

Allison, Marvin J. 1984. Paleopathology in Peruvian and Chilean populations. *Paleopathology at the Origins of Agriculture*: 515-529.

Applebaum, N. and Applebaum, Y.H. 2005. Chapter 4-1: The Use of Medical Computed Tomography (CT) Imaging in the Study of Ceramic and Clay Archaeological Artifacts form the Ancient Near East. *X-rays for Archaeology*. Uda, M., Demortier, G. and Nakai, I. (Eds.). The Netherlands: Springer: 231-245.

Appleyard, H.M. 1978. *Guide to the Identification of Animal Fibers*. Leeds: British Textile technology Group.

Andreev, G. N., Schrader, B, Schulz, H., Fuchs, R., Popov, S. and Handjieva, N. 2001. Non-destructive NIR-FT-Raman analyses in practice. Part 1. Analyses of plants and historic textiles. *Fresenius Journal of Analytical Chemistry* 371: 1009-1017.

Antúnez de Mayolo, K.K. 1989. Peruvian Natural Dye Plants. *Economic Botany* 43(2): 181-191.

Arriaza Torres, B. 2016. Personal correspondence, 10 May 2016.

Arriaza, B., Cárdenas-Arroyo, F., Kleiss, E., and Verano, J.W. 1998. Chapter 10: South American Mummies: Culture and Disease. *Mummies, Disease & Ancient Cultures*, second ed. Cockburn, A., Cockburn, E. and Reyman, T.A. (Eds.). New York: Cambridge University Press: 190-234.

Aufderheide, A.C. 2003. *The Scientific Study of Mummies*. Cambridge: Cambridge University Press.

Baitzel, S.I. and Goldstein, P.S. 2014. More than the sum of its parts: Dress and social identity in a provincial Tiwanaku child burial. *Journal of Anthropological Archaeology* 35: 51–62.

Bass, W. M. 1995. *Human Osteology: A Laboratory and Field Manual.* Fourth ed. Columbia: Missouri Archaeological Society, Inc.

Bernardino, D., de Faria, D.L.A. and Negrón, A.C.V. 2015. Applications of Raman spectroscopy in archaeometry: An investigation of pre-Columbian Peruvian textiles. *Journal of Archaeological Science: Reports* 4: 23–31.

Byers, S. N. 2002. *Introduction to Forensic Anthropology: A Textbook*. Boston: Allyn and Bacon.

Bird, J.S. 1988. *Excavaciones en el Norte de Chile, Arica: Ediciones Universidad de Tarapacá*.

Bonavia, D. 2008. *The South American Camelids: An Expanded and Corrected Edition*. Los Angeles: The Cotsen Institute of Archaeology, UCLA.

Bowron, E.L. 2010. A new approach to the storage of human skeletal remains. *The Conservator* 27(1): 95-106.

Brill, T.B. 1980. *Light: Its Interaction with Art and Antiquities*. New York: Plenum Press.

Brown, J.P. and Robert D. Martin. 2014. Restoration by other Means: CT Scanning and 3D Computer Modeling for the re-Restoration of a Previously Restored Skull from the Magdalenian Era. *Objects Specialty Group Postprints* 21: 81-101.

Canaza-Cayo, A.W., Cozzolino, D., Alomar, D. and Quispe, E. 2012. A feasibility study of the classification of Alpaca (Lama pacos) wool samples from different ages, sex and color by means of visible and near infrared reflectance spectroscopy. *Computers and Electronics in Agriculture* 88: 141-147.

Cardon, D. 2007. *Natural Dyes: Sources, Tradition, Technology and Science*. London: Archetype.

Cassman, V. and Odegaard, N. 2007. Storage and Transport. *Human Remains: A Guide for Museums and Academic Institutions*, Cassman, V., Odegaard, N. and Powell, J. (Eds.). Lanham, MD: AltaMira Press: 103-128.

Cassman, V. 2000(a). Prehistoric Ethnicity and Status Based on Textile Evidence from Arica, Chile. *Beyond Cloth and Cordage: Archaeological Textile Research in the Americas*. Drooker, P.B. and Webster, L.D. (Eds.). The University of Utah Press: Salt Lake City: 253-266.

Cassman, V. 2000(b). Prehistoric Andean Ethnicity and Status: The Textile Evidence. *Revista de Antropología Chilena* 32(2): 253 -257.

Centeno, S.A., Williams, V.I., Little, N. and Speakman, R.J. 2012. Characterization of surface decorations in Prehispanic archaeological ceramics by Raman spectroscopy, FTIR, XRD and XRF. *Vibrational Spectroscopy* 58: 119-124.

Clementi, C., Doherty, B., Gentili, P.L., Miliani, C., Romani, A., Brunetti, B.G. and Sgamellotti, A. 2008. Vibrational and electronic properties of painting lakes. *Applied Physics A: Materials Science & Processing* 92: 25-33.

Comelli, D., Nevin, A., Valentini, G., Osticioli, I., Castellucci, E.M., Toniolo, L., Gulotta, D. and Cubeddu, R. 2010. Insights into Masolino's wall paintings in Castiglione Olona: Advanced reflectance and fluorescence imaging analysis. *Journal of Cultural Heritage* 12: 11-18.

Conlogue, G. 2015. Considered Limitations and Possible Applications of Computed Tomography in Mummy Research. *The Anatomical Record* 298: 1088-1098.

Davey, J., Stewart, M.E.B. and Drummer, O.H. 2013. The value of CT imaging of Horus in determining the method of mummification and the sex of the mummy. *Journal of Medical Imaging and Radiation Oncology* 57: 657-662.

Degano, I. and Colombini, M.P. 2009. Multi-analytical techniques for the study of pre-Columbian mummies and related funerary materials. *Journal of Archaeological Science* 36: 1783-1790.

Díaz, O.P., Leyton, I., Muñoz, O., Núñez, N., Devesa, V., Súñer, M.A., Vélez, D. and Montoro, R. 2004. Contribution of Water, Bread, and Vegetables (Raw and Cooked) to Dietary Intake of Inorganic Arsenic in a Rural Village of Northern Chile. *Journal od Agriculture and Food Chemistry* 52: 1773-1779.

Dutra Moresi, C.M., Wouters, J., 1997. HPLC analysis of extracts, dyeings and lakes, prepared with 21 species of Relbunium. *Dyes in History and Archaeology* 15: 85-97.

El-Najjar, M.Y. and Dawson, G.L. 1977. The Effect of Artificial Cranial Deformation on the Incidence of Wormian Bones in the Lambdoidal Suture. *American Journal of Physical Anthropology* 46: 155-160.

Flewett, S., Saintenoy, T., Sepúveda, M., Mosso, E.F., Rolbes, C., Vega, K., Gutierrez, S., Romero, A., Finney, L., Maxey, E. and Vogt, S. 2016. Micro X-ray Fluorescence Study of Late Pre-Hispanic Ceramics from the Western Slopes of the South Central Andes Region in the Arica y Parinacota Region, Chile: A New Methodological Approach. *Applied Spectroscopy* 70(10): 1759-1769.

Florian, M.L.E., Kronkright, D.P. and Norton, R.E. 1990. *The Conservation of Artifacts Made from Plant Materials*. Marina del Rey: Getty Conservation Institute.

Florian, M.L.E. 1990. Freezing for Museum Insect Pest Eradication, *Collection Forum* 6(1), (Spring): 1-7.

Frenais, M., Richardin, P., Gimat, A., Sepúlveda, M., Leize-Wagner, E. and Charrié, A. 2015. Recent advances in the characterization of hair of mummies from the Chilean Andean coast. *Forensic Science International* 249: 25-34.

Fujita, M.Q., Taniguchi, M., Zhu, B., Quan, L., Ishida, K., Oritani, S., Kano,T., Kamikodai, Y. and Maeda, H. 2002. Inca bone in forensic autopsy: a report of two cases with a review of the literature. *Legal Medicine* 4: 197-201.

Gerszten, P.C. 1993. An Investigation into the Practice of Cranial Deformation among the Pre-Columbian Peoples of Northern Chile. *International Journal of Osteoarchaeology* 3: 87-98.

Gishen, M. and Cozzolino, D. 2007. Feasibility study on the potential of visible and near infrared reflectance spectroscopy to measure alpaca fibre characteristics. *Animal* 1(6): 899-904.

Gordon, H.B. 1931. The Identification of Fibers. *The Melliand Textile Monthly* 3(6).

Grazia, C., Clementi, C., Miliani, C., and Romani, A. 2011. Photophysical properties of alizarin and purpurin Al (III) complexes in solution and in solid state. *Photochemical & Photobiological Sciences* 10(7): 1249-1254.

Gulmini, M., Idone, A., Diana, E., Gastaldi, D., Vaudan, D. and M. Aceto. 2013. Identification of dyestuffs in historical textiles: Strong and weak points of a non- invasive approach. *Dyes and Pigments* 98: 136-145.

Kakoulli, I., Radpour, R., Lin, Y., Svoboda, M. and Fischer, C. 2017. Application of forensic photography for the detection and mapping of Egyptian blue and madder lake in Hellenistic polychrome terracottas based on their photophysical properties. *Dyes and Pigments* 136: 104-115.

Kilby, V. 1995. Buffered And Unbuffered Storage Materials. *Conserve O Gram*, National Park Service (4/9), (July): 1-4.

Langley, K.D. and Kennedy, Jr., T.A. 1981. The Identification of Special Fibers. *Textile Research Journal:* 703-709.

Lee, P.C. and D. Meisel. 1982. Adsorption and Surface-Enhanced Raman of Dyes on Silver and Gold Sols. *Journal of Physical Chemistry* 86: 3391-3395.

Lewis, V.R. and Seybold, S.J. 2010. Wood-boring Beetles in Homes: Integrated Pest Management in the Home. *Pest Notes, University of California Statewide Integrated Pest Management Program Agriculture and Natural Resources* (7418): 1-4.

Leona, M., Stenger, J., and Ferloni, E. 2006. Application of surface-enhanced Raman scattering techniques to the ultrasensitive identification of natural dyes in works of art. *Journal of Raman Spectroscopy* 37: 981-992.

Leona, M., Casadio, F., Bacci, M. and Picollo, M. 2004. Identification of the Pre-Columbian Pigment Maya blue on Works of Art by Noninvasive UV-Vis and Raman Spectroscopic Techniques. *Journal of the American Institute for Conservation* 43(1): 39-54.

Meighan, C.W. & True, D. L. 1980. *Prehistoric trails of Atacama: Archaeology of Northern Chile.* Los Angeles: Institute of Archaeology, the University of California.

Melo, M.J. and Claro, A. 2010. Bright Light: Microspectrofluorimetry for the Characterization of Lake Pigments and Dyes in Works of Art. *Accounts of Chemical Research* 43(6): 857-866.

Minkes, W. 2005. *Wrap the Dead: The funerary textile tradition from the Osmore Valley, South Peru, and its social-political implications*. The Netherlands: Faculty of Archaeology, Leiden University.

Museum Conservation Institute. 2006. Insects and Wool Textiles. Smithsonian Institution. https://www.si.edu/mci/english/learn_more/taking_care/insects.html. Accessed 16 May 2018.

Niemeyer, H.M. and Agüero, C. 2015. Dyes used in pre-Hispanic textiles from the Middle and Late Intermediate periods of San Pedro de Atacama (northern Chile): new insights into patterns of exchange and mobility. *Journal of Archaeological Science* (57): 14-23.

Niemeyer, H.M., Zapata, V., Cantillana, P., Missene, A., Aguilera, J. and Torres, A. 2013. Computed Tomography study of snuff trays from San Pedro de Atacama (Northern Chile). *Journal of Archaeological Science* 40: 2036-2044.

Pardo, F., Jordan, M.M. and Montero, M.A. 2018. Ceramic behavior of clays in Central Chile. *Applied Clay Science* 157: 158–164.

Paterakis, A.B. 1987. The deterioration of ceramics by soluble salts and methods for monitoring their removal. *Recent Advances in the Conservation and Analysis of Artifacts*, Jubilee Conservation Conference, London: 6-10.

Peters, A., Cassman, V., and Gustafsson. 2007. Associated Artifacts. *Human Remains: A Guide for Museums and Academic Institutions*, Cassman, V., Odegaard, N. and Powell, J. (Eds.). Lanham, MD: AltaMira Press.

Philadelphia Museum of Art. 2018. Preventative Conservation Activities: Light. *Conservation Research*. Web. http://www.philamuseum.org/conservation/10.html?page=1. Accessed 16 May 2018.

Phipps, E. *The Peruvian Four-Selvedge Cloth: Ancient Threads, New Directions*. Los Angeles: The Fowler Museum at UCLA.

Rambaldi, D.C., Pozzi, F., Shibayama, N., Leona, M. and Preusser, F.D. 2015. Surface pseudopurpurin in the interpretation of the spectra. *Journal of Raman Spectroscopy* 46: 1073–1081.

Reycraft, R.M. 2005. Style Change and Ethnogenesis among the Chiribaya of Far South Coastal Peru. *Us and Them: Archaeology and Ethnicity in the Andes*. Reycraft, R.M. (Ed.). Los Angeles: The Cotsen Institute of Archaeology, UCLA.

Rivera, M. 2008. Chapter 48: The Archaeology of Northern Chile. *Handbook of South American Archaeology*. Silverman, H. and Isbell, W.H. (Eds.). New York : Springer Science + Business Media, LLC: 963-977.

Rodman, A.O. 2000. Andean Textiles from Village and Cemetery: Casserones in the Tarapaća Valley, North Chile. *Beyond Cloth and Cordage: Archaeological Textile Research in the Americas*. Drooker, P.B. and Webster, L.D. (Eds.). Salt Lake City: The University of Utah Press: 229-251.

Roquero, A. 2008. Identification of red dyes in textiles from the Andean region. *Textile Society of America Symposium Proceedings*, Paper 129.

Salazar, D., Niemeyer, H.M., Horta, H., Figueroa, V. and Manríquez, G. 2014. Interaction, social identity, agency and change during Middle Horizon San Pedro de Atacama (northern Chile): A multidimensional and interdisciplinary perspective, *Journal of Anthropological Archaeology* 35: 135-152.

Scheuer, L., Black, S. and Christie A. 2016. *Developmental Juvenile Osteology,* Second Edition. London: Elsevier Ltd.

Schweppe, H. 1986. *Practical Hints on Dyeing with Natural Dyes: Production of comparative dyeing for the identification of dyes on historic textile materials*. Washington, DC: Conservation Analytical Laboratory, Smithsonian Institution.

Seifert, S.A, Boyer, L.V., Odegaard, N., Smith, D.R. and Dongoske, K.E. 2000. Arsenic Contamination of Museum Artifacts Repatriated to a Native American Tribe. *Journal of the American Medical Association* 283 (20) (May 24-31): 2658-2659.

Sibley, L. R. and Jakes, K. A. 1994. Implications of coloration in Etowah textiles from burial 57. *Archaeometry of Pre-Columbian Sites and Artifacts: Proceedings of the Archaeometry Conference, UCLA*. Scott, A. D. and Meyers, P. (Eds.). Los Angeles: The Getty Conservation Institute: 395-418.

Splitstoser, J.C., Dillehay, T.D., Wouters, J. and Claro, A. 2016. Early pre-Hispanic use of indigo blue in Peru. *Science Advances*, 2: 1-4.

Stanford Children's Health. 2018. Anatomy of a Newborn Skull. http://www.stanfordchildrens.org/en/topic/default?id=anatomy-of-the-newborn-skull-90-P01840. Web. Accessed 4 February 2018.

Stolow, N. 1987. *Conservation and Exhibitions: Packing, transport, storage and environmental considerations*. London: Butterworth & Co. (Publishers) Ltd.

Sutter, R. C. 2006. The Test of Competing Models for the Prehistoric People of the Azapa Valley, Northern Chile using Matrix Correlations. *Chungara: Revista de Antropología Chilena*, 38(1): 63–82.

Sutter, R.C. 2005. A Bioarchaeological Assessment of Prehistoric Ethnicity among Early Late Intermediate Period Populations of the Azapa Valley, Chile. *Us and Them: Archaeology and Ethnicity in the Andes*. Reycraft, R.M. (Ed.). Los Angeles: The Cotsen Institute of Archaeology, UCLA:183-205.

Timar-Balazsy, A. and Eastop, E. 2012. *Chemical Principles of Textile Conservation,* First Edition, London: Routledge.

Torres-Rouff, C. 2008. The influence of Tiwanaku on life in the Chilean Atacama: Mortuary and bodily perspectives. *American Anthropologist* 110(3): 325-337.

Torres-Rouff, C. 2002. Cranial Vault Modification and Ethnicity in Middle Horizon San Pedro de Atacama, Chile. *Current Anthropology* 43(1): 163-171.

Uribe Rodrigues, M.I. 2016. Personal communication, 1 June 2016.

Wallert, A. and Boytner, R. 1996. Dyes from the Tumilaca and Chiribaya Cultures, South Coast of Peru. *Journal of Archaeological Science* 23: 853-861.

Whitney, A.V., Van Duyne, R.P., and Casadio, F. 2006. An innovative surface-enhanced Raman spectroscopy (SERS) method for the identification of six historical red lakes and dyestuffs. *Journal of Raman Spectroscopy* 37: 993-1002.

Workman, Jr., J. and Weyer, L. 2008. *Practical Guide to Interpretive Near-Infrared Spectroscopy.* Boca Raton: Taylor & Francis Group, LLC.

Wouters, J. and Rosario-Chirinos, N. 1992. Dye Analysis of Pre-Columbian Peruvian Textiles with High-Performance Liquid Chromatography and Diode-Array Detection. *Journal of the American Institute for Conservation* 31(2): 237-255.